A STUDY OF THE GROSS, MICROSCOPIC, ULTRASTRUCTURAL, AND COMPARATIVE ANATOMY AND DEVELOPMENT OF THE ARTICULAR SURFACES OF THE HUMAN SACROILIAC JOINT

VOLUME I

JOHN DAVID CASSIDY

1994

A STUDY OF THE GROSS, MICROSCOPIC, ULTRASTRUCTURAL, AND COMPARATIVE ANATOMY AND DEVELOPMENT OF THE ARTICULAR SURFACES OF THE HUMAN SACROILIAC JOINT

A Thesis Submitted to the College of
Graduate Studies and Research
in Partial Fulfilment of the Requirements
for the Degree of Doctor of Philosophy
in the Department of Pathology
University of Saskatchewan
Saskatoon

By

John David Cassidy, D.C., B.Sc., M.Sc.

October, 1993

In presenting this thesis in partial fulfilment of the requirements for a Postgraduate degree from the University of Saskatchewan, I agree that the Libraries of this University may make it freely available for inspection. I further agree that permission for copying of this thesis in any manner, in whole or in part, for scholarly purposes may be granted by the professor or professors who supervised my thesis work or, in their absence, by the Head of the Department or the Dean of the College in which my thesis work was done. It is understood that any copying or publication or use of this thesis or parts thereof for financial gain shall not be allowed without my written permission. It is also understood that due recognition shall be given to me and to the University of Saskatchewan in any scholarly use which may be made of any material in my thesis.

Requests for permission to copy or to make other use of material in this thesis in whole or part should be addressed to:

Head of the Department of Pathology
University of Saskatchewan
Saskatoon, Saskatchewan S7N 0W0

ABSTRACT

In this study, the gross, microscopic, ultrastructural, and comparative anatomy and development of the sacroiliac joint are presented. Sacroiliac joints were obtained from 108 human, 43 bovine, 24 equine, 21 porcine, and 21 canine autopsies, spanning a full range of ages. The specimens were photographed and examined under the light microscope. The human specimens were also examined under the transmission and scanning electron microscopes. The sacroiliac joint angle and the relative lengths of the caudal and cephalad limbs of the joint were compared between species.

On gross inspection, the sacral surface has the smooth, shiny, creamy-white appearance of normal articular cartilage. The iliac surface has the rough, dull, bluish appearance of a thin layer of fibrocartilage. Histological and ultrastructural examination confirms the presence of hyaline cartilage on the sacral side and fibrocartilage on the iliac side in all species. The equine joint has a greater angle and a relatively shorter caudal limb than the other species.

The unique juxtaposition of hyaline and fibrocartilage in the sacroiliac joint is explained by the developmental anatomy of the joint. The sacral articular cartilage develops directly from the primary hyaline cartilage anlage. Enchondral ossification progresses from the primary centre of ossification toward the articular surface. At maturity, a hyaline cartilage cap is left as the articular cartilage. On

the iliac side, ossification of the cartilage anlage precedes cavitation of the joint space. Therefore, the iliac articular cartilage is derived from other progenitor cells and not directly from the primary cartilage anlage. As a result, it contains undifferentiated spindle cells and secondary cartilage that matures into a thin layer of fibrocartilage. The same situation is observed in the young animal specimens.

Premature degenerative changes develop in the iliac cartilage in all species. In the human, ultrastructural signs of degenerative change can be observed in specimens from the second decade of life onward. Similar changes are observed on the sacral side by the third decade of life. A similar chronology of events occurs in the animal specimens. The iliac cartilage is affected at a very young age, followed soon after by the sacral cartilage.

ACKNOWLEDGEMENTS

I wish to extend my sincere thanks to my two supervisors, Professor F. N. Ghadially for introducing me to the field of cartilage ultrastructure and to Professor H. E. Emson for his support and encouragement to continue with this work. I consider myself fortunate to have been able to work in the Department of Pathology, and I am most grateful to the members of that Department for their assistance. My sincere appreciation goes to the other members of my graduate committee, Dr. J. Kalra, Dr. F. Murphy, Dr. J. D. Newstead, Dr. K. Yong-Hing, and Dr. H. G. G. Townsend for their patience and support of this project.

I gratefully acknowledge the expert technical assistance of Mr. N. K. Yong, Mrs. D. McCullum, Mr. R. Van den Beuken, Mr. D. Mandeville, Dr. H. Pham, Dr. D. Proctor, and Mr. D. Geary. Financial assistance for this study was provided by the Chiropractors' Association of Saskatchewan, the Canadian Memorial Chiropractic College, and the Chiropractic Foundation for Spinal Research.

Finally, my deepest appreciation goes to my wife, Helena, whose patience and loving support made the completion of this thesis possible.

TABLE OF CONTENTS

LIST OF TABLES

LIST OF FIGURES

LIST OF ABBREVIATIONS

C ..... centigrade

CCR ..... caudal/cephalad limb-length ratio

C.I. .....colour Index

cm .....centimetre

e.g. .....for example

E.M. .....electron microscopy

g .....gram

H & E .....Haematoxylin and Eosin

i.e. .....that is

JI_i .....iliac cephalad limb length

JI_m .....mean cephalad limb length

JI_s .....sacral cephalad limb length

keV .....kiloelectron-volt

KI_i .....iliac caudal limb length

KI_m .....mean caudal limb length

KI_s .....sacral caudal limb length

LM .....light micrograph

M .....molar

ml .....millilitre

mm .....millimetre

MO .....month

N .....newton

N-m .....newton-metre

NB .....new born

nm .....nanometres

No. .....number

SEM .....scanning electron micrograph

S-O .....Safranin O

T-B .....Toluidine Blue

TEM .....transmission electron micrograph

WG .....weeks gestation

YR .....years

θ_i .....iliac angle JIK

θ_m .....mean angle JIK

θ_s .....sacral angle JIK

μm .....micrometer

LIST OF APPENDIX TABLES

1. INTRODUCTION

1.1 The Problem of Low Back Pain

Low back pain is an extremely common disorder. Various studies have indicated that between 60 to 80% of adults will suffer from it at some time in their lives (Cassidy and Wedge, 1988). At any given time, between 20 to 30% of us have it (Biering-Sorensen, 1983; Nagi et al., 1973; Valkenburg and Haanen, 1982). Even children are affected. Twenty-three percent of primary school children and 33% of secondary school children have experienced an episode of moderate low back pain (Mierau et al., 1984). In a more recent study, 30.4% of 1242 adolescents reported low back pain (Olsen et al., 1992). In one third of these cases it restricted activity, and 7.3% required medical attention.

Back pain is the most frequent cause of disability below the age of 45 years (Kelsey, 1982), the second most frequent reason for physician visits, the third ranking reason for surgical procedures, and the fifth most frequent reason for hospitalization in the United States (Andersson, 1991). The Canada Health Survey detected a prevalence of "serious trouble with back and spine" in 4.4% of the Canadian population (Lee et al., 1985). The average duration of disability was estimated at 21.4 days per person per year, for a total of 21,735,000 disability days. In 1981, the one-year incidence of work-related low back pain resulting in absenteeism was 1.4% in the province of

Quebec (Abenhaim and Suissa, 1987). Ten percent of the cases accounted for 75% of the cost ($125 million), and the recurrence rate was 36.3% at three years (Rossignol et al., 1988).

Although back pain is a relatively benign condition, the sheer magnitude of the problem is of great economic concern (Burton and Cassidy, 1992). It has been estimated that the direct cost of treatment of low back pain is about $23.5 billion annually in the United States (Cats-Baril and Frymoyer, 1991). Indirect costs, including compensation and disability payments, could account for another $50 to $70 billion, resulting in a total annual cost of up to $100 billion in the U.S. (Pope et al., 1991). Canadian estimates are not available, but per capita the cost is probably similar. Only four out of 12 provincial workers' compensation boards (i.e. Saskatchewan, B.C., N.W.T., and the Yukon) currently operate without a deficit, and low back injuries account for 28% of the claims (Maynard, 1993). Low back injuries alone cost the Saskatchewan Workers Compensation Board $50 Million in 1988 (Gamborg et al., 1991). In the U.S., back injuries have been estimated to account for between 33 and 41% of all compensation costs (Andersson et al., 1991).

Not only is back pain common and costly, it has a profound effect on its sufferers. Although most acute episodes subside before three months, those that persist or

become recurrent often lead to physical and psychological deconditioning and, in some cases, long-term disability. McGill (1968) found that the chance of successfully rehabilitating back-injured patients was only 50% in those disabled for six months, 20% in those disabled for one year, and 0% for those disabled for two years. This situation has not improved over the years. In the U.S. the number of persons disabled with low back pain increased to 14 times that of the rate of growth of the population between 1971 and 1981 (Naylor, 1990). These dramatic increases have continued through the 1980s (Waddell, 1990). Chronic back pain sufferers develop psychological dysfunctions such as depression, anxiety, hypochondriasis, and hysteria, which complicate treatment and recovery (Waddell et al., 1980; Frymoyer et al., 1985). In addition, the inactivity associated with chronic back pain leads to severe physical deconditioning that is difficult to reverse (Mayer, 1990). Clearly, there is a need to prevent chronic low back pain and stop the development of the associated disability.

1.2 Pathogenesis of Low Back Pain

One of the difficulties facing health care providers that deal with low back pain patients is that the cause and source of the pain is unknown in the majority of cases (Dillane et al., 1966; Spitzer et al., 1987). Without this

knowledge, treatment directed at specific structures in the spine is problematic. Primary prevention is possible through the reduction of risk factors, but secondary and tertiary prevention are complicated by a lack of knowledge on the pathogenesis of low back pain and an inability to identify, and therefore, treat the acute lesion. This state of confusion has led to numerous theories implicating every structure in and around the lumbar spine as a cause for low back pain. Often, the various theories are championed by different disciplines, usually because their mode of therapy is directed at the implicated structure. For example, chiropractors manipulate "subluxed" zygapophyseal and sacroiliac joints, physiotherapists retrain " dysfunctional" muscles, surgeons inject, lyse, and remove "contained" disc herniations.

Different diagnoses and causes for back pain have been in and out of vogue over the years. At the beginning of this century, most back pain was attributed to poor posture, or associated with imprecisely defined disorders such as muscular rheumatism, fibrositis and neuritis (Naylor, 1990). With the advent of osteopathy and chiropractic, mechanical causes of back pain became popular (Gibbons, 1992). Prominent orthopaedists such as Albee (1909), Goldthwait (1911), and Yeoman (1928) considered sacroiliac arthritis and subluxation to be the most common cause for backache and sciatica. Others, including

Goldthwait (1911), thought that facet joint arthritis was responsible for a great deal of backache and neuralgia (Putti, 1927; Ghormley, 1933; Bradgley, 1941).

The surgical era of back treatment flourished after Mixter and Barr (1934) reported their observations relating intervertebral disc herniation to back pain and sciatica. Since then, the intervertebral disc has dominated medical theories on the cause of back pain. This tendency led McNab (1977) to call this period the "dynasty of the disc". Even today, some prominent orthopaedic scientists consider the disc to be the most significant cause of mechanical backache (Nachemson, 1992).

There is no doubt that the intervertebral disc is responsible for some backache and sciatica, but it is unlikely that disc lesions explain all back and leg pain (Mooney et al., 1989). Certainly disc herniations are the main cause of sciatica associated with neurological deficit (Weber, 1983), but back pain and sciatica without neurological deficit can be produced by hypertonic saline injections into paraspinal muscles and ligaments (Kellgren, 1938), facet (zygapophyseal) joints (Mooney and Robinson, 1976; Marks, 1989) and by provocative injection of contrast material into the sacroiliac joints (Fortin et al., 1992). This suggests that noxious stimulation of these structures may explain the symptoms. However, this approach does not explain how or why these structures would cause backache in

the absence of trauma in the first place.

One explanation for insidious back pain is degenerative joint disease (Bland, 1983). Its occurrence in the spine has been the subject of many radiographic studies (Hult, 1954; Kellgren and Lawrence, 1958; Magora and Swartz, 1976; Witt et al., 1984; Frymoyer et al., 1984, Symmons et al., 1991). It is generally agreed that disc degeneration increases with age, but its relationship to back pain is less clear. Moderate disc-space narrowing and associated osteophyte formation in younger subjects seems to be associated with low back pain (Lawrence, 1969; Torgerson et al., 1976; Frymoyer et al., 1984; Symmons et al., 1991). However, in middle-aged and older individuals back pain and degenerative disc disease are both common, and their relationship might be coincidentally associated with advancing age. In addition, patients with mechanical backache don't always have degenerative disc disease and those that do have it, don't always have symptoms.

Arthrotic changes in the facet and sacroiliac joints are more difficult to reliably detect on radiographs than disc degeneration (Bellamy et al., 1984; Deyo et al., 1985; Coste et al., 1991). Indeed, early spinal osteoarthrosis cannot be detected radiographically since the initial changes are in the cartilage. It is only after cartilage breakdown and subsequent reactive subchondral bone formation that radiographic detection is even possible.

Furthermore, these changes must be moderately advanced to be detected by radiographic examination. Part of the problem is due to the small size of these joints, and their oblique orientation.

As an alternative to radiographic examination of the spine, post-mortem examination of the disc (Videman et al., 1987; Miller et al., 1988; Thompson et al., 1990), the facet joints (Lewin, 1964; Taylor and Twomey, 1986; Wang et al., 1989), and the sacroiliac joints (Sashin, 1930; MacDonald and Hunt, 1952; Resnick et al., 1975; Bowen and Cassidy, 1981) have been undertaken. Although this approach allows direct examination of the joints, clinical correlation in autopsy cases is difficult and not usually reported. Nevertheless, the relationship of degenerative changes to age is important in order to identify deviations from the norm.

Miller et al. (1988) compared macroscopic disc degeneration with age from 16 previously published reports. In total, 600 autopsy lumbar intervertebral discs from 273 cadavers were studied. Significant degenerative changes were more common in males and began to appear in the fourth decade of life. Thompson et al. (1990) found a significant correlation between age and the amount of disc degeneration in a blinded quantitative study of gross specimens. Only minor degenerative changes were seen before the age of 36 years. In another study, Videman et al. (1987) found no

correlation between disc and facet joint degeneration in middle-aged autopsy specimens. In general, it would appear that degenerative disc disease appears during middle ages and is independent of changes in the posterior facet joints.

Lewin (1964) studied age-related changes in the disc and facet joints in 104 autopsy specimens. Gross changes in the nucleus pulposus and annulus fibrosus were seen in the 20-45 years age group. However, significant changes in the facet joints rarely occurred before the age of 45 years. Morphological changes in the facet joints were compatible with the same process in other synovial joints. These included a mixture of degenerative and restorative processes, such as cartilage fibrillation, chondrocyte cloning, surface erosion, subchondral bone plate remodelling, and osteophyte formation. Other studies by Taylor and Twomey (1986) and Wang et al. (1989) found histological age-related changes in the lumbar facet joints to occur after the age of 40 years. Therefore, facet joint arthrosis tends to occur independent of and later than disc degeneration.

In the first study to publish histological sections through the sacroiliac joint, Sashin (1930) found that degenerative changes occurred in 91% of males and 77% of females after the age of 30 years. However, only two of 32 cases under the age of 30 years showed early degenerative

changes. MacDonald and Hunt (1952) reported on 57 autopsy cases over the age of 20 years and two newborn cases. They found increasing degenerative changes in the articular cartilage in specimens 30 years and older. Resnick et al. (1975) reported on 46 sacroiliac joints, 40 of which were over the age of 50 years. They found that degenerative changes increased after the age of 50 years. Bowen and Cassidy (1981) were the first to report on a complete series of autopsy specimens from fetal life to the eighth decade. They also were the first to clearly document the different morphology of the two articular surfaces, the iliac being fibrocartilage and the sacral being hyaline cartilage. This finding was later confirmed by Walker (1986). Bowen and Cassidy (1981), noted degenerative changes in the iliac cartilage as early as the second decade of life. Based on these observations, it would appear that degenerative changes in the sacroiliac joint precede those found in the disc and facet joints.

Given the rich nociceptive nerve supply to the capsule and synovium of the facet joints (Bogduk, 1983; Giles and Taylor, 1987) and of the sacroiliac joints (Solonen, 1957; Ikeda, 1991), it is likely that these joints do contribute to low back pain. They are both subject to osteoarthrosis, which can produce pain by chronic synovitis that results from the absorption of joint detritus, ligamentous strain from altered joint mechanics, and increased stress on

subchondral bone (Kellgren, 1983; Radin and Rose, 1986; Hammerman, 1989). However, it remains uncertain how to best assess this hypothesis in vitro and in vivo.

1.3 The Sacroiliac Joint and Back Pain

The role of the sacroiliac joint as a primary source of low back pain is an old hypothesis that is resurgent, but still controversial (Bernard and Cassidy, 1991). Several problems complicate this issue. Firstly, the function of the sacroiliac joint is uncertain. Secondly, because of its anatomical location, it is difficult to examine. Finally, because its role in the pathogenesis of low back pain is not clear, there are no definitive tests to objectively measure altered sacroiliac function or physiology that correlate to low back pain (Cassidy and Mierau, 1992).

Many attempts have been made to describe and measure motion in the sacroiliac joints. The first studies came from the specialty of obstetrics and gynecology when it became apparent that the fetal head could not pass through the pelvis without some separation of the sacroiliac joints. According to Lynch (1920), in 1812 Le Gallois showed that the pelvis of the female guinea pig had a diameter of 11 mm, yet the fetal head measured 20 mm. Obviously, separation of the pelvis was a necessary precursor to birth. This led Lynch (1920) to publish a

case series of radiographs in post-partum females. He observed widening of the sacroiliac joint and attributed this to sacroiliac slipping, which he considered the main cause for the back pain in his cases. Four years later, Brooke (1924) reported the results of manually stressing 200 cadaveric specimens, including an unspecified number of pregnant female specimens. Although he did not publish his measurements, he reported that females were more mobile than males, and that mobility was increased during pregnancy to two and one half times above the maximum degree present in the non-pregnant female specimens.

Weisl (1955) was the first to publish radiographic measurements of sacral position in different postures. On 27 male and 30 female volunteers, he found an average of 5.6 (± 1.4) mm of ventral sacral movement (x-axis rotation) between the recumbent and standing positions. There were no differences between the sexes. However, when Borell and Fernstrom (1957) used x rays to measure changes in sacral position in 191 women of reproductive age, including 40 women during labour, greater mobility was found in the pregnant and puerperal women than in the nulliparae women.

The first direct, in vivo measurement of sacroiliac mobility was performed by inserting Kirschner pins into the iliac spines of 11 male medical students and one male professor of medicine (Colachis et al., 1963). Displacements between the pins were measured in various

postures. According to the authors, a variable amount of displacement was reported. The maximum amount of five mm was observed in the x axis during forward flexion while standing. Unfortunately, like all of the preceding studies, this report did not contain a table of the measurements, so that the quality of the data is hard to assess.

With the advent of stereoradiographic techniques, more sophisticated three dimensional data were reported by Frigerio et al. (1974) and later by Egund et al. (1978). In the former study, measurements were made in one cadaver and one male volunteer (ages unknown). In the cadaver, movement between points on the sacrum and ilium ranged up to 12 mm, and averaged 2.7 mm with different leg positions. In vivo, these movements were considerably larger, ranging up to 26 mm. In the later study, tantalum balls were inserted into the sacrum and ilia of three female volunteers (age 30, 42, and 45 years) and one male volunteer (age 25 years). Measurements were obtained in seven different recumbent and weight-bearing postures. The distance between the two superior posterior iliac spines varied at most 0.4 mm between the seven different positions. Rotations between the ilium and sacrum about any of the three main axes were in the magnitude of two degrees (± 0.2 degrees).

Grieve (1983) used the same biplanar orthogonal

technique to analyze x-axis rotational displacements of the posterior superior iliac spines with respect to the sacrum on photographs rather than x rays. Measurements were made from a series of photographs taken while the subjects stood on one leg during alternate hip and knee raising. A sample of 61 joints (age and sex not specified) were studied. Her results were reported in histograms with no raw data, summary statistics, or analysis. According to her interpretation of the results, movements were found to be between one and 16 mm. All of the women subjects and six subjects with back pain had more mobility than the male subjects and those subjects without back pain. Unfortunately, the methods and results are not presented in enough detail to substantiate her findings.

Lavignolle et al. (1983) used a more advanced stereoroentgenographic technique to measure iliac displacements during straight leg raising in five subjects, two women and three men under 25 years of age. The average displacement was determined to be 12 degrees of x-axis rotation with 6 mm of z-axis translation. Sturesson et al. (1989) used the same technique to investigate rotations in 25 back pain patients, 21 females, and four males between 18 and 45 years of age. Prior to testing, the patients were examined by clinicians who decided whether or not the joints were symptomatic. Tantalum balls were inserted percutaneously as reference markers and the subjects were

studied in the supine, prone, standing, and sitting positions. The mean x-axis rotation of the sacrum was 2.5 degrees (range from 0.8 to 3.9 degrees), and the mean z-axis translation was 0.7 mm (range from 0.1 to 1.6 mm). There was no difference in the displacements between the symptomatic and asymptomatic joints. As a result, the authors concluded that the analysis of mobility could not identify symptomatic joints. However, one might also conclude that the clinical tests used in the study were not valid or reliable, or that the patients had other causes for their back pain.

Load-displacement behaviour of the sacroiliac joints from eight cadaveric specimens (seven males and one female) between the ages of 59 and 74 years was studied by Miller et al. (1987). With the ilia fixed, the specimens were subjected to test forces of 294 N and moments up to 42 N-m in flexion, extension, lateral bending, and axial torsion. Displacements did not exceed 0.5 mm in response to the test forces, and rotations were less than two degrees in response to the 42 N-m test moments. In addition, the specimens were tested to failure. All eight specimens resisted loads up to 500 N or 50 N-m in all test directions. These results are consistent with previous estimates of in vivo sacroiliac shear loads in the range of 300 to 1750 N in daily activities with simultaneous flexion and lateral bending moments of 25 to 50 N-m (Millar, 1985).

In a series of in vitro experiments, Brunner et al. (1991) reported their results on the mobility, morphology and histology of the sacroiliac joints. Two male pelves (age 24 and 55 years) and two female pelves (age 49 and 59 years) were subjected to vertical forces of 100 to 300 N at the sacrum. Maximum nutation movements (i.e. x-axis rotation) of 0.6 to 1.2 degrees were recorded in the male specimens, and 1.9 to 2.8 degrees in the female specimens. Moiré topographic measurements showed great variation in surface topography, but the usual pattern was to find an elevation along the iliac surface that fit into a depression along the sacral surface. In all cases, the iliac cartilage was more degenerated and thinner than the sacral cartilage. Generally, there was less mobility in the male specimens and in specimens with more degenerative cartilage.

More recently, Vleeming et al. (1992b) subjected four embalmed, but intact pelves to physiologic loads to induce ventral rotation (x-axis rotation). A cranially-directed preload of 300 N was applied to simulate gravity, then a ventrally-directed force of 200 N was applied to induce rotation. The specimens were fixed by the acetabuli in order to allow physiologic deformations of the pelvic bones. The three female and one male specimen were all over 70 years of age. Under these conditions, the eight joints allowed an average of about two degrees of rotation,

and there were significant variations within and between specimens. Mobility was decreased in arthrotic sacroiliac joints and increased in one joint adjacent to a total hip replacement. These results suggest that even in elderly specimens, the sacroiliac joint is mobile. In addition, mobility decreases with arthrotic change and might be increased by ipsilateral coxarthrosis. These results are consistent with an earlier study of sacroiliac joint friction coefficients by the same group of investigators (Vleeming et al., 1990a&b). Higher friction coefficients were associated with increasing degenerative roughening of the articular surfaces of the sacroiliac joint. Therefore, degenerative change decreases sacroiliac mobility, as it does in other synovial joints.

Several other studies have looked at biomechanical factors that might influence sacroiliac mobility. Wilder et al. (1980) measured the joint surface contours from eleven innominate bones in order to mathematically model the best-fit axes of rotation. From these data, they proposed that the joint surfaces must first separate to allow rotation, which must also include translation. In their opinion, the sacroiliac joint functions as a shock-absorbing structure, rather than a freely moving articulation because of its irregular surface structure. However, Vukicevic et al. (1991) showed that removal of the interosseous ligament from 12 fresh pelves caused the

sacroiliac articulations to wedge together and limit mobility. With this ligament intact, they observed sacroiliac motion under physiologic loadings of 50 to 300 N. Therefore, it is not possible to model motion without taking into account the affect of the soft tissues. Furthermore, Vleeming et al. (1989a and 1989b) showed that there are direct attachments between the sacrotuberous ligament and the long head of the biceps femoris, the piriformis, and the gluteus maximus, and that these muscles could dynamically influence sacroiliac mobility.

It is obvious from the preceding discussion that there is little agreement between studies on the quality and quantity of sacroiliac mobility. Both the in vivo and in vitro kinematic studies cited show a variable degree of mobility using various methods of analysis on different cohorts of subjects and specimens. Nevertheless, the following trends have emerged (Cassidy and Mierau, 1992).

1. The range of motion is small and decreases with age and degenerative change.
2. The range of motion is greater in women and increased during pregnancy.
3. The motions are coupled and dependent on some degree of joint separation.
4. The predominant motion is x-axis rotation, coupled with a small amount of z-axis translation. (Figure 1.1)

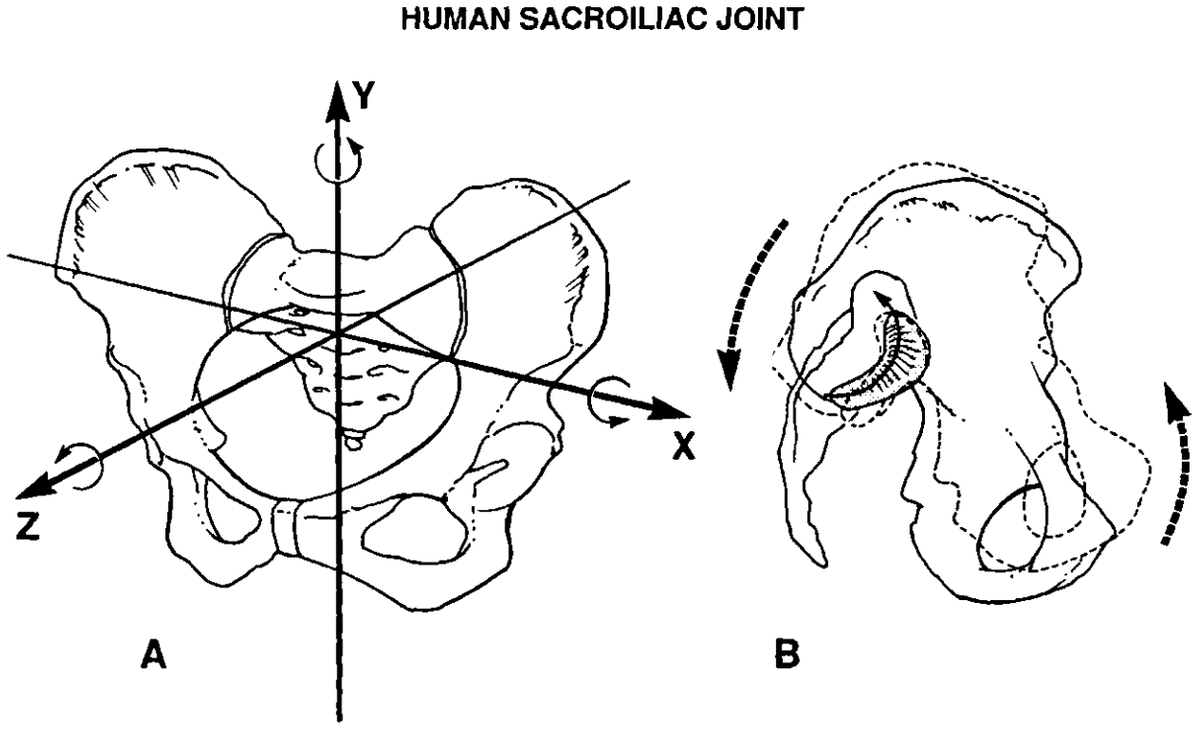

FIGURE 1.1 Part A illustrates the three axes of movement superimposed over the human pelvis. Part B shows x-axis rotation of the sacroiliac joint.

Clinicians have put a lot of emphasis on the pathologic significance of altered sacroiliac mobility. Various tests have been proposed to diagnose decreased mobility (Kirkaldy-Willis and Hill, 1979), hypermobility (Lee, 1989), and displacement (Greenman, 1986). However, the test-retest reliability of these tests is unacceptably poor (Haas, 1991) and the validity of such testing is questionable (Cassidy, 1992), especially after considering the preceding discussion. Yet despite this lack of diagnostic precision, a plethora of treatment options have been recommended, including manipulation (McGregor and Cassidy, 1983), mobilizations (DonTigny, 1985), immobilization by external support (Grieve, 1983) and arthrodesis (Waisbrod et al., 1987).

Another common treatment approach is to ignore the issue of mobility and rely on palpatory tenderness over the posterior aspect of the joint in the buttock. However, because of its deep anatomical location, it is not possible to directly palpate the sacroiliac joint. In addition, tenderness over the posterior location of the sacroiliac joint could be due to any number of problems, including referred pain from the lumbar spine (Clements et al., 1991) or trauma to the overlying muscles and ligaments (McGill, 1987). Proponents of this approach often diagnose and treat sacroiliac syndrome by local anesthetic and corticosteroid injection (Broadhurst, 1989). If the local

abolishes the pain, the injection is diagnostic. The steroid is directed at joint inflammation.

In support of the hypothesis that sacroiliac joint inflammation is a cause of low back pain, Davis and Lentle (1978) found scintigraphic evidence of sacroiliitis in 22 of 50 female patients with low back pain. Only one of the 22 patients with a positive scan had ankylosing spondylitis. Therefore, the increased radionuclide uptake was attributed to a different, non-specific, inflammatory process. Chisin et al. (1984) observed the same phenomenon in four males with sacroiliac strain. The increased radionuclide uptake was on the same side as the symptoms and returned to normal after recovery. All the symptomatic joints were tender to palpation and were associated with a positive Gaenslen test (i.e. pain on sacroiliac joint hyperextension).

In a follow-up to their 1978 study, Rothwell, Davis and Lentle (1981) reported scintigraphic findings in 60 female patients with low back pain. Twenty-four patients had increased uptake suggesting sacroiliitis. At six-month follow-up, 18 patients showed clinical improvement associated with a return to normal values on quantitative sacroiliac scintigraphy. More recently, Mierau (1991) studied 27 patients with unilateral sacroiliac joint pain and tenderness. After initial quantitative sacroiliac scintigraphy, the patients were treated by sacroiliac

manipulation and then rescanned six weeks later. The mean uptake was greater on the symptomatic side and associated with the presence of two or more positive sacroiliac stress tests. At follow-up, a majority of the patients had recovered and their scans were normal.

In summary, the role of the sacroiliac joint in the pathogenesis of low back pain remains an enigma. However, the weight of the evidence suggests that this joint is prone to early degenerative arthrosis that could lead to inflammation and low back pain. So far, kinematic studies have yet to demonstrate pathologically altered biomechanics that could account for lower back symptoms.

LITERATURE REVIEW

2.1 Anatomy

The sacroiliac joints join the sacrum to the ilium to form the pelvic ring. (Figure 2.1) The articular surface is usually auricular or c-shaped, with the convex side facing anteriorly and slightly inferiorly. (Figure 2.2) The shorter, cephalad limb is directed posteromedially and cranially, while the longer caudal limb is directed posterolaterally and caudally. The vertically-oriented auricular surfaces twist obliquely at an angle to the sagittal plane. (Figure 2.1) The articular portion of the sacral side most often includes the first, second, and upper half of the third sacral segments (Solonen, 1957). In the adult, there is usually a saddle-shaped elevation along the length of the iliac side that fits into a corresponding sacral depression (Bowen and Cassidy, 1981). There can be marked variations in the size, shape, contour, orientation, and relative lengths of the limbs of the joint.

The surface area of the articular surface of the sacroiliac joint was first reported by Sashin (1930) to be 18 cm^2. Later, Miller et al. (1987) reported it to be 14 cm^2, using a much more precise method of measurement. Weisl (1954) was the first to carefully study the contours of the articular surface. He meticulously recorded relief maps from 62 post-mortem specimens, including 11 full-term fetuses and 51 adults of various ages. In addition, he

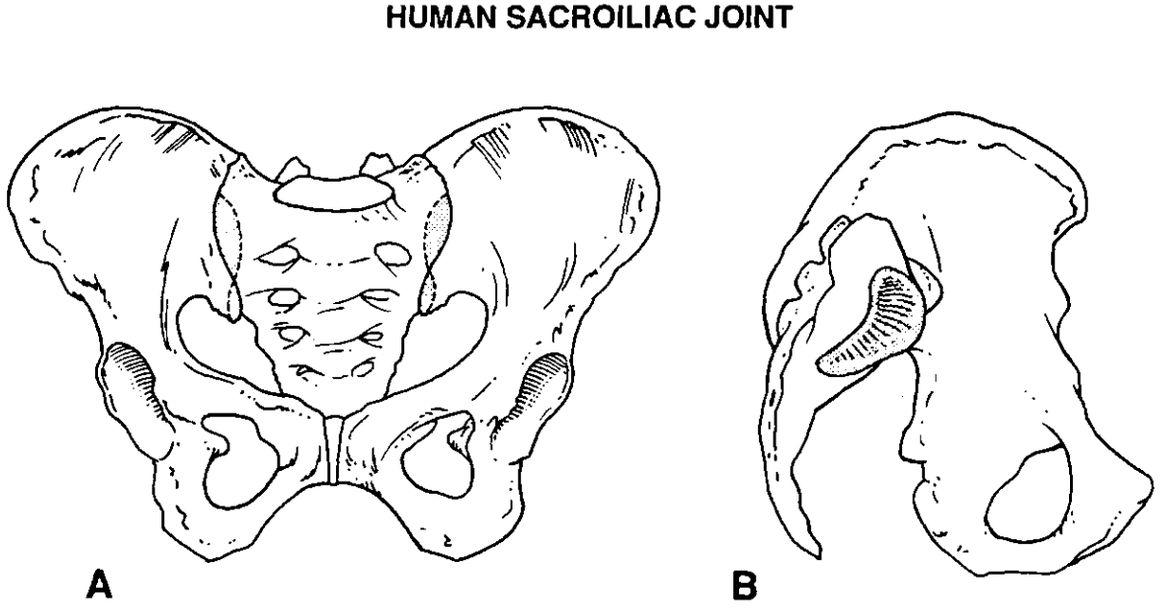

FIGURE 2.1 Anteroposterior (A) and lateral (B) views of the human pelvis showing the location of the sacroiliac joints.

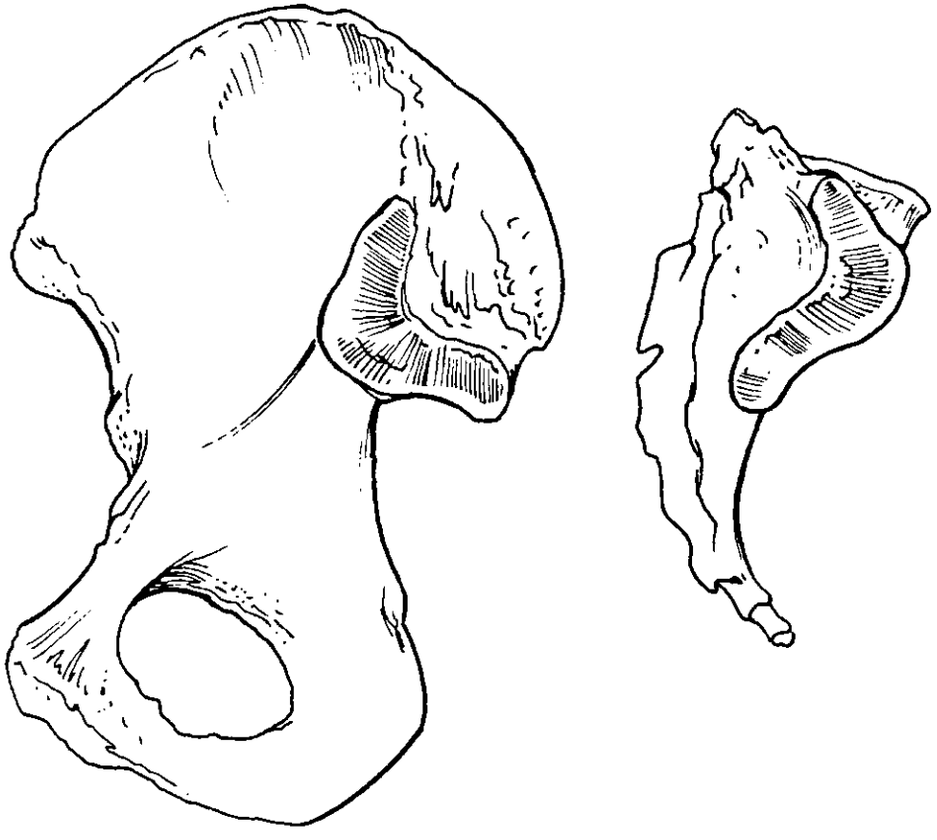

FIGURE 2.2 Illustrations of the iliac and sacral surfaces of the sacroiliac joint.

measured various points on the articular surface to help describe its shape. The sacral surfaces were characterized by a large central depression and two small elevations at the ends of the caudal and cranial limbs. The iliac surfaces had a reciprocal relief. These irregularities were found to increase with age. The mean angle between the two limbs was measured dorsally at 87° ± 1.23°. Based on these results, he described the joint as a cranial and caudal condyloid joint with an intermediate saddle joint.

Ohba (1985) modified Weisl's methods of measurement and repeated them on 24 adult cadaver sacroiliac joints. Eight of his specimens were under 70 years of age, and the rest were older. The mean angle between the two limbs of the joint was 106° ± 7.1°. The caudal limb was always longer than the cephalad limb with mean lengths measured at 39 mm ± 5.0 and 28.5 mm ± 4.8 mm respectively. He also measured the mean joint surface area at 14.3 cm^2 ± 2.03 cm^2. Female specimens had slightly smaller surface areas, shorter caudal limbs, and more acute joint angles. These sex differences were small.

When Weisl's measurements were repeated by Valojerdy and Hogg (1989) on a set of 153 dried bones of Indian origin, the angle between the two limbs of the joint was found to be more acute in females. In 108 males and 45 females, the mean angle on the sacral side was 99.2° ± 7.86° for males and 96.0° ± 9.85° for females. On the

iliac side, the measurements were 93.35° ± 7.23° for males and 88.73° ± 8.73° for females. The joint surfaces were always larger in the male specimens, and the auricular surface of the ilium was located more caudally in the female specimens.

Using similar measurements to Weisl, Bakland and Hansen (1984) found the mean length of the caudal limb of the sacroiliac joint to be 52 mm and the cranial limb to be 39.5 mm. In 92% of their 24 autopsy specimens (ages not reported), they found an extra-articular or "axial" sacroiliac joint, located approximately 15 mm dorsocranial to the main articulation. It is described as an iliac prominence that fits into a sacral depression, and could easily be mistaken for an accessory sacroiliac joint. In 50% of the cases, the axial joint surfaces were covered by either hyaline or fibrocartilage.

Past studies have focused on the presence of extra-articular or accessory sacroiliac joints. These are usually described as small oval articulations that occur between the sacrum and ilium, posterior to the main articular surfaces of the sacroiliac joint. Hadley (1952) described two types of accessory articulations based on his dissections of 185 half sacra and 163 ilia from anatomy-room specimens. The superficial accessory joint occurs between the posterior superior iliac spine and the lateral crest of the sacrum, opposite to the second sacral foramen.

The less common deep variant is located opposite the first sacral foramen. In 18% of his specimens, he was able to find at least one accessory joint. Although he claimed that they are surrounded by a capsule and covered by hyaline cartilage, he did not publish any histological evidence for this claim. Schunke (1938) found these articulations in 16 (34%) of his 47 specimens. In all cases, the articular surface was covered with fibrocartilage. Other studies of dried bones found a prevalence of accessory articulations in 10.4% (Derry, 1911), and 36% (Trotter, 1937) of specimens. According to Trotter (1937) their incidence is increased in males and increases with age. According to Bakland and Hansen (1984), Hadley's deep articulation should be considered a separate "axial" sacroiliac joint.

The sacroiliac joint is a weight-bearing articulation that is stabilized by a series of strong ligaments. These include the sacrospinous and sacrotuberous ligaments, which originate from the anterior and posterior surface of the sacrum and insert into the ischial spine and tuberosity, respectively. The interosseous ligament binds the sacrum to the ilium and forms the posterior margin of the sacroiliac joint. Dorsal to this strong ligament is the smaller and weaker posterior sacroiliac ligament. It forms several short fasciculi that run between the dorsolateral sacrum and the medial aspect of the posterior superior

iliac spine. A long portion of this ligament runs inferiorly from the posterior superior iliac spine to the sacrum. These ligaments are separated from the interosseous ligament by the dorsal rami of the sacral nerves and accompanying vessels (Cassidy and Mierau, 1992). The anterior sacroiliac ligament is little more than a thickening of the anterior joint capsule. (Figure 2.3) This capsule is well-developed anteriorly, but missing along the posterior margin of the articular surface (Solonen, 1957; Bowen and Cassidy, 1981). Here, fasciculi of the interosseous ligament extend into the joint and appear to be intraarticular. The long posterior sacroiliac ligament may give partial origin to the sacrospinalis (erector spinae) muscles. The piriformis muscle takes part of its origin from the anterior sacroiliac ligament.

The lumbosacral plexus crosses in front of the sacroiliac joint, directly over the anterior ligament and beneath the psoas major muscle (Sashin, 1930). Solonen (1957) was the first to study the innervation of the sacroiliac joint by macroscopic dissection. In nine cadavers (18 joints) the anterior ligament was most often innervated by branches of the fourth and fifth lumbar nerves. However, innervation was not always symmetrical on the two sides and contributions were also observed from as high as L-3 and as low as S-2. The superior gluteal nerve, which is a branch of the sacral plexus (L-4 to S-2), also

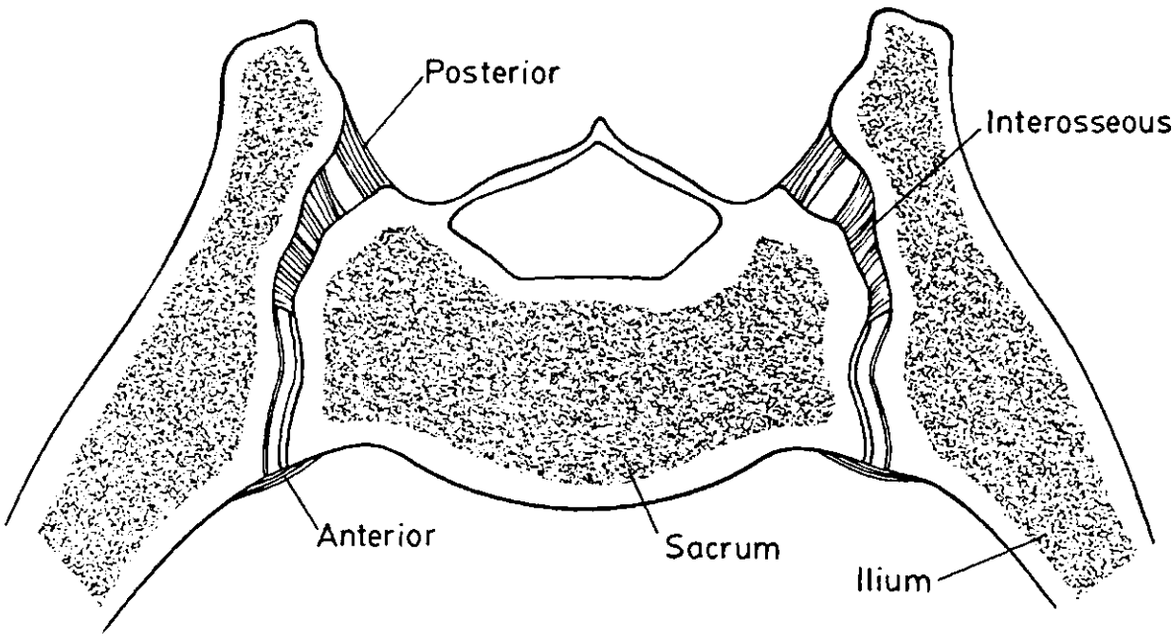

FIGURE 2.3 An axial illustration through the middle of the sacroiliac joint shows the posterior, interosseous, and anterior ligaments.

contributed to the anterior innervation of the joint in most cases. In all eighteen specimens, the dorsal aspect of the joint received branches from the first and second sacral nerves. This wide range of segmental innervation could account for the large spectrum of somatic referred pain patterns attributed to sacroiliac disorders.

A more recent and detailed study used gross and histological methods to study the nerve supply of the sacroiliac joint in eighteen adult cadavers (Ikeda, 1991). The upper ventral portion of the joint was mainly innervated by the ventral ramus of L-5 and the lower ventral portion by the ventral ramus of S-2. The upper dorsal portion of the joint was mainly innervated by lateral branches of the dorsal ramus of L-5 and the lower dorsal portion by lateral branches of the dorsal rami of the sacral nerves. The diameters of these nerves ranged from 0.292 mm to 0.997 mm. Nerve fibres varying in diameter from 0.2 microns to 2.5 microns were observed to terminate with five morphologically different terminals in the sacroiliac joint capsule. These findings are in agreement with Wyke (1982), who also reported that the sacroiliac joint capsule contains a dual nociceptive receptor system, one from a dense plexus of unmyelinated nerve fibres and the other located in the adventitial sheaths of minute articular blood vessels.

The anterior blood supply to the sacroiliac joint

occurs by anastomoses between the middle sacral artery and lateral sacral branches from the internal iliac artery (Bernard and Cassidy, 1991). They enter the anterior sacral foramina and anastomose with the posterior sacroiliac blood supply from the gluteal arteries. Venous drainage occurs through tributaries of the middle and lateral sacral veins.

The anatomical classification of the sacroiliac joint has been problematic. The joint was considered to be an immovable synarthrosis (i.e. united by fibrous tissue) long after Hippocrates (fifth century B.C.) and Vaesalius (1543) described it as a fixed connection (Vleeming et al., 1992a). According to Lynch (1920), obstetricians of the 17th and 18th centuries debated whether or not the joint separated during birth, until Bernhard Siegfried Albinus (1697-1770) and William Hunter (1718-1783) demonstrated that the connection was a flexible joint. Merkel has been credited with the first detailed description of the joint in his textbook of human anatomy published in 1816 (Sashin, 1930). He noted that the surfaces were covered with cartilage that became rougher with advancing age. According to Sashin (1930), Von Luschka in 1854 was the first to consider the sacroiliac joints as diarthroses (i.e. freely-moving, synovial joints). However, many anatomists disputed this and classified the joint as either a synarthrosis (Allen, 1882) or as an amphiarthrosis

(Cooke, 1878; Gray, 1901), where the two surfaces are united by fibrocartilage.

Sashin (1930) published the first micrographs of the sacroiliac joint. His study included 43 fresh specimens up to 29 years of age, 111 fresh specimens between 30 to 59 years of age, and 103 fresh specimens 60 years and older. He reported that the younger specimens were freely movable and both surfaces were covered with hyaline (articular) cartilage. Therefore, he classified the younger joints as diarthrodial. In his older specimens, the joints became fibrous, so he classified them as amphiarthroses. However, careful review of his one micrograph of a young specimen shows fibrocartilage on the iliac side of the sacroiliac joint.

Eight years later, Schunke (1938) published a histological study of the development of the sacroiliac joint. In his opinion, the sacral articular cartilage could be either hyaline or fibrous, but after birth it was mostly hyaline cartilage. He reported the iliac cartilage as either hyaline or fibrous, but mostly fibrocartilage after the fourth fetal month. He did not offer an anatomical classification for the joint, and he was generally unsure about the histology of the cartilage surfaces.

In 1962, Carter and Loewi described the cartilage surfaces of the sacroiliac joint in eight autopsy

specimens, all under 22 years of age. Although they were more interested in comparing two of their cases with Still's disease to the normals, they did note that the matrix and cell alignment was different in the iliac cartilage. Although they acknowledged the controversy surrounding the anatomical classification of the joint, they did not offer an opinion on it.

Confusion over the classification of the sacroiliac joint continued into the nineteen seventies, when it was often classified as an amphiarthrosis by anatomical authorities (Schmorl and Junghanns, 1971; Gray, 1973). In an attempt to settle this debate, Bowen and Cassidy (1981) published their results of a histological survey of 40 autopsy specimens from fetal life to the eighth decade. They reported that the iliac side is fibrocartilage and the sacral side hyaline cartilage from fetal life onward. The joint was classified as a diarthrosis because of its synovial cavity, anterior joint capsule, and free mobility. However, they emphasized that other diarthrodial joints are covered by hyaline cartilage, and the sacroiliac is an unusual or atypical diarthrosis. However, Paquin et al. (1983) challenged this notion when they were able to isolate type II, but not type I, collagen from one 49-year-old specimen of human iliac cartilage. Since type I collagen is associated with fibrocartilage and type II with hyaline cartilage, they concluded that both surfaces were

hyaline cartilage. However, Both type I and II collagen are found in the fibrocartilage of the annulus fibrosus of the intervertebral disc (Eyre and Muir, 1976) and in other fibrocartilages (Miller, 1978). So it is possible that their small sample biased the study. In fact, they admitted that detailed biochemical analysis of the iliac cartilage was limited by the paucity of tissue obtained from their limited sample. Also, they compared the ultrastructure of the sacral and iliac collagen in one sample. The collagen fibrils of the sacral cartilage were randomly oriented, while those of the iliac cartilage were arranged in parallel bundles. For some unknown reason, they further confused the issue by classifying the joint as an amphiarthrosis.

There have been two other histological studies of the sacroiliac cartilage. Walker (1986) examined 36 fetal joints ranging from 12 weeks gestation to term and 15 adult anatomy-room cadavers from 49 to 84 years of age. Her observations confirmed those of Bowen and Cassidy (1981). In all cases, the iliac side was fibrocartilage and the sacral side was hyaline cartilage. However, Ishimine (1989) stated that both surfaces were composed of hyaline cartilage. He studied 13 fetuses and 42 adult specimens by light and scanning electron microscopy. A review of the micrographs published in his report shows marked differences in morphology between the iliac and sacral

sides. In particular, his micrographs of a five month old and a seven month old specimen show fibrocartilage on the iliac side. The scanning electron micrographs confirm the more collagenous nature of the iliac matrix.

It is well accepted that the articular cartilage of synovial joints is hyaline cartilage. This point is important for more than academic interest or for joint classification by anatomists. Hyaline cartilage is better suited to withstand the loads involved in joint motion. Its high water content contributes to its stiffness to compression, resiliency to loading, and its ability to participate in joint lubrication. On the other hand, fibrocartilage has a lower water content because of its higher matrix collagen-to-proteoglycan ratio (Mitchell and Shepard, 1976). It is biomechanically inferior and cannot withstand the repetitive loads that hyaline articular cartilage is regularly exposed to (Coletti, et al., 1972). After full-thickness articular cartilage injury, hyaline cartilage is replaced by fibrocartilage, which eventually undergoes degenerative breakdown under the stress of joint loading (Buckwalter et al., 1988b).

Hyaline (Gr. Hyalos, glass) cartilage has a glassy homogeneous appearance when viewed under the microscope. This is because of its high water content, which in turn is due to its high proteoglycan content. It is composed of cells (mostly chondrocytes) and matrix, which is between 60

to 80% water by weight, depending on age and degree of degenerative change (Mankin and Thrasher, 1975). After removing the water content, collagen contributes about 50%, proteoglycans between 30 to 35%, and non-collagenous proteins with glycoproteins between 15 to 20% of the dry weight of the matrix. Collagen forms the framework (fibrillary matrix) that gives cartilage its tensile strength and form (Kempson, 1980). It serves to trap the ground substance (interfibrillary matrix) of water, proteoglycans, and other proteins.

Proteoglycans form the major macromolecule of hyaline cartilage matrix. They can occur in various forms, including individual monomers to large aggregating forms that are visible as electron-dense dots under the electron microscope. The monomer consists of a protein core filament with multiple covalently-bound oligosaccharides and glycosaminoglycans. The glycosaminoglycans, chondroitin and keratan sulfate, form about 95% of the molecule. Their attachment to the protein core filament is limited to specific regions. In the matrix, most of the monomers associate with hyaluronic acid filaments and link proteins to form aggregates. (Figure 2.4) The hyaluronic acid forms the backbone of the aggregate and the link proteins stabilize the association between it and the monomers. The aggregates are trapped, either mechanically or by some other possible interaction, by the collagen

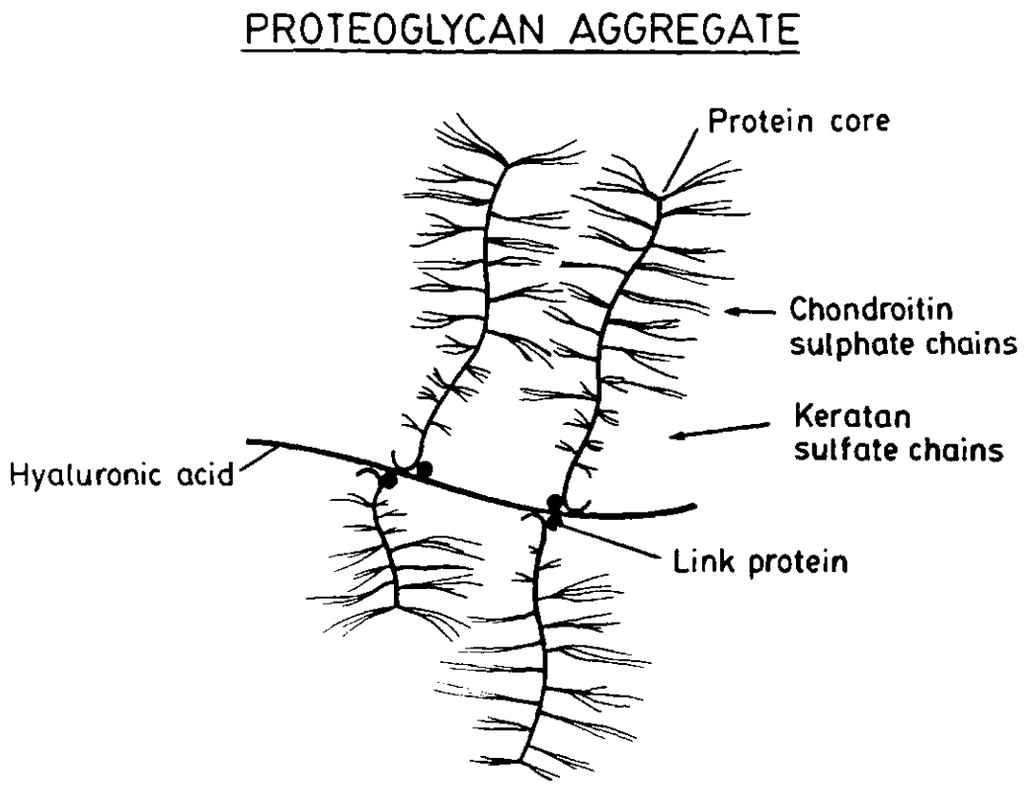

FIGURE 2.4 An illustration of the proteoglycan aggregate shows four monomers attached to a hyaluronic acid filament by link protein. The glycosaminoglycans, chondroitin and keratan sulfate, are seen in their specific regions along the protein core.

fibrils in the matrix (Poole et al., 1982). (Figure 2.5)

Because the sugars in the proteoglycan monomer contain carboxylate and sulfate groups, they are negatively charged and repel each other while imbibing water. This ability to interact with matrix fluid gives cartilage its resilience and stiffness to compression. (Figure 2.6) Loading the cartilage compresses the monomers together, increasing their negative charge density and forcing fluid out of their molecular domain. Releasing the load allows the monomers to expand again and decrease their charge density. The proteoglycan aggregates are under a constant pressure to expand, restrained only by the collagen fibril meshwork. (Figure 2.5)

The principle collagen of articular or hyaline cartilage is type II. It forms the characteristic cross-banded fibrils seen in the matrix under the electron microscope. The length or period of each band (i.e. one light band + one dark band) depends on the hydration of the fibril. In unfixed specimens it ranges from 64 to 70 nm, and in processed specimens from 52 to 62 nm (Ghadially, 1988). The fibrils form fibres that can be arranged in bundles. (Figure 2.7) Because the diameter of the collagen fibril is usually less than 0.1 μm, it cannot be seen under the light microscope, which has a limit of resolution between 0.2 to 0.25 μm (Ghadially, 1983). The collagen fibril is comprised of filaments made up of five rows of

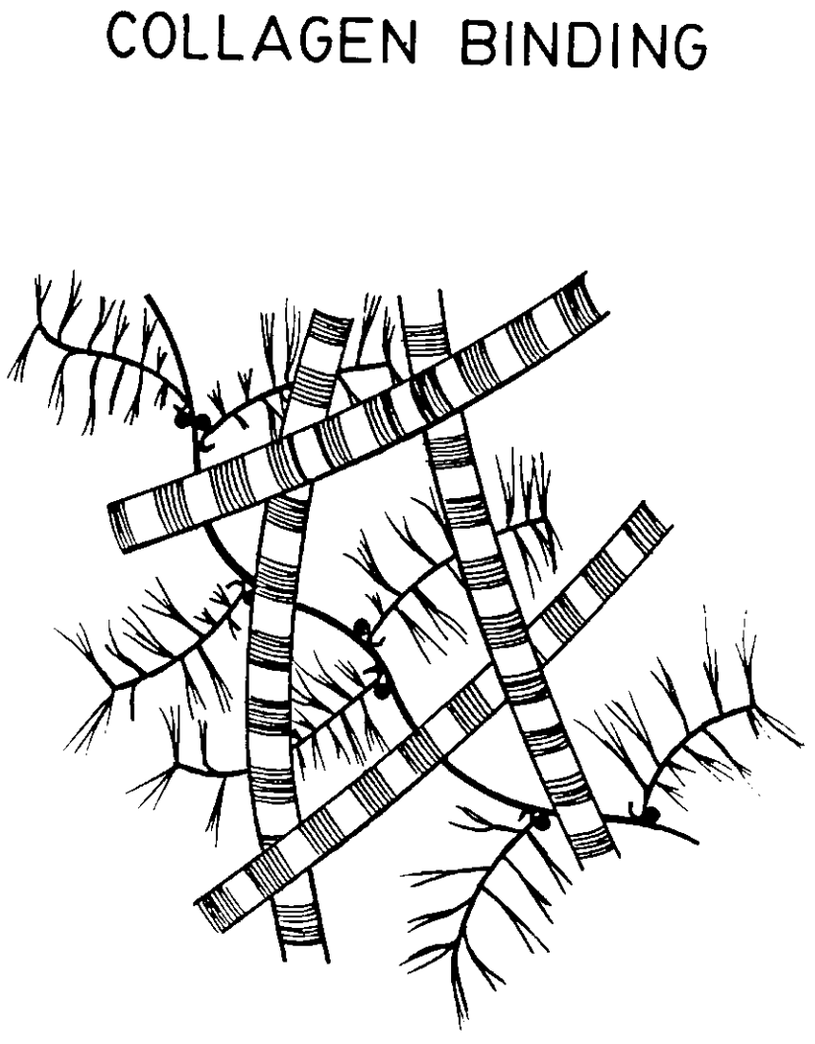

FIGURE 2.5 An illustration of a proteoglycan aggregate trapped by collagen fibrils in the cartilage matrix.

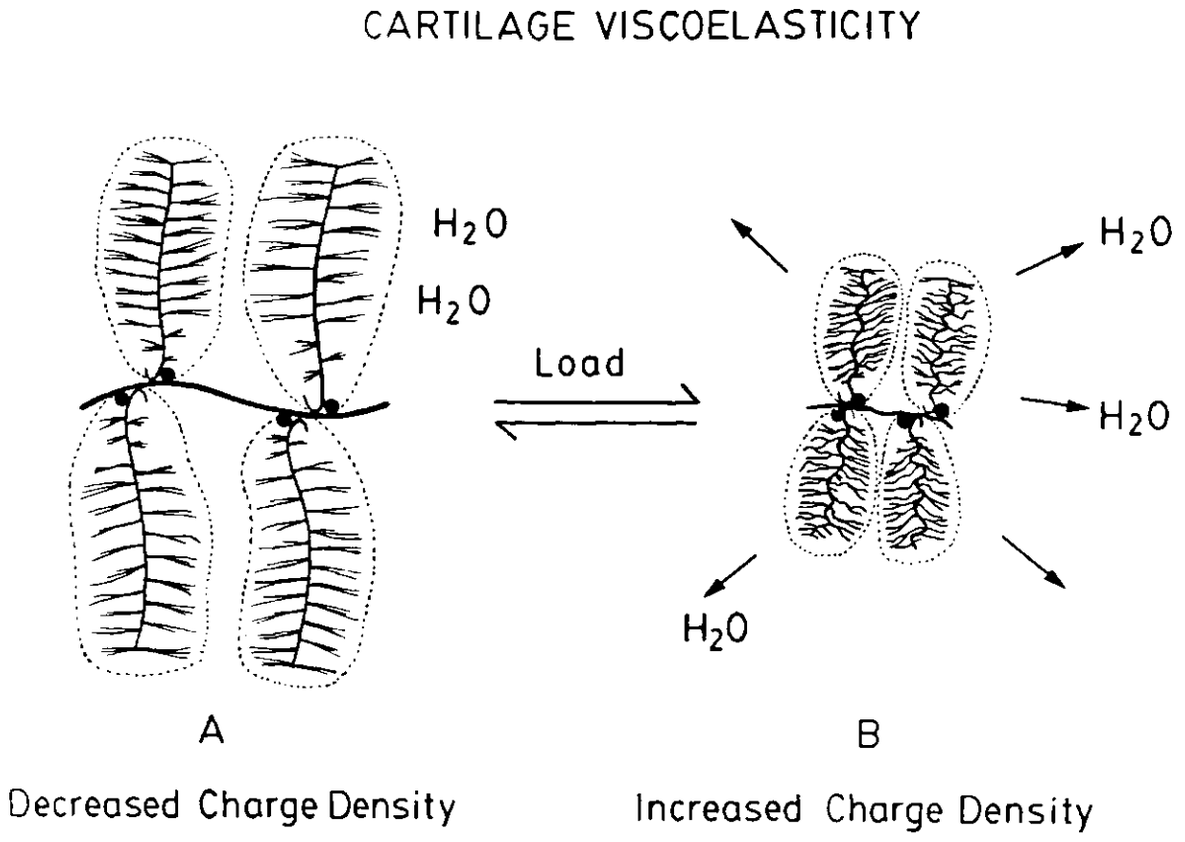

FIGURE 2.6 An illustration of cartilage viscoelasticity shows the decreased charge density (A) associated with the extended position of the proteoglycan monomers. When a load is applied to the cartilage surface, the monomers are compressed, resulting in an increased charge density (B).

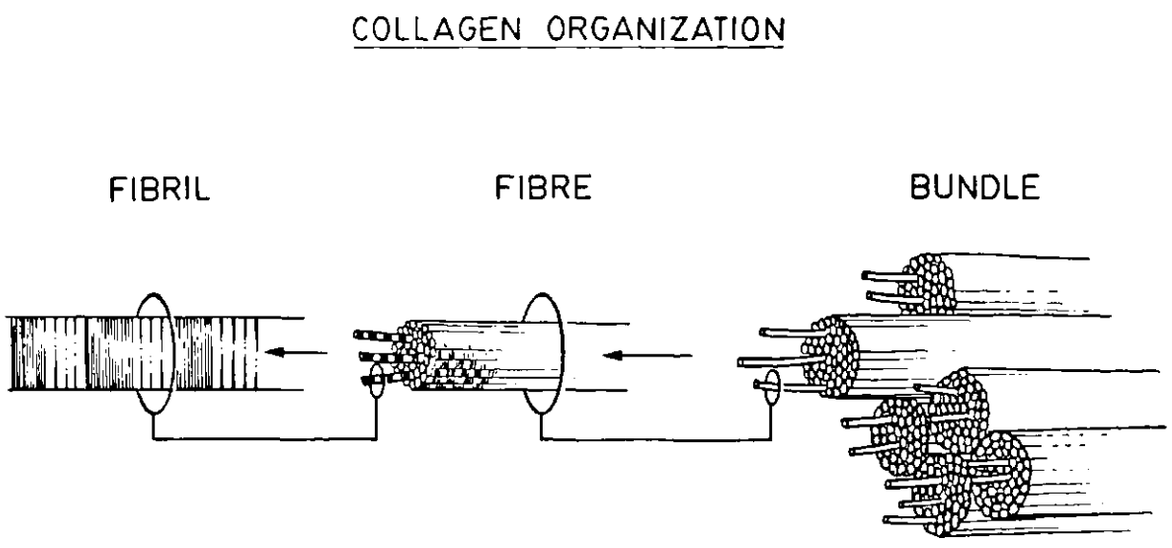

FIGURE 2.7 An illustration of collagen organization shows how a fibril forms a fibre, which forms a bundle.

approximately quarter-staggered tropocollagen molecules (Smith, 1968). (Figure 2.8) This molecule consists of three helical polypeptide α-chains that form a triple helix about 280 nm in length. The staggered alignment of these molecules is responsible for the collagen fibril banding. There are different types of collagen, depending on amino-acid composition and sequence and glycosylation of the hydroxylysine residues. For example, type I collagen fibrils are larger, have fewer hydroxylysine residues, and are less glycosylated than type II fibrils (Buckwalter et al., 1988a).

The existence and maintenance of the matrix of cartilage depends on the chondrocyte. Like other mesenchymal cells, chondrocytes surround themselves with extracellular matrix, and do not normally contact other cells. In addition to the organelles responsible for matrix synthesis, such as the endoplasmic reticulum and Golgi complex, chondrocytes may also contain mitochondria, glycogen, lipid droplets and lysosomes. Rarely they contain intracytoplasmic filaments, microtubules, centrioles and cilia (Ghadially, 1983). Normally these cells are round, with short cell processes. However, chondrocytes in zone I (i.e. adjacent to the joint surface) present oval or elongated profiles. Their nuclei are round (elongated in zone I) and the nucleoli are not prominent. Normally the cells are surrounded by a territorial matrix

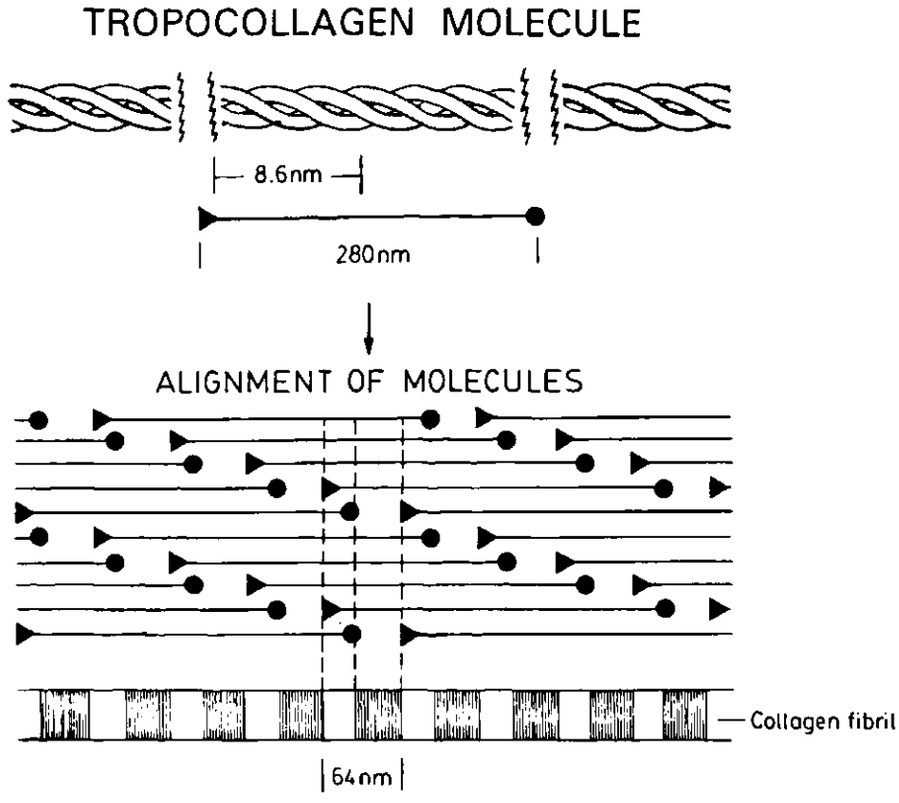

FIGURE 2.8 An illustration of the tropocollagen molecule shows its triple helix structure, and how the alignment of the molecules accounts for the length or period of the bands on the fibril.

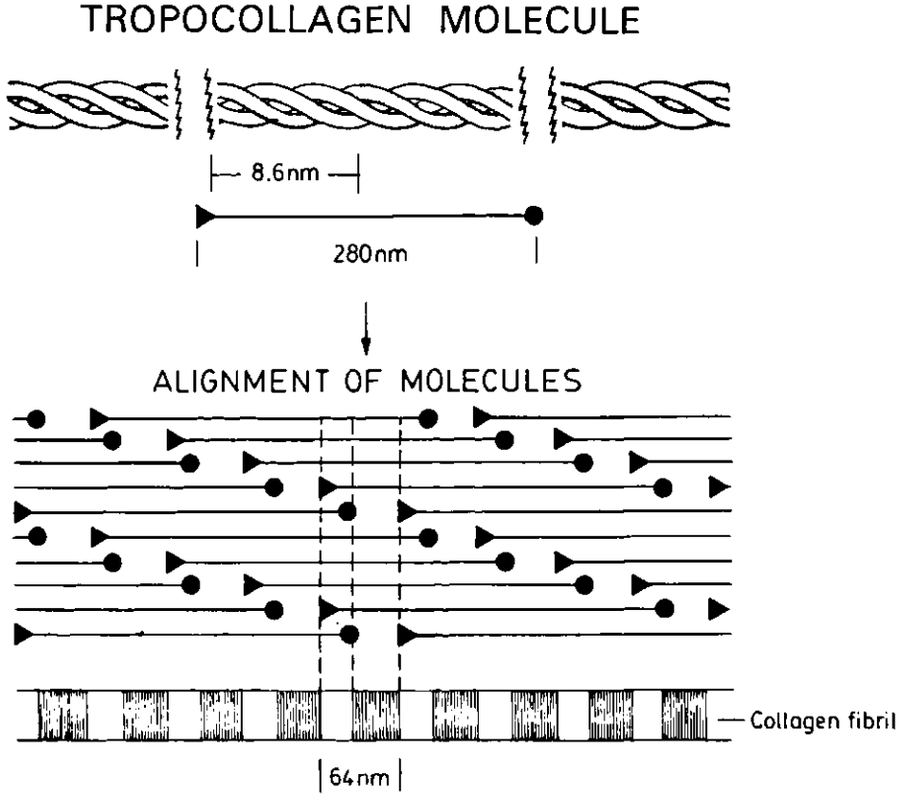

FIGURE 2.8 An illustration of the tropocollagen molecule shows its triple helix structure, and how the alignment of the molecules accounts for the length or period of the bands on the fibril.

that usually contains more fine, short filaments and proteoglycans than the general or interterritorial matrix.

Fibrocartilage differs from hyaline cartilage in several respects. The matrix contains a lower percentage of water and proteoglycans and a higher percentage of collagen fibrils, which are mostly type I (Buckwalter and Cooper, 1987). It usually consists of alternating layers of hyaline cartilage matrix containing chondrocytes and thick layers of dense collagen fibres oriented in a specific direction (Wheater et al., 1979). Elongated, fibroblast-like cells and more plump chondrocyte-like cells occur singly or in a group, surrounded by a fine-textured territorial matrix (Ghadially, 1978). It is generally considered a regressive form of cartilage, since damaged and cultured hyaline articular cartilage dedifferentiates into fibrocartilage (Sokoloff, 1980).

It is unusual to find fibrocartilage on the articular surfaces of healthy joints, but this occurs on the iliac side of the sacroiliac joint (Bowen and Cassidy, 1981), the clavicular side of the sternoclavicular joint (Davies, 1969), and the mandibular condyle of the temporomandibular joint (Bont et al., 1984). Both the sternoclavicular and the temporomandibular joints also contain an intraarticular fibrous meniscus. A small transitional area of fibrocartilage is normally present in synovial joints between the hyaline articular cartilage and the surrounding

synovial membrane (Van Sickle and Kincaid, 1978).

2.2 Embryology

Synovial joints undergo several stages in their development. (Figure 2.9) The mesenchyme blastema skeleton forms as a continuous structure, without separation to differentiate the major anlagen from each other. As the blastema undergoes chondrification, the anlagen separate to create a presumptive joint interzone. Chondrification does not spread across these zones, and the cartilage anlagen are surrounded by a perichondrium (O'Rahilly and Gardner, 1978). The joint interzone is a blastema condensation that gives rise to the joint cavity and articular surfaces. It consists of two dense chondrogenic layers and an intermediate loose layer. The chondrogenic layers are continuous with the perichondrium and are responsible for appositional growth of the adjacent cartilage. The central loose layer merges laterally into the surrounding mesenchyme. The future joint capsule appears as a condensed layer of mesenchyme surrounding the interzone.

The next major event is cavitation of the joint space. (Figure 2.9) Minute cavities appear in the interzone and eventually coalesce to form the joint space. This process quickly expands to firmly establish most joint spaces by ten weeks gestation (O'Rahilly and Gardner, 1978; Ogden and Grogan, 1987). Synovial tissue is formed by the more

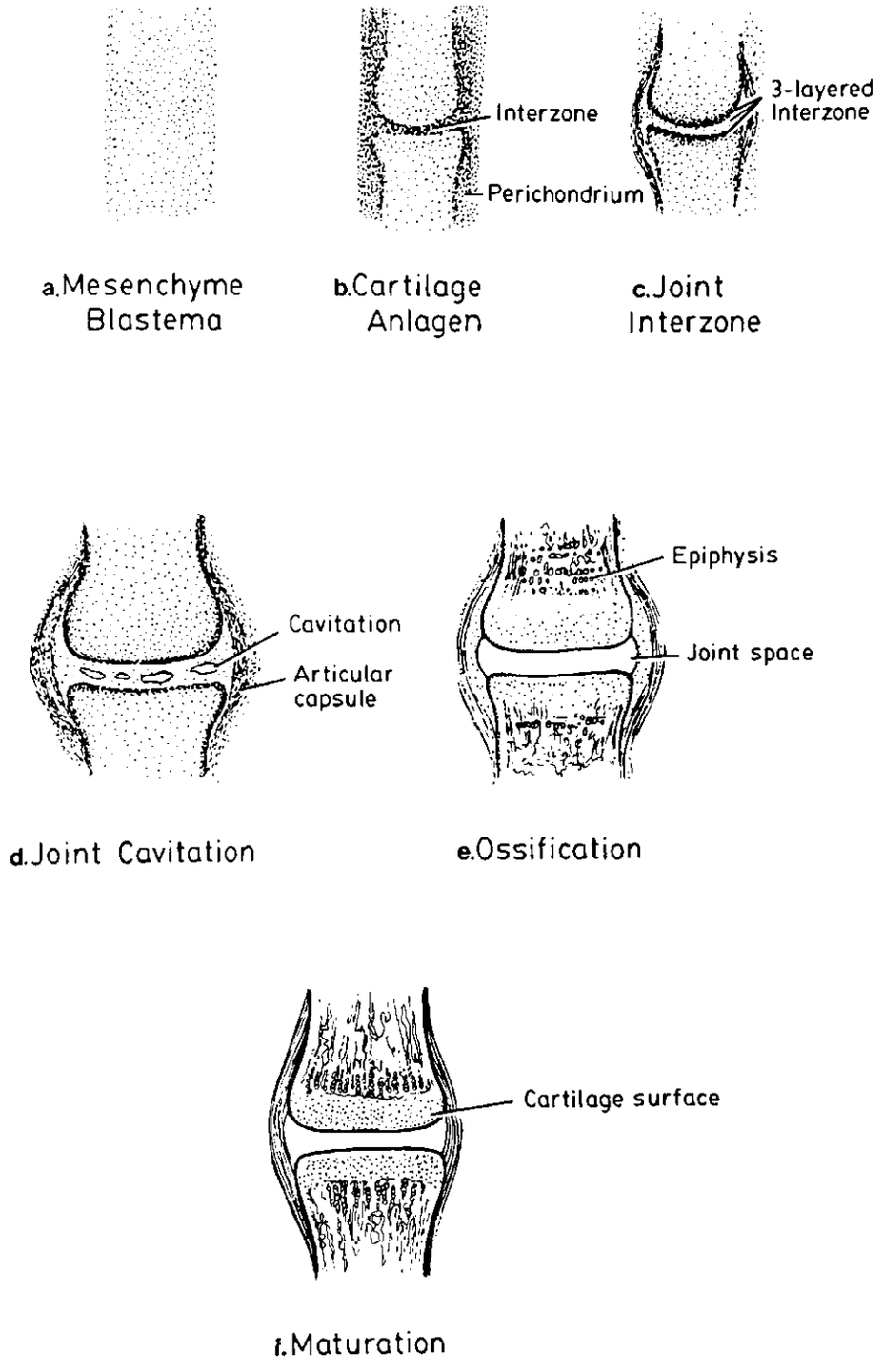

FIGURE 2.9 An illustration of the stages of joint development.

peripheral extensions of the interzone intermediate layer. Predetermined central regions of the anlagen undergo chondrocyte hypertrophy, followed by replacement with bone to form the primary centres of ossification. Secondary centres of ossification develop in the epiphyses in the same manner and grow until they reach the growth plate on one side and the articular cartilage on the other side. (Figure 2.9) This process leaves a hyaline cartilage cap on the articular surface of the bone.

In the sacrum, there are several primary centres of ossification (Davies, 1969; Dihlmann, 1980). Centres for the sacral bodies and each half of the lamina appear between 10 to 12 weeks gestation. The primary centres for the costal elements for the upper three sacral vertebrae appear between six to eight months. These elements mature and unite with the laminae between the second and fifth years of life, then the conjoined elements unite with the centra about the eighth year. The lateral epiphyses of the costal elements grow towards the articular surface of the sacroiliac joint to leave a hyaline cartilage cap. (Figure 2.10)

The three primary ossification centres for the innominate appear at different intervals (Davies, 1969; Dihlmann, 1980). The ilium appears about the eighth week of gestation, making it the first centre to appear in the pelvis. It matures quickly and is quite large by the time

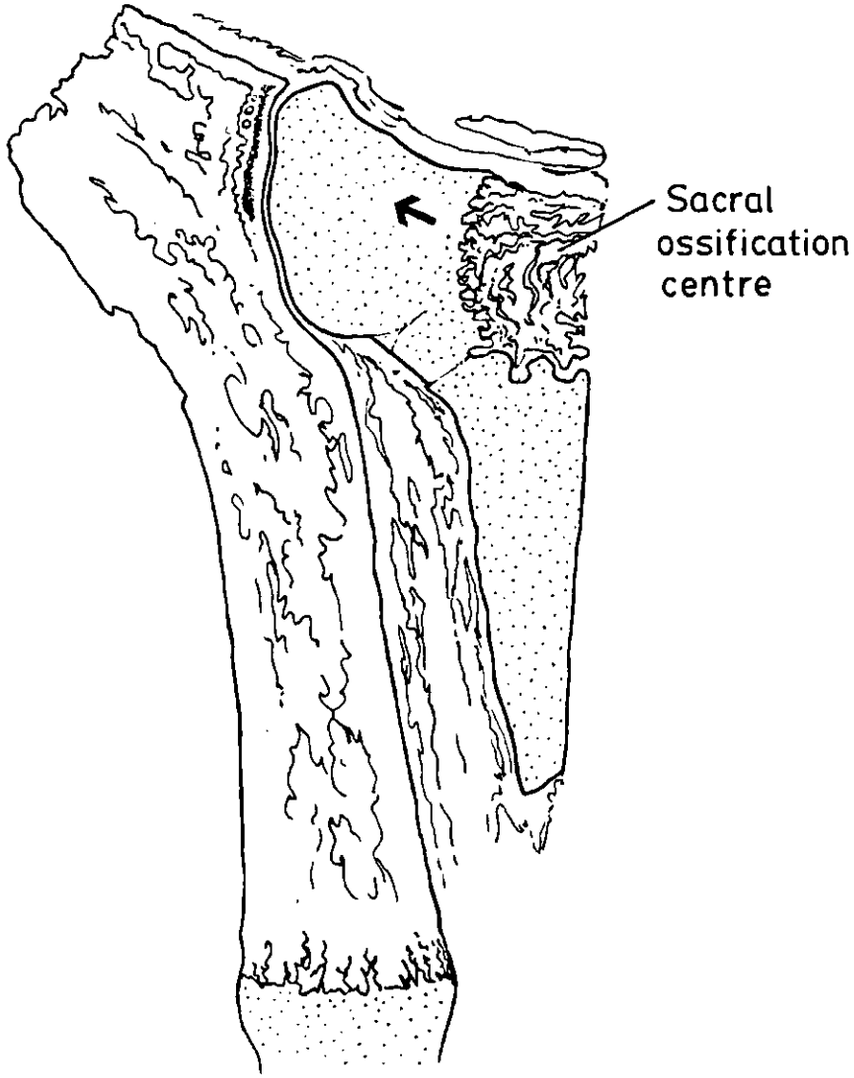

FIGURE 2.10 An illustration of the primary ossification centre in the sacral ala growing toward the surface of the sacroiliac joint (arrow).

the ischium and pubis appear, between the sixteenth and twentieth weeks. (Figure 2.11) At the time of birth, the iliac crest, acetabulum, and much of the ischium and pubis are still cartilage. At seven to eight years of age, the ischium and pubis fuse. Secondary centres appear at puberty, and the remaining bones fuse between the fifteenth and twenty-fifth years.

There have been only a few studies of sacroiliac joint development. The first study was published by Schunke (1938). His observations were made on 35 fetal specimens between eight weeks gestation and term. Cavitation of the sacroiliac joint first appeared in a ten-week specimen. It began simultaneously at several places between the cartilage anlagen of the sacrum and ilium and proceeded slowly from the most cranial part of the joint to the most caudal region. The process was not completed until term. Intraarticular bands were demonstrated, attaching the two surfaces throughout fetal life. He described them as resembling degenerate, hyalinized fibrocartilage. With respect to the auricular cartilage, he described fibrocartilage on the iliac side at the time of cavitation, but did not comment on its origin. However, he also stated that the iliac cartilage could be hyaline, and that the sacral cartilage could be hyaline or fibrocartilage. Overall, he was not sure about the histology of the surfaces, and he stated that "in most specimens it was

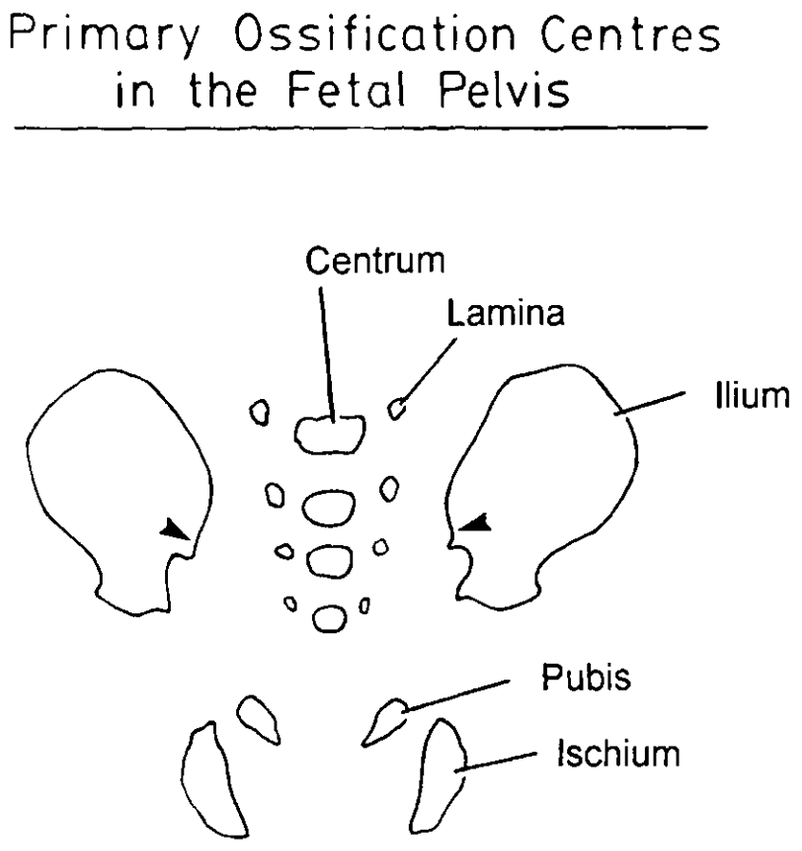

FIGURE 2.11 An illustration of the primary ossification centres that are visible in the second trimester fetus. The ilium is quite large and is ossified adjacent to the sacroiliac joints (arrowheads).

difficult to tell, even at term, whether the cartilage was fibrous or hyaline."

In their series of 40 sacroiliac autopsy specimens, Bowen and Cassidy (1981) included gross and microscopic observations on seven fetal specimens, all over two months gestational age. All of the fetal joints had well-formed articular surfaces, with a thin anterior capsule and ligament. The articular surfaces were smooth, flat, and mobile. The iliac surface appeared blue, dull, and striated, while the sacral surface was smooth and clear. A thin, fibrous, intraarticular septum was observed in most specimens. In all cases, the iliac cartilage matrix was fibrous and the sacral matrix was hyaline.

In another study, Walker (1986) examined 36 fetal sacroiliac joints, aged 12 to 40 weeks gestation. She did not observe joint cavitation until 16 weeks gestation, and the process was not completed until 34 weeks gestation. Intraarticular fibrous bands were observed, and in all cases, the iliac side was fibrocartilage and the sacral side was hyaline cartilage.

Ishimine (1989) included 11 fetal specimens in his histological study of sacroiliac joints. He also described intraarticular fibrous bands, but claimed that both the sacral and iliac cartilages are hyaline. However, the three fetal micrographs that he published show a thick layer of dense fibrous tissue covering the chondrocytes on

the iliac side of the joint.

The only other study of sacroiliac development was published by Salsabili and Hogg (1991). In 13 fetal specimens, aged seven to 22 weeks gestation, they described the early development of the joint. Observations were made on the three-layered joint interzone and the cartilage anlagen of the sacrum and ilium. Cavitation was observed to begin in a 10 week specimen in the cranial region of the joint. The process was observed to spread caudally, to include the entire joint by 22 weeks gestation. Fibrous septa were seen between the joint surfaces after cavitation. They described both sides of the joint as hyaline cartilage, but their micrographs show fibrocartilage on the iliac side. However, they did comment on a thick layer of fibrous tissue covering the iliac surface, and they stated that it could develop into fibrocartilage.

2.3 Ageing and Degeneration

Studies by Sashin (1930), Macdonald and Hunt (1952), Resnick et al. (1975), Bowen and Cassidy (1981), Walker (1986), Ishimine (1989), and Vleeming et al. (1990a) have established that the sacroiliac joint undergoes early degenerative changes. Some suggest that the process begins some time before the age of 50 years (Rsenick et al, 1975; Walker, 1986). Others suggest that it starts as early as

30 years of age (Sashin, 1930; MacDonald and Hunt, 1952; Ishimine, 1989). Two studies have described degenerative changes beginning in the iliac cartilage in teenage specimens (Carter and Loewi, 1962; Bowen and Cassidy, 1981).

A spectrum of macroscopic changes have been described. These include yellowing, roughening, splitting, flaking, sloughing, erosion, fibrosis, and fusion of the joint surfaces. The consensus is that these changes are more marked on the iliac side of the joint and occur more commonly in males (Bernard and Cassidy, 1991).

There is less agreement about the incidence of joint fusion. Brooke (1924) stated that bony ankylosis occurred in 37% of the 105 males specimens he examined and in none of the 105 female joints examined. The proportion of ankylosed joints in subjects over 50 years of age was 76%, and no joint under this age was affected. In a study of 257 fresh and macerated pelves, Sashin (1930) found bony ankylosis in 60% of male and 14% of female joints up to the age of 59 years. In the 103 specimens older than 59 years, most of the males were affected and about one quarter of the females were affected. Ishimine (1989) reported fusion of the two surfaces in 24% of 27 adults over the age of thirty. However, MacDonald and Hunt (1952) observed two cases of bony ankylosis in 42 specimens over 50 years of age, and one was due to ankylosing spondylitis. Bowen and

Cassidy (1981) observed only one case of bony fusion in 12 cases over 50 years of age, and Walker (1986) did not find any in her series of 15 adults between 49 and 84 years of age.

The studies by Resnick et al. (1975) and Stewart (1984) offer an explanation for the various rates of sacroiliac fusion. In the former study, 46 male sacroiliac joints between the ages of 24 to 80 years were radiographed and dissected. Only two of these joints were fused. However, 10 had bridging osteophytes or para-articular ankylosis. In the latter study, 701 dried skeletons over 29 years of age were carefully examined. Internal ankylosis was present in only three specimens, but para-articular ankylosis occurred in a much higher percentage. It is obvious from the above results that bony fusion of the articular surfaces is rare, and studies that are confined to this area have a low incidence of synostosis. However, in those studies that examine the para-articular region, there is a higher incidence of fusion. A more recent study found that para-articular synostosis occurs primarily along the ventral border of the cranial limb and that fibrous fusion occurs more commonly in the caudal limb (Valojerdy et al., 1989). Although exact figures are not available, most studies agree that fibrous fusion of the joint is very common in older specimens (Cassidy, 1992). In all cases, both fibrous and bony synostosis are more

common in males.

A number of studies have concentrated on microscopic age-related and degenerative changes in the sacroiliac joint cartilage. In Sashin's (1930) series, microscopic evidence of degenerative change was evident in cases over 30 years of age. He described surface fibrillation and chondrocyte clumping as occurring in all sections examined, and that these changes were more marked in the males. Fibrous replacement of cartilage was the rule in his cases over 60 years of age. MacDonald and Hunt (1952) found mild fibrillation and erosion of the articular cartilage in cases aged 30 to 39 years of age. These changes became moderate in cases 40 to 49 years of age and severe in cases over 50 years of age.

Carter and Loewi (1962) reported on the histology of the sacroiliac joints in nine pelves, 21 years of age and younger. They were primarily interested in the pathology of Still's disease (juvenile rheumatoid arthritis that can affect the sacroiliac joints), and compared two cases with it to seven controls. However, they did describe iliac cartilage splitting and chondrocyte clumping in several non-arthritic teenage specimens.

Resnick et al. (1975) graded degenerative changes in the cartilage of 40 specimens over 50 years of age and six specimens under 50 years of age. An increasing degree of degeneration was associated with increasing age in all of

the specimens. In the younger specimens the cartilage was fibrillated, but in the cases over 50 years old there was marked erosion. These changes were more common in the iliac cartilage. Four of their 18 cases over 70 years of age had undergone cartilaginous fusion.

Bowen and Cassidy (1981) studied histological changes in the sacroiliac joints from fetal life onward in 40 autopsy specimens. They noted fibrillation and crevice formation in the iliac cartilage in some teenage specimens. These changes, along with iliac chondrocyte clumping, became more pronounced during the third and fourth decades of life. Similar changes did not occur on the sacral side until the fifth and sixth decades. By this time, the iliac cartilage was often eroded and covered with amorphous debris. Iliac subchondral bone sclerosis was common in these specimens. Walker (1986) found fibrillation, crevice formation, and erosion of both cartilage surfaces in 12 of her 18 specimens, all over 48 years of age.

The distinction between the normal ageing process and degenerative arthrosis can be difficult. Regions of fraying and splitting (i.e. fibrillation) normally develop at the surface of all synovial joints, and can be seen as early as the second decade (Meachim and Emery, 1973). This "wear and tear" phenomenon is usually asymptomatic, but can be the precursor for more destructive changes associated with symptomatic osteoarthrosis.

It has been established that the water content of osteoarthrotic cartilage is increased, while that of ageing cartilage is decreased (Hamerman, 1989). When the collagen network of the articular surface becomes fibrillated, water absorption may occur (Mankin and Treadwell, 1986). This causes dilution and diffusion of the matrix proteoglycans, leading to a functional deterioration in the ability of the cartilage to withstand mechanical stress. This increases the contact pressure on the subchondral bone plate, which leads to remodeling and stiffening of the plate and increased pressure on the cartilage above (Radin and Rose, 1986). In turn, the cartilage is subjected to stresses that can result in further splitting and crevice formation.

In response to the breakdown in the cartilage matrix, chondrocytes proliferate and form clusters. The cells increase their proteoglycan and collagen output. This reparative process produces an intense metachromatic staining of the surrounding matrix with safranin O. Since there is an increase in protein synthesis, the cells often contain a well-developed endoplasmic reticulum, which is frequently dilated (Ghadially, 1983). Unfortunately, these newly synthesized proteoglycans are smaller, fragmented, and less aggregated. (Figure 2.12) They are more easily extracted from the matrix, and more susceptible to degradative enzymes (Roughley, 1987). The newly synthesized collagen is thicker and may contain traces of

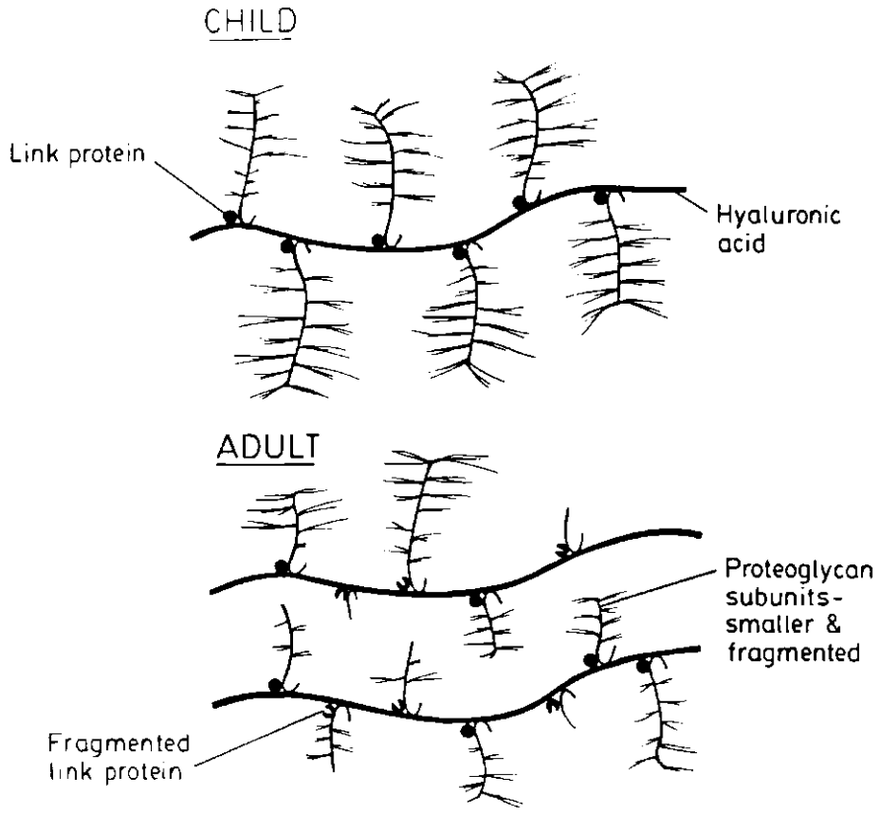

FIGURE 2.12 An illustration showing the effect of ageing on the proteoglycan aggregate. In the adult, the proteoglycan subunits and link proteins are smaller and fragmented.

type I and glycosylated variants of type II fibres (Nimni, 1983). These new species of collagens and proteoglycans do not supply the strength or stiffness of their healthy counterparts.

Eventually, further damage results in the production of degradative enzymes that attack both matrix collagen and proteoglycans (Ehrlich et al., 1986). Joint detritus results in synovitis and the release of collagenase and other hydrolytic enzymes from synovial cells and macrophages (Brandt and Slowman-Kovacs, 1986). In addition, the chondrocytes produce proteoglycan-degrading lysosomal enzymes and latent metalloproteinases (Roughley and Mort, 1986). This further insult leads to chondrocyte degeneration and necrosis. The cells become laden with lipid, glycogen, and intracytoplasmic filaments (Ghadially, 1983). In situ necrosis of chondrocytes occurs, leaving lipidic debris in the matrix.

2.4 Comparative Anatomy

There are major differences between the bipedal human pelvis and that of the quadrupeds. These include a ninety degree rotation to the upright posture, shortening of the ilium and ischium, broadening and forward rotation of the ilium, and broadening of the pelvic ring (Napier, 1967). These adaptations enable the hip musculature to stabilize the trunk during the act of biped walking (Lovejoy, 1988).

The sacroiliac joints are more horizontally oriented in the quadruped, with the convex surface facing in a cephalad direction. (Figure 2.13) In the domestic species of quadrupeds, both the pubis and ischium participate in the symphyseal joint. This joint tends to ossify with advancing age, but the process is variable between species (Dyce et al., 1987).

The sacroiliac joints have not received much attention in the veterinary literature, with one exception. In the horse, sacroiliac subluxation or strain has been implicated as a cause of poor performance and lameness (Herrod-Taylor, 1967; Rooney et al. 1977; Jeffcott et al., 1985). This is particularly true in the high-speed trotter and pacer, where counter-rotation of the pelvis places more stress on the sacroiliac joints (Rooney, 1977). (Figure 2.14) These horses increase their speed by increasing the length of their stride, placing more stress on the sacroiliac joints. In contrast, a galloping horse protracts and retracts the limbs together. This type of gait causes flexion and extension at the lumbosacral level and less stress on the sacroiliac joints. Interest in this problem is a direct result of the economics of horse racing.

Herrod-Taylor (1967) was the first to implicate pelvic subluxation as a cause for lameness in the horse. He described a chiropractic manipulation to treat the condition. Rooney et al. (1977) examined the sacroiliac

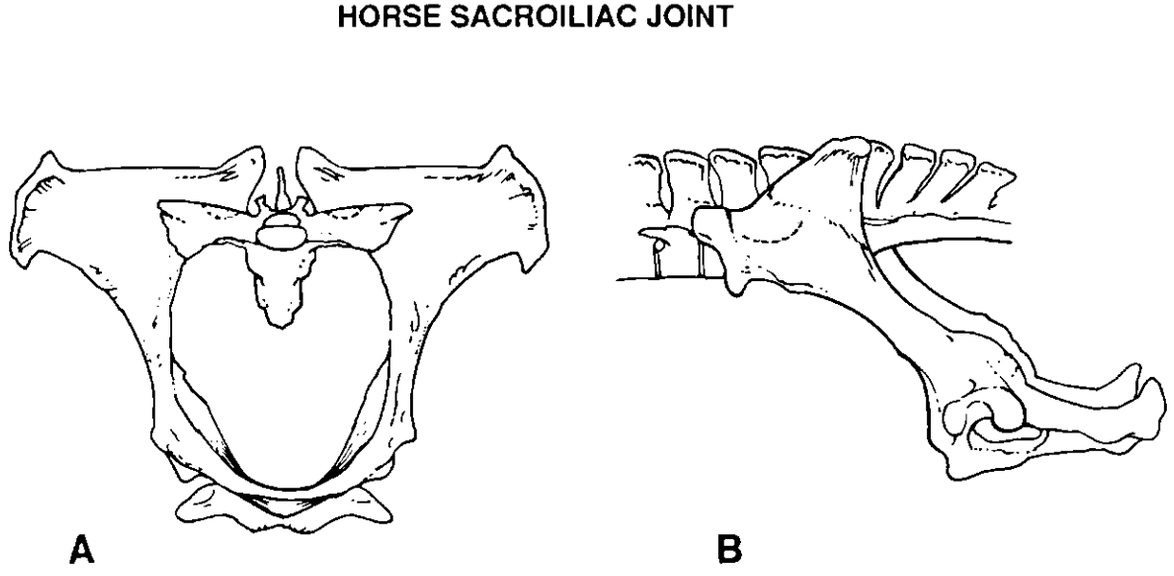

Figure 2.13 The quadruped pelvis and sacroiliac joints are oriented horizontally. A. The pelvic inlet view illustrates the position of the sacroiliac joints in the horse. B. A lateral illustration shows the orientation of the sacroiliac joint.

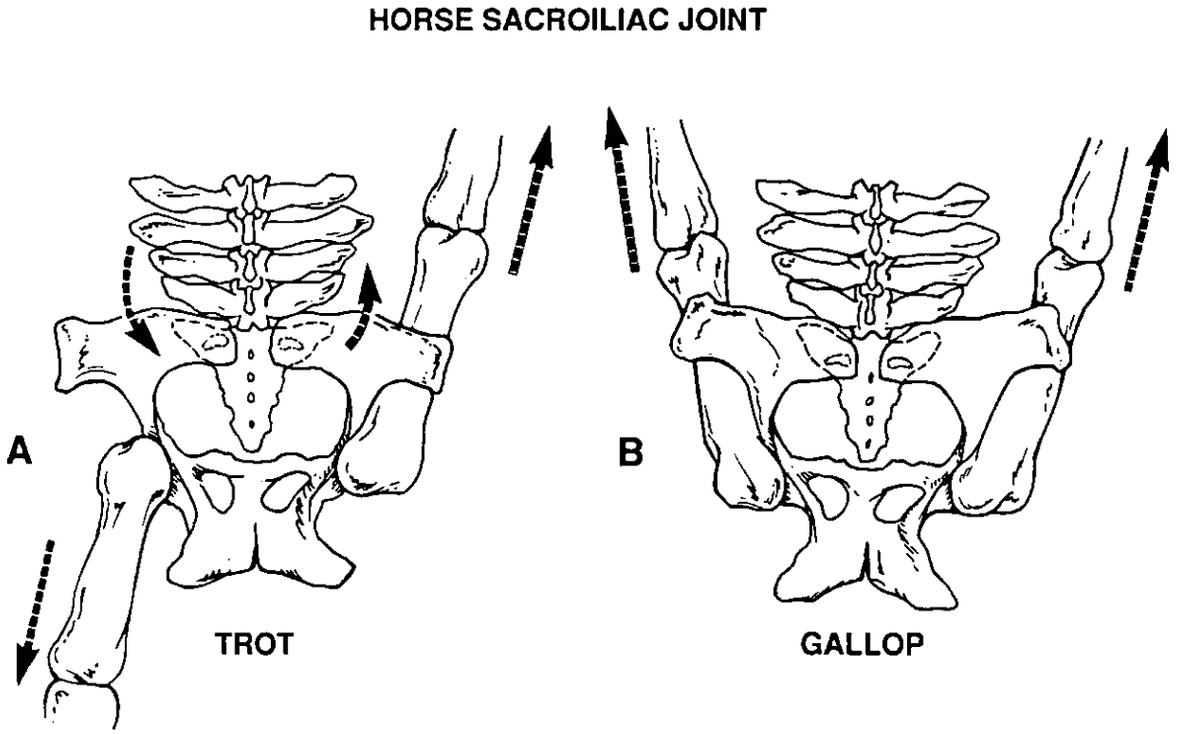

Figure 2.14 A. This illustration of a trotting horse's pelvis shows the counter-rotation forces at the sacroiliac joints (arrows). B. When a horse gallops, there is more movement at the lumbosacral level and less stress on the sacroiliac joints.

joints during postmortems of six cases of hindquarter lameness in pace-setting Thoroughbred horses. They found tearing and haemorrhage in the sacroiliac joints of two acute cases and stretching of the sacroiliac ligaments with cranio-dorsal luxation of the sacrum in the four chronic cases.

In a series of 55 postmortem examinations of the sacroiliac joint, Rooney (1977) noted a variable size and shape of the joint. He also observed that yellowish-brown discoloration of the joint was more common in Standardbreds (77% of 22 cases aged one to over 10 years), than in Thoroughbreds (42% of 33 cases aged two to over 10 years). He concluded that sacroiliac arthrosis is more common in Standardbreds. Jeffcott et al. (1985) performed postmortem examination of the sacroiliac joints in 11 horses with long-standing poor performance due to low-grade hindlimb lameness. In two cases, there was severe degeneration of the articular cartilage. In the other nine cases, there were osteophytic extensions of the joint surface. They interpreted this remodelling of the surface as an attempt to stabilize the sacroiliac joint.

The first detailed anatomical description of the sacroiliac joint in the horse was provided by Dalin and Jeffcott (1986a, 1986b) and Ekman et al. (1986). This group of researchers examined 82 sacroiliac joints from 41 horses spanning late fetal life to 14 years of age. The

majority of joint surfaces were flat and angled at 30° to the horizontal plane. Even though the joints were relatively immobile, there were no cases of fusion. Their size and shape varied, but many were sock-shaped with the convex border facing caudally and ventrally. The surface area of the articulation varied from one cm^2 to 17.8 cm^2, depending on age. In the adult, the joint was up to nine cm long and 4.6 cm wide. There were no apparent sex or breed differences. The iliac side was covered with fibrocartilage and the sacral side with hyaline cartilage. Degenerative changes were first observed on the iliac side of the joint as early as one year of age. After two years of age, both surfaces were involved in all cases, but the changes were more advanced on the iliac side of the joint.

In an attempt to use the dog as a model to study the human sacroiliac joint, Gregory et al. (1986) studied mobility and histology in the sacroiliac joints of 10 dogs from 1.5 to 10 years of age. A rotational force representing 25% of the dog's body weight was applied to the sacrum in the freshly dissected, but intact pelves. The median range of motion was 7° (95% confidence interval of 4-13°), with a median of 3° flexion and 4° extension. This mobility was constant regardless of age or sex. They described both surfaces of the joint as hyaline cartilage. Degenerative changes were present as early as five months of age, consisting of fibrillation and chondrocyte

clustering. One six-year-old dog had a partial synchondrosis of one joint. According to the authors, degenerative changes were common, occurred at an early age, and affected both sides of the joint equally.

2.5 Objectives of the Study

Certainly, there is some controversy about the anatomy of the sacroiliac joint. The development of the sacroiliac joint has not been adequately studied. Differences between the two cartilages might be due to developmental factors. How is the iliac cartilage different from the sacral cartilage, and what are the functional implications of this difference? At what age does the cartilage develop degenerative changes and how quickly do they progress? With the exception of one study on the horse (Dalin and Jeffcott, 1986a&b; Ekman et al., 1986) and one study of the dog (Gregory et al., 1986) the comparative anatomy of the sacroiliac joint has not been adequately studied. There are no studies on the ultrastructure of the sacroiliac joint.

The objectives of this study are to:

(1) investigate the development of the sacroiliac joint, with the aim to observe any differences between the two sides of the joint,

(2) study the ultrastructure of the articular cartilage, with the aim to accurately classify the

cartilage types,

(3) document the prevalence and age of onset of degenerative changes in the articular cartilage,

(4) study the comparative anatomy of the sacroiliac joint in several species, and

(5) compare the joint angle and relative lengths of the two limbs of the joint between species.

3. MATERIALS AND METHODS

3.1 Human Autopsy Specimens

Specimens of the articular surfaces of the sacroiliac joint were obtained at 108 autopsies. Both right and left sides were sampled in 78 cases, and one side was sampled in 30 cases. A total of 186 sacroiliac joints were studied altogether.

Of the 108 cases sampled, 62 were male and 22 were female. In the other 24 cases, it was not possible to identify the sex, since they were all under 15 weeks gestational age. The youngest specimen was five weeks gestational age and the oldest was 87 years. Specimens were selected by age in order to obtain adequate representation from embryonic life through to the eighth decade. (Figure 3.1) Unfortunately, it was not possible to obtain female specimens between the ages of 23 and 60 years of age because of a lack of autopsy cases in this group. The cause of death was recorded in all cases. (Appendix A)

3.2 Animal Autopsy Specimens

Both sacroiliac joints were removed from 115 animals. There were 44 bovine, 25 equine, 23 porcine, and 23 canine cases. A total of 230 sacroiliac joints was included in the study. Of the 44 bovine cases, 35 were female and nine were male. There were 16 male and nine female equine cases, 19 female and four male porcine cases, and 14 female and nine male canine cases. In all cases, an attempt was made to

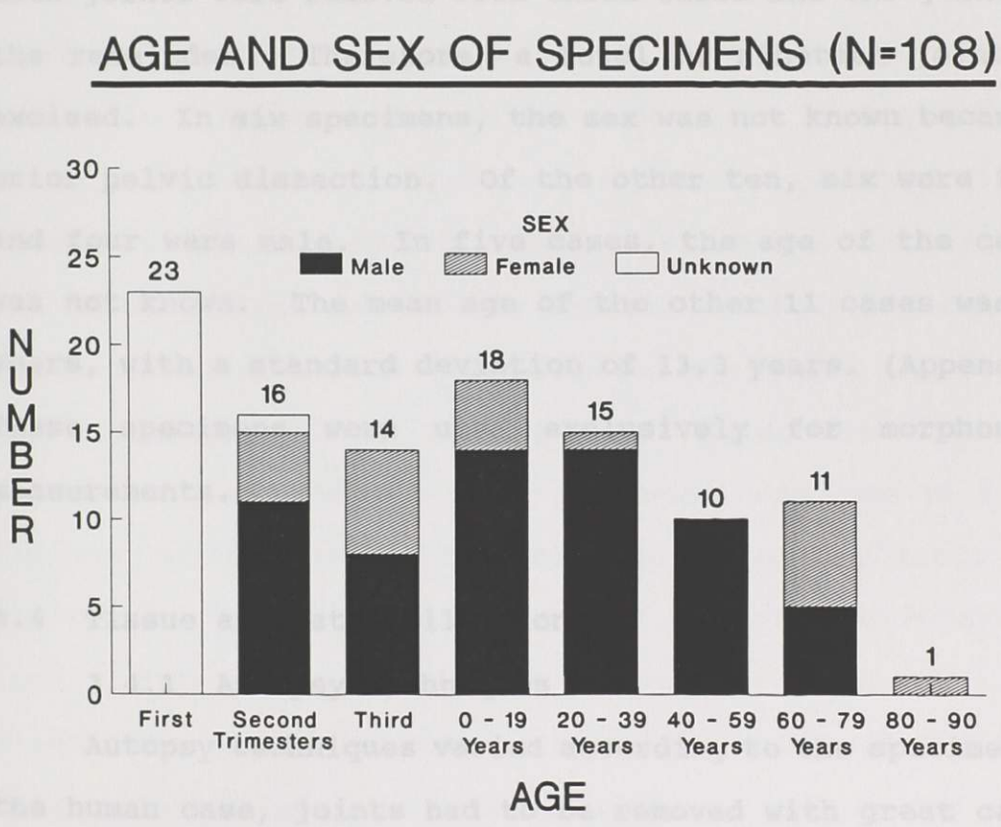

FIGURE 3.1 The age and sex of the human autopsy specimens is illustrated in this figure.

obtain specimens from all age groups. The cause of death was recorded for each case that underwent an autopsy. The other cases were euthanized for the Society for the Prevention of Cruelty to Animals. (Appendices B, C, D, and E)

3.3 Human Cadaveric Specimens

Sacroiliac joints were removed from sixteen embalmed cadaveric pelves from the gross anatomy teaching laboratory. Both joints were removed from three cases and one joint from the remainder. Therefore, a total of nineteen joints was excised. In six specimens, the sex was not known because of prior pelvic dissection. Of the other ten, six were female and four were male. In five cases, the age of the cadaver was not known. The mean age of the other 11 cases was 70.2 years, with a standard deviation of 13.3 years. (Appendix F) These specimens were used exclusively for morphometric measurements.

3.4 Tissue and Data Collection

3.4.1 Autopsy Techniques

Autopsy techniques varied according to the specimen. In the human case, joints had to be removed with great care in order to reconstruct the pelvis after the autopsy. However, reconstruction was not necessary for human fetal or cadaveric specimens. In the former case, the fetus is not usually reconstructed after autopsy, and in the latter case, the

remains are incinerated after use. Reconstruction is not done after animal autopsies. In all cases, permission to remove specimens was obtained from the pathologist in charge of the case.

In human and animal autopsy cases where pelvic reconstruction was not necessary, the entire pelvis was dissected, and in most cases, both sacroiliac joints were removed. With animal specimens, a coin was flipped to determine which joint (right for heads and left for tails) would be studied microscopically. The opposite joint was stored in a freezer and subjected to gross photography at a later time. In human cases where pelvic reconstruction was necessary, the sacroiliac joint(s) was removed at the end of the autopsy, from an anterior approach. After evisceration, the psoas major muscle was dissected away from the front of the sacroiliac joint. (Figure 3.2) After identifying the anterior joint margins, curved scissors were used to dissect tissues behind the joint, from the greater sciatic notch inferiorly to the iliac crest and sacral ala superiorly. Once a path was cleared from behind the joint, two Gigli wires were passed behind and on either side of the joint. This allowed for two cuts on either side of the joint. (Figure 3.3) A three to four cm block containing iliac and sacral bone with the interposed joint was removed. In order to stabilize the pelvic ring, three Steinmann pins were hammered through the greater trochanter, femoral neck,

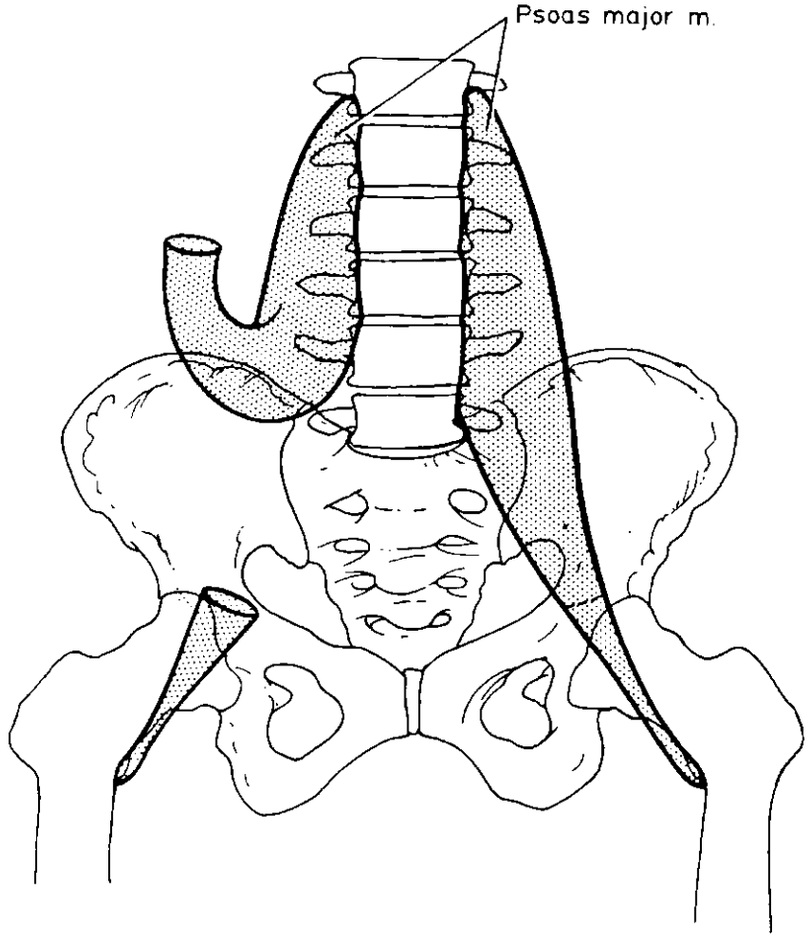

FIGURE 3.2 The psoas muscle group was dissected and reflected away from the surface of the sacroiliac joint, prior to its removal.

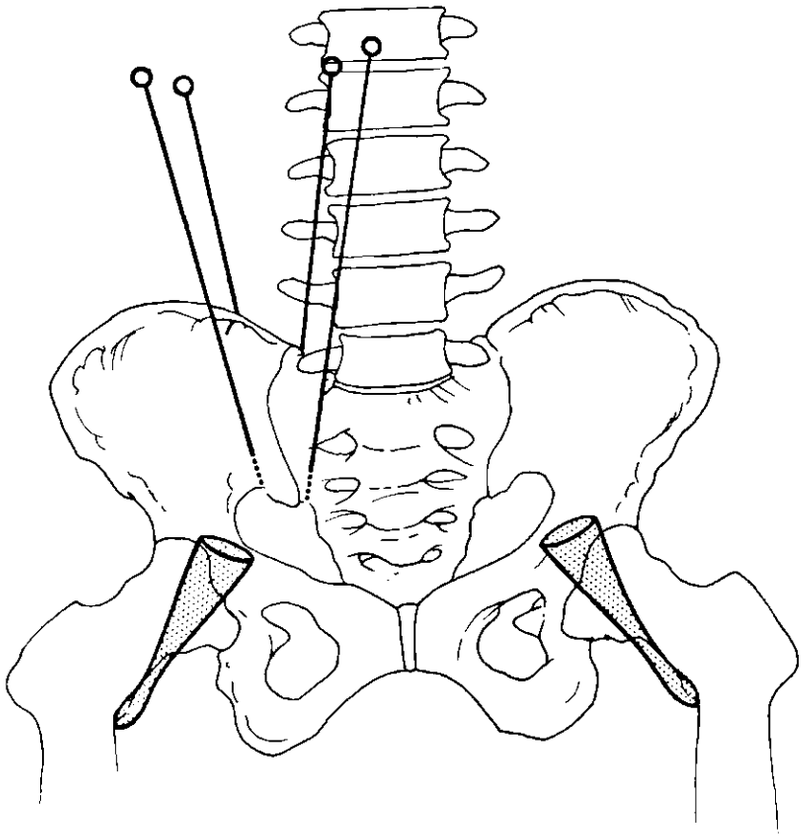

FIGURE 3.3 Gigli wires were passed behind the sacroiliac joint and the entire joint was removed as illustrated.

femoral head, and acetabulum to the sacrum and L5 vertebral body. This secured the hip to the spine.

After removing the sacroiliac joint, an incision was made through the anterior ligament and capsule. This allowed the joint to be gently pried open like a book, with the interosseous ligament acting as the binding. During this process, the cartilage surfaces were cleaned and kept moist with normal saline. Care was taken not to touch the surfaces, or to allow them to dry.

Specimens for photography were placed in plastic bags and either photographed within the hour or frozen and photographed at a later date. Some of the photographed human specimens were later processed for light microscopy. In the case of animals, one side was always saved for photography, while the opposite side was processed for light microscopy only. Specimens for light microscopy were trimmed and placed in 10% neutral buffered formalin. In the human specimens, small areas of the cartilage surface were excised from the underlying bone for transmission electron microscopy. This tissue was trimmed into one cubic millimetre tissue blocks and placed into cold 2% glutaraldehyde. The joint surface region of the block was marked with eosin, in order to properly orient the specimen during processing. In some of the human specimens, an area of articular cartilage and its subchondral bone was excised for scanning electron microscopy. This tissue was trimmed and placed in cold 2%

glutaraldehyde. Care was taken to sample different areas of the joint surface for transmission and scanning electron microscopy.

3.4.2 Gross Photography

A limited number of human specimens were photographed. All animal specimens had one joint photographed. In most cases, it was necessary to freeze the specimens and photograph them at a later time. Therefore, human specimens processed for electron microscopy could not be photographed. Those human specimens that were frozen, were later processed for light microscopy, after they were photographed. In total, 20 human specimens were photographed in this manner. In all but one case, both right and left joints were removed, and one side was saved for photography while the other side was processed for microscopy immediately after removal. In the case of animal specimens, a coin was flipped to see which side would be saved for photography, and the other side was processed for examination under the light microscope.

Specimens were thawed at room temperature for one hour and then photographed on a back-lite stage, under a main light and a fill light to reduce shadows. Photographs were taken with a 35 mm Leicaflex camera and a 90 mm lens with bellows. Kodak EPR ASA 100 daylight professional film was used for colour slides, and Ilford Pan-F ASA 50 film was used for black and white prints. In some cases, black and white

prints were produced from colour slides by rephotographing the slide onto black and white film. After being photographed, the specimens were placed in 10% neutral buffered formalin.

3.4.3 Morphometric Technique

Nineteen human cadaveric sacroiliac joints, 19 bovine autopsy joints, 16 canine autopsy joints, and 13 equine autopsy joints were subjected to morphometric comparison. Both the sacral and iliac surfaces were studied. None of these specimens were used for microscopic study.

In each case, the joint was opened anteriorly and dissected apart. The iliac and sacral surfaces were studied separately. Each surface was pushed into a plasticine mould, to create an imprint of the joint. All imprints were analyzed using the method of Ohba (1985), which is based on the technique developed by Weisl (1954). (Figure 3.4)

1. A straight-edge ruler was placed against the posterior aspect of the cephalad and caudal limbs of the joint, and these two points were marked by pins as points A and B.
2. Using a right-angled ruler, the most superior and inferior aspects of the cephalad and caudal limbs were identified with pins as points C and D. The right angles were labelled E superiorly and F inferiorly.
3. A square was completed around the joint by placing a line against the anterior aspect of the joint margin,

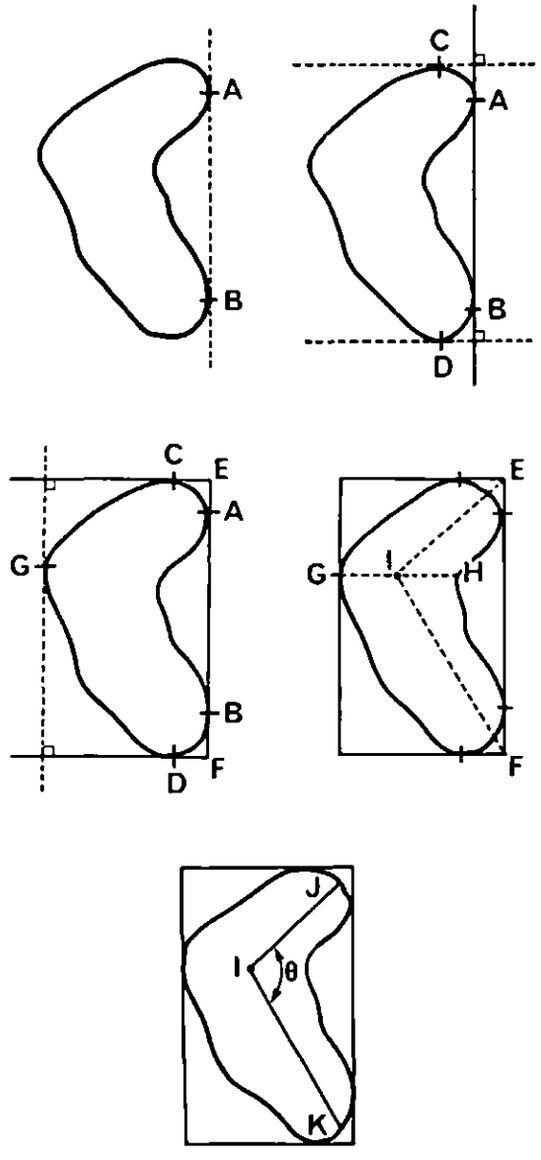

FIGURE 3.4 The method for measuring the cephalad (J-I) and caudal (K-I) limbs of the sacroiliac joint is illustrated in this figure. The angle of the sacroiliac joint is labelled θ. (see text for detailed explanation)

perpendicular to the line EF. The point where this line intersects with the anterior joint margin was identified and labelled with a pin as point G.

4. Using Line EF as a reference, the most anterior aspect of the posterior joint margin was located and labelled with a pin as point H.

5. A point midway between points G and H was identified and labelled with a pin as point I.

6. Two points were identified on the cephalad and caudal limbs of the joint. Point J was identified and labelled with a pin as the point were the line IE crosses the joint margin of the cephalad limb. Point K was identified and labelled with a pin as the point were the line IF crosses the joint margin of the caudal limb.

7. The cephalad (line JI) and caudal (line KI) limbs of both surfaces (e.g. iliac are JI_i and KI_i, while sacral are JI_s and KI_s) were measured on each specimen. The mean of the two values (e.g. $[JI_s + JI_i] \div 2 = JI_m$ and $[KI_s + KI_i] \div 2 = KI_m$) was used as an estimation of the length of the two limbs in each case. A ratio of the mean caudal length over the mean cephalad length (e.g. $[KI_m + JI_m] \div 2 = CCR$) was calculated for each specimen so that comparisons could be made between species. (Appendices F-I)

8. The Joint angle JIK was measured with a protractor and labelled θ_s on the sacral surface and θ_i on the iliac surface. The mean of these two measurements (e.g. $[\theta_s + \theta_i] \div 2 = \theta_m$)

was used as an estimation of the angle formed by the cephalad and caudal limbs of the joint.

3.5 Processing of Tissues

Most of the human sacroiliac joint specimens were processed for light microscopy. In addition, some specimens were processed for both transmission and scanning electron microscopy. (Figure 3.5) In the case of animal specimens, both left and right sacroiliac joints were removed at autopsy. Depending on a coin toss (heads for histology on the right side and tails for histology on the left side) one side was always processed for light microscopy. The other side was photographed and studied morphometrically in some cases. None of the animal specimens were processed for ultrastructural examination. It was not possible to sample both sides in all of the human autopsies.

3.5.1 Light Microscopy

Tissue fixation was achieved in a solution of 10% neutral-buffered formalin for a minimum of 48 hours. Following fixation, specimens were decalcified in Kristensen's Decalcifying Fluid (Lillie, 1965). (Appendix J) Following decalcification, tissues were further trimmed and then processed in an autotechnicon, on a 24-hour paraffin-processing schedule. During the cycle, the tissues were dehydrated by graded changes of ethyl alcohol, consisting of

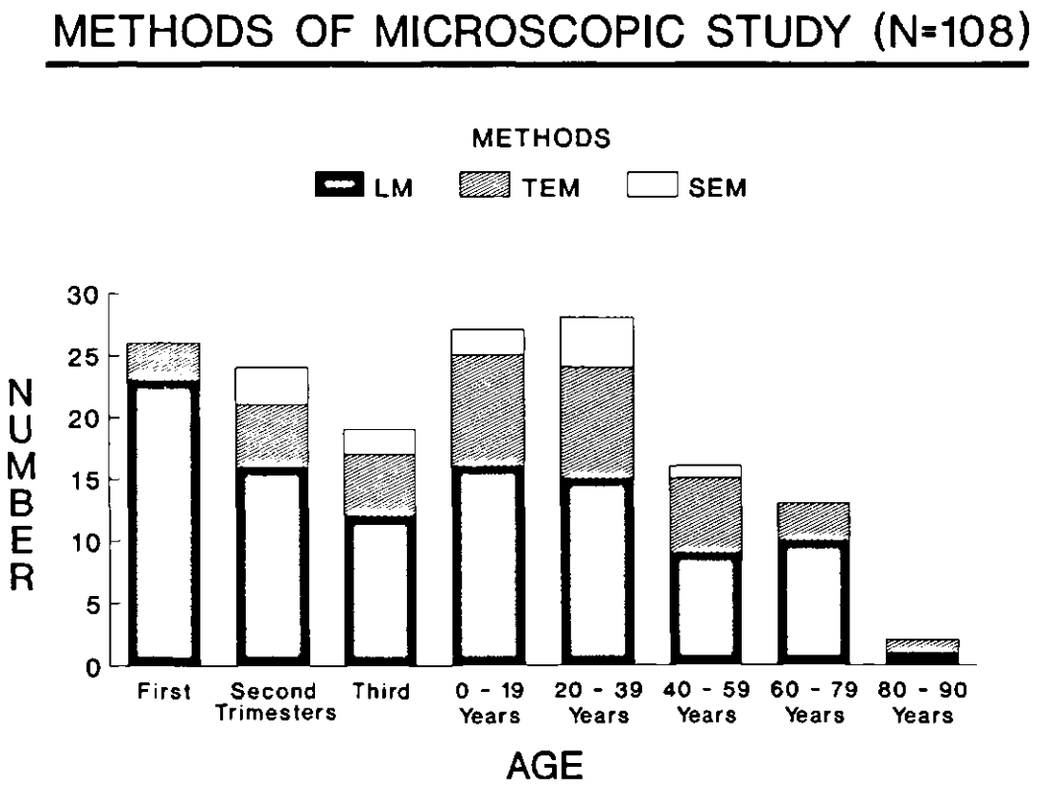

FIGURE 3.5 The methods of microscopic examination are illustrated in this figure.

two hours in each of 70% and 95% ethanol, followed by two hours in each of five changes of absolute ethanol. Clearing was undertaken by three two-hour changes in chloroform. Impregnation of the tissues was accomplished by two, two-hour changes in molten paraffin (Paraplast X-tra). After this cycle, the specimens were embedded in molten paraffin and allowed to solidify into blocks suitable for sectioning. The tissues were orientated so that cross-sections would include the cartilage surfaces of the joint.

Cross-sections of the paraffin-embedded tissues were cut at 6μm in thickness, using a Spencer 820 microtome. The sections were floated on a warm water bath, picked up on glass slides and dried in a 60°C oven.

All histological sections were stained with haematoxylin and eosin (H & E) (Bancroft and Stevens, 1982) and with safranin O (Lillie, 1965). (Appendices K and L) The slides were arranged in a staining rack, and the paraffin was removed by placing them into two changes of xylene for two minutes each. Then the slides were hydrated through a series of decreasing alcoholic and increasing aqueous dilutions as follows: two minutes in each of absolute, 95%, and 70% ethanol, and finally distilled water.

The slides stained with H & E were placed into Harris haematoxylin for 90 seconds, rinsed in tap water, differentiated by dipping three times in 0.35% acid-alcohol, washed and blued in warm-running tap water for five minutes,

and rinsed in distilled water. They were then placed into the eosin solution for 90 seconds, rinsed in distilled water, and dehydrated by quick rinses through two changes of 95% ethanol and three changes of absolute ethanol. The sections were then passed through two changes of xylene and were mounted with glass cover slips using Permount.

The slides stained with safranin O were placed into Weigert's haematoxylin for eight minutes, rinsed in tap water, dipped three times in 0.35% acid-alcohol, and washed well in tap water. They were then placed into 0.02% fast green FCF for three minutes, washed in four dips of 1% acetic acid, placed in 0.1% safranin O for six minutes, and then dehydrated, cleared, and mounted in the usual fashion. This metachromatic staining procedure was chosen for its ability to stain cartilage proteoglycans stoichiometrically (Rosenberg, 1971).

3.5.2 Transmission Electron Microscopy

Tissue fixation was achieved in a solution of cold 2% glutaraldehyde buffered in cacodylic buffer (pH 7.35) for one hour, followed by three changes of cacodylic buffer (0.1 M, pH 7.35), and one hour in 2% osmium tetroxide on ice. Following fixation, the tissues were dehydrated for 10 minutes each in 50%, 70%, and 90% ethanol. This was followed by three 15 minute changes of absolute ethanol, and three 15 minute changes of propylene oxide. Finally, the tissues were

left in 1:1 propylene oxide and Epon overnight, under the fume hood with the specimen vial cap off. The next day, the specimens were orientated and blocked in a flat embedding mould. These were polymerized at 45°C for 24 hours, then at 65°C for 48 hours. (Appendix M)

After polymerization, the Epon blocks were trimmed with a razor blade under a Riechart Om U3 ultramicrotome, in order to expose the cartilage specimen. Then one-micron sections were cut using a glass knife. These sections were picked up on glass slides with a wire loop and dried at 70°C on a hot plate. After drying, the sections were covered with toluidine blue for 30 seconds, rinsed with distilled water, dried on the hot plate, and mounted with a coverslip. (Appendix N) After staining, the sections were examined for areas suitable for ultrathin sectioning. Once a suitable area was identified, the block was trimmed with a razor blade accordingly. Ultrathin sections were cut with a diamond knife on a Riechart Ultracut E ultramicrotome set at a section thickness of 90 to 110 nm. The silver to gold coloured sections were picked up on 300-mesh copper grids.

Ultrathin sections on copper grids were double stained with uranyl acetate and lead citrate. (Appendix O) The staining solutions were removed from the refrigerator and allowed to warm up to room temperature. The grids were placed, section side down, on to a droplet of 4% aqueous uranyl acetate for 30 minutes. Afterwards, the grids were

rinsed with double distilled water and allowed to dry. Then they were placed on a drop of lead citrate for 3-5 minutes (Reynolds, 1963), and rinsed again with double distilled water. The grids were dried on filter paper and stored in plastic grid boxes.

3.5.3 Scanning Electron Microscopy

Tissues for scanning electron microscopy were fixed in cold 2% glutaraldehyde in 0.1 M cacodylic buffer (pH 7.3) for two weeks, followed by dehydration in increasing concentrations of ethanol over the next week. The specimens were placed in 50% ethanol for one day, 70% ethanol for one day, and 90% ethanol for one day. This was followed by 3-5 changes of absolute ethanol over a 3-4 day period. Subsequently, the specimens were placed in 1:1 ethanol to amyl acetate for a day, followed by 2-3 changes over two days in amyl acetate. Then, the specimens were quickly transferred to a Polaron Critical Point Dryer and dried by the critical point method using liquid CO_2. Dry specimens were mounted with the aid of double-sided tape on aluminum specimen mounts. In all cases, specimens consisted of the cartilage surface and a substantial piece of subchondral bone. Specimens were then vacuum coated with gold in a Technics Hummer Sputter Coater and stored in plastic boxes.

3.6 Examination of tissues

3.6.1 Gross Observations

All tissues were examined with the naked eye and the gross appearance of the articular surface was ranked as 1 = smooth, 2 = moderate degeneration, 3 = severe degeneration, and 4 = fused. In animals, an attempt was made to estimate the degree of mobility in the joint by standing on the intact pelvis and stressing the sacrum manually. The degree of mobility was ranked as 0 = none, 1 = barely detectable, 2 = easily detectable, and 3 = very mobile. It was not possible to estimate mobility in human specimens since the whole pelvis could not be removed. In addition, it was difficult to remove human specimens with the joint entirely intact.

3.6.2 Light Microscopy

Paraffin-embedded sections stained with H & E and safranin O were examined under the light microscope. In addition, Epon-embedded, one-micron sections stained with toluidine blue were examined. All sections were examined under a Leitz Orthoplan light microscope, and photomicrographs were recorded on Kodak Technical Pan, black and white film with a Wild MPS45 35 mm Photoautomat camera. The film was developed in HC 110 mixed in a 1:19 dilution for eight minutes at 20°C and fixed in Kodak Rapid Fix.

3.6.3 Transmission Electron Microscopy

Epon-embedded ultrathin sections were examined under a Zeiss EM-9S, or a Philips EM-400, or a Zeiss EM-10C transmission electron microscope. Each grid was systematically examined and electron micrographs were recorded on Kodak 4489 Electron Microscopic Film. The film was developed in D19 developer 1:2 for 3.25 minutes at 20°C and fixed in Kodak Rapid Fix.

3.6.4 Scanning Electron Microscopy

Gold-coated specimens were examined under a Cambridge Stereoscan Scanning Electron Microscope Mark 2A using an accelerating voltage of 20 keV. Polaroid pictures were made of areas of interest in order to confirm the exposure. Then, electron micrographs were taken on a Linhof 6X9 camera using Kodak PXP-120 film. The film was developed in Agfa Rodinol developer 1:50 for 10.5 minutes at 20°C and fixed in Kodak Rapid Fix.

3.7 Data Analysis

3.7.1 Morphometric Data

Measurements of the cephalad and caudal limbs of the human and animal sacroiliac joints were used to calculate a ratio of the caudal to cephalad limb length. This had the effect of standardizing the measurements for between-species comparisons. The mean of this ratio was compared between

species by an analysis of variance (ANOVA). The mean angle formed between the two limbs of the joint was also compared by an ANOVA. These measurements were made to investigate between-species differences and to compare the upright, bipedal pelvis of man to the quadruped animals.

4. EXPERIMENTS AND RESULTS

4.1 Prenatal Human Specimens

4.1.1 First Trimester

The youngest specimen examined was five weeks gestational age. At this stage of development, the iliac and sacral mesenchyme blastema are visible as one dense condensation of mesenchymal cells anterior to the developing spinal cord. (Figure 4.1a) It roughly defines the future shape of the sacrum and ilium. It is composed of densely-packed, stellate or polymorphous cells with prominent nuclei. The notochord is visible in the centre of the sacral blastema. (Figure 4.1b)

By eight weeks gestational age, the mesenchyme blastema has undergone chondrification, and the cartilage anlagen of the sacrum and ilium can be clearly identified as separate structures. (Figure 4.2a) Each anlage is surrounded by a layer of undifferentiated mesenchymal cells, known as the perichondrium. These cells span the future site of the sacroiliac joint. (Figure 4.2b) Within the ilium, there are some chondrocytes that have increased in size, taking on a cuboidal shape. These cells will undergo vacuolation and involution before being replaced by bone.

By the ninth week, chondrocytes in the ilium adjacent to the sacrum become vacuolated, and there is extracellular matrix formation. (Figure 4.3) The sacroiliac joint interzone can be identified as two parallel chondrogenic layers and an intervening, less dense layer of cells. The

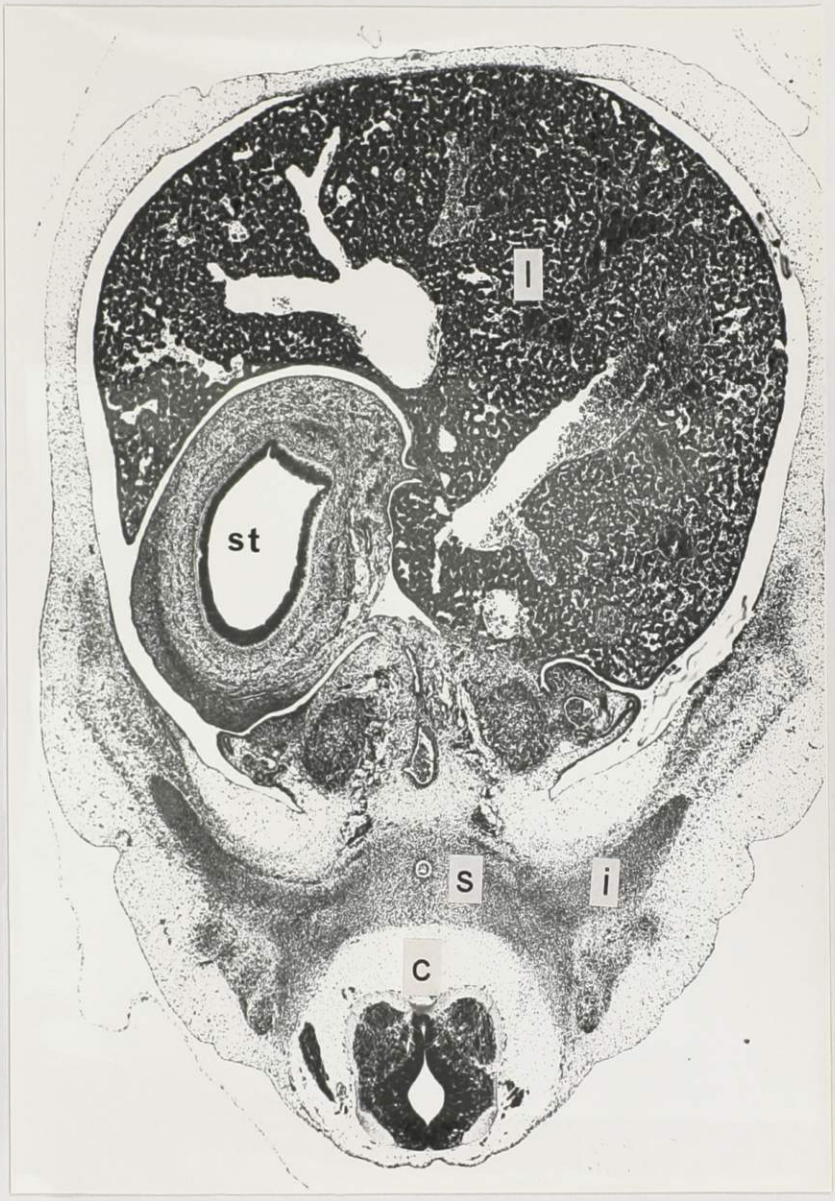

Figure 4.1a A cross section through the sacral region of this 5 WG fetus shows a large liver (l) and stomach (st) ventrally, and a developing spinal cord (c) dorsally. The sacral (s) and iliac (i) mesenchyme blastema can be seen ventral to the spinal cord. H & E, X 35

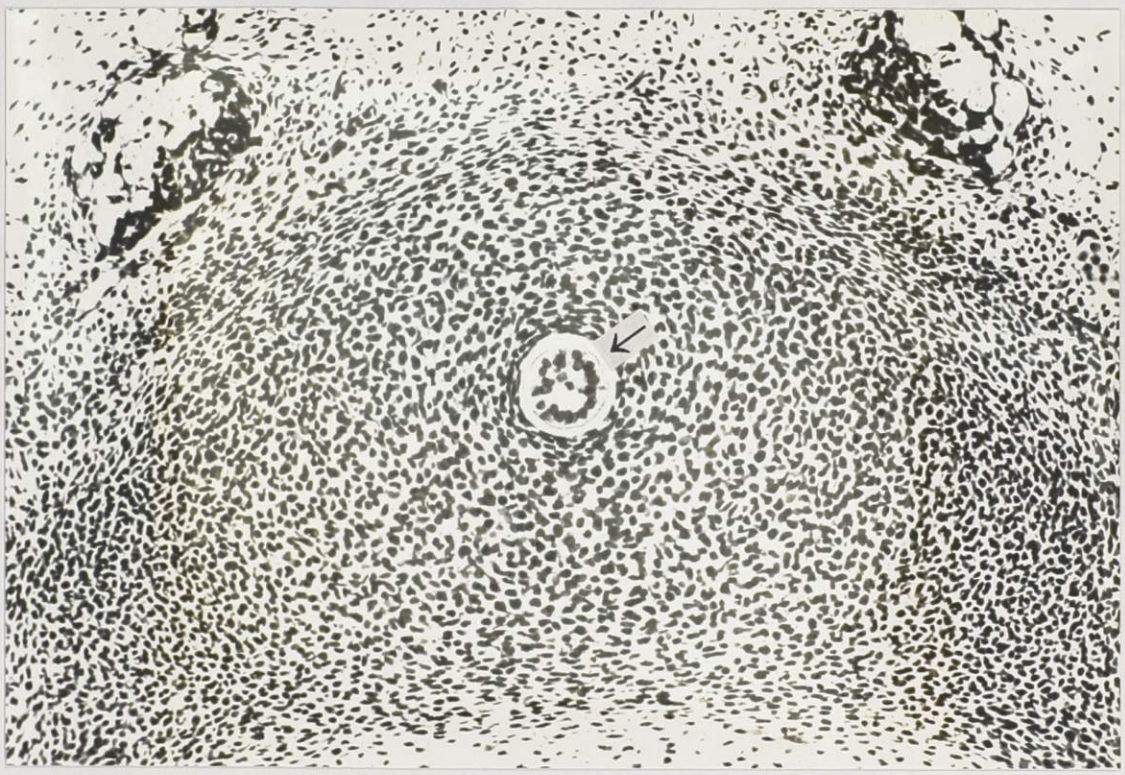

Figure 4.1b A high-power view of the cells of the sacral mesenchyme blastema shows that they appear stellate or polymorphous, with prominent nuclei. The notochord (arrow) is visible in the centre of the sacral blastema. H & E, X 220

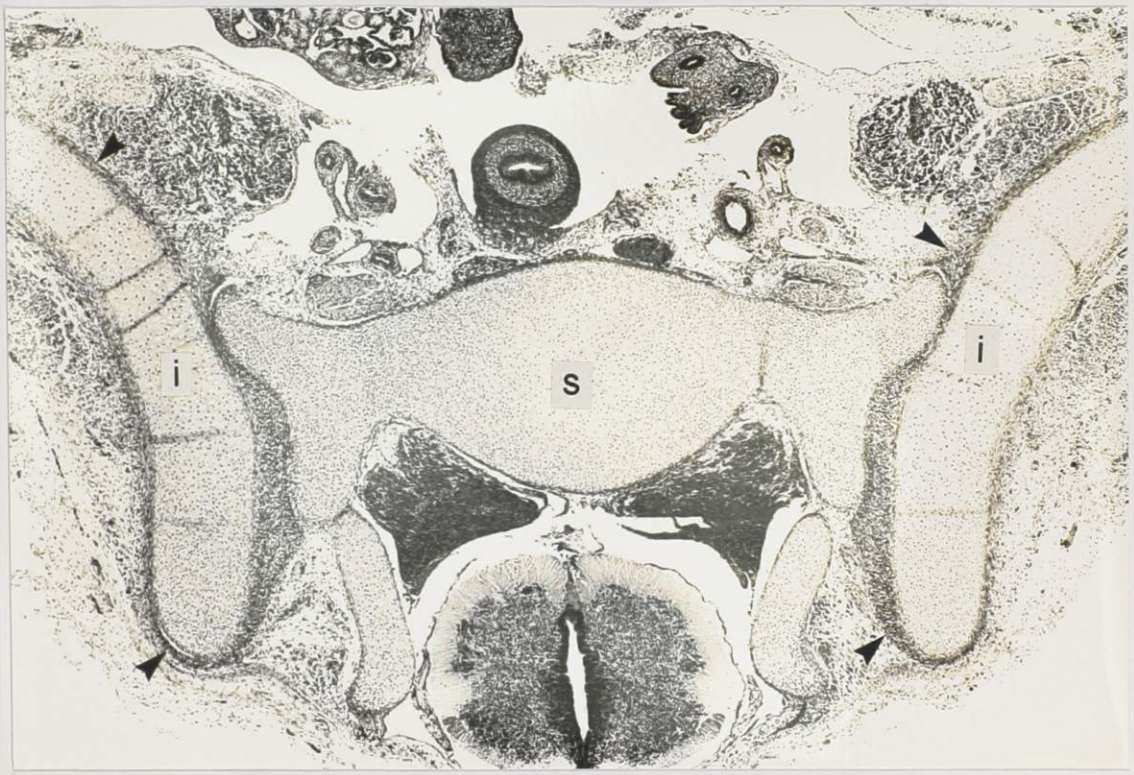

Figure 4.2a A cross section through the cartilage anlagen of the sacrum (s) and ilium (i) in an 8 WG fetus shows that both structures appear as separate entities surrounded by a layer of condensed cells known as the perichondrium (arrowheads). H & E, X 35

Figure 4.2b A high-power view of the future site of the sacroiliac joint in the specimen above shows that the perichondrium spans the space between the ilium (i) and the sacrum (s). Chondrocyte hypertrophy is visible within the iliac anlage, adjacent to the future sacroiliac joint (arrow). H & E, X 88

Figure 4.3a This 9.5 WG specimen shows marked chondrocyte hypertrophy (arrow) with vacuolation and extracellular matrix formation in the left ilium. H & E, X 22

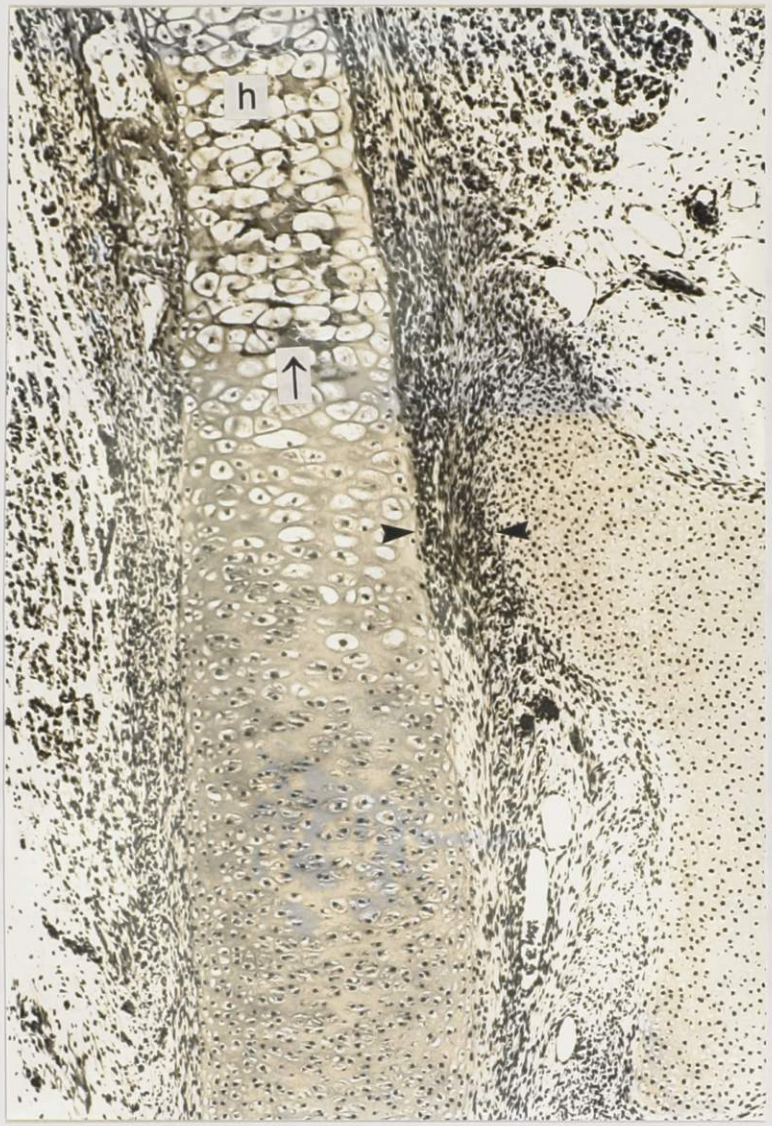

Figure 4.3b This high-power micrograph of the left ilium shows the details of the sacroiliac joint interzone. Adjacent to the interzone, there is chondrocyte hypertrophy (h) and extracellular matrix formation (arrow) within the iliac anlage. The three-layered joint interzone is comprised of two parallel layers of densely-packed cells (arrowheads) and an intervening layer of differently-oriented cells. H & E, X 88

Figure 4.69a The iliac surface of this 23-year-old male specimen is intact, but there is marked chondrocyte clustering. S-O, X 22

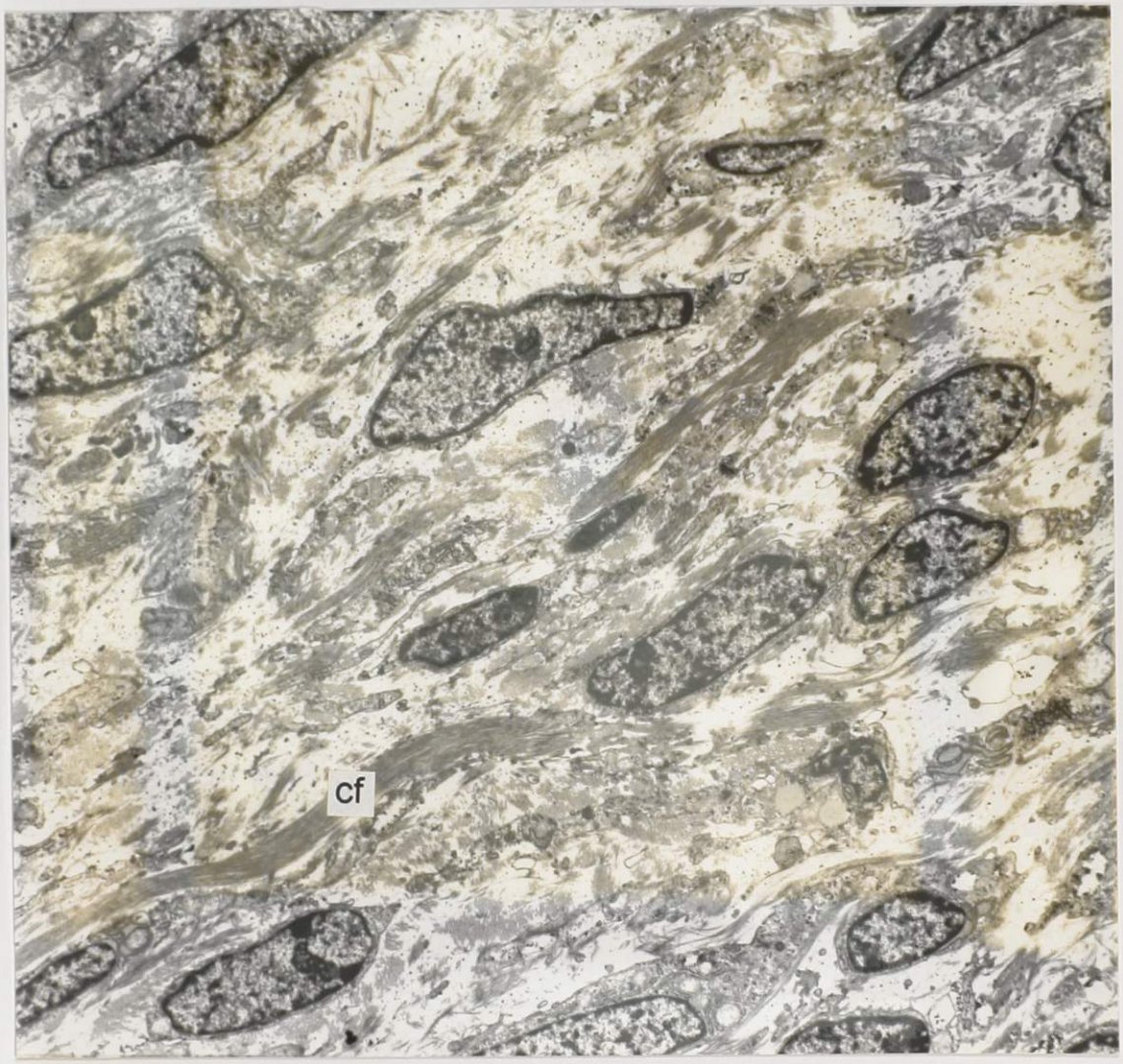

Figure 4.4 This TEM of the sacroiliac joint interzone of a 12 WG fetus shows fibroblast-like cells within a matrix with an abundance of collagen fibrils (cf). X 3,800

Figure 4.5 This histological section through the ilium shows osteoid formation (arrowheads) in the iliac perichondrium adjacent to the sacroiliac joint interzone (arrows) in a 9.5 WG specimen. The sacral cartilage anlage (s) is composed of chondrocytes in a hyaline matrix. S-O, X 88

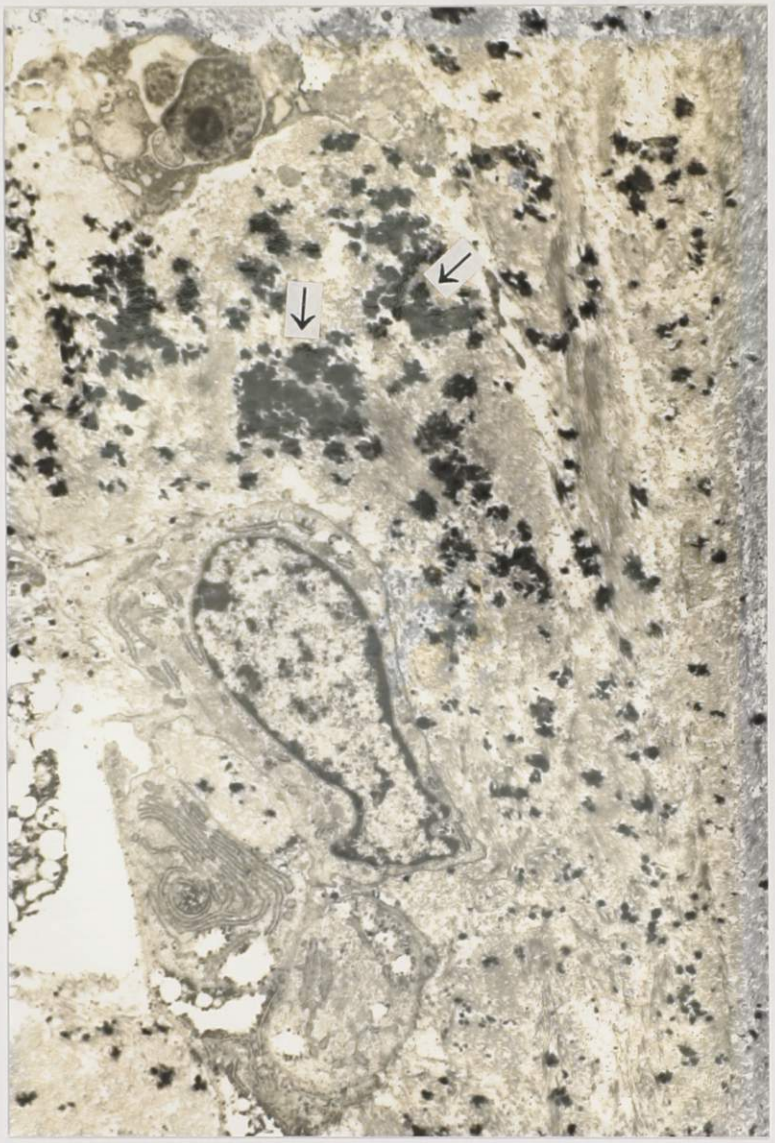

Figure 4.6 This TEM shows early mineralization of the iliac perichondrium adjacent to the sacroiliac joint interzone in a 12 WG fetus. There are numerous foci of mineralization (arrows) within the collagen-rich matrix. X 5,400

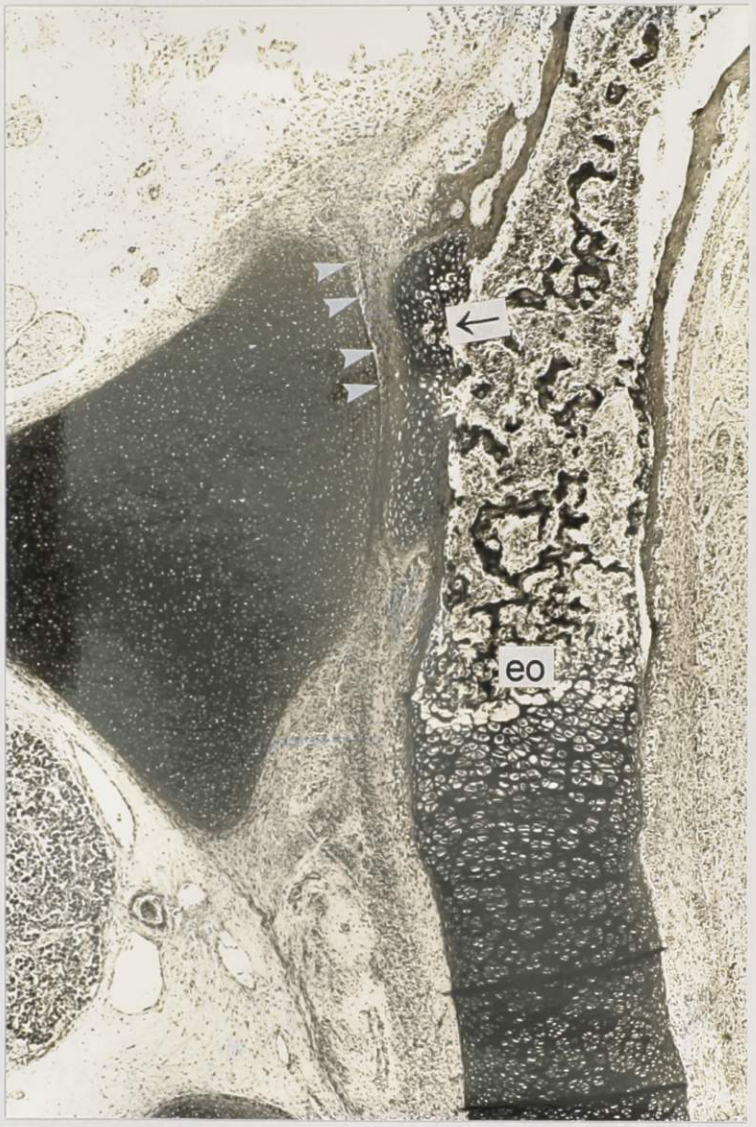

Figure 4.7a This 16 WG female specimen shows cavitation of the sacroiliac joint space (arrowheads) with new chondrocyte formation (arrow) within the undifferentiated cells that cover the ilium. Note that the process of endochondral ossification (eo) of the ilium has progressed past the area of the sacroiliac joint. S-O, X 35

the undifferentiated mesenchyme of the joint interzone. They form columns between the ilium and the iliac mesenchyme, and their immediate surrounding matrix stains metachromatically, indicating the presence of proteoglycans. Therefore, at the time of cavitation, the iliac surface of the sacroiliac joint is composed of undifferentiated mesenchyme with pockets of large developing chondrocytes surrounded by an area of metachromatic matrix.

On the other side of the joint, the sacral surface is derived from the sacral cartilage anlage. It has the typical appearance of fetal hyaline cartilage. The chondrocytes are evenly distributed throughout a hyaline matrix that has a high proteoglycan content. (Figure 4.8)

The process of sacroiliac joint cavitation begins in the cranial region of the joint and spreads caudally. (Figure 4.9) In more caudal areas of the joint, there is no evidence of chondrocyte formation on the iliac side at the time of cavitation. (Figure 4.10) In addition, cavitation begins in the ventral part of the joint and then spreads dorsally. Minute spaces occur in the joint interzone and coalesce to form the joint cavity. (Figure 4.11) In some cases, complete separation of the two joint surfaces is delayed by fibrous septa that bridge across the joint. These are common in the dorsal part of the joint cavity during the second trimester. (Figure 4.12) They sometimes persist after birth.

From an ultrastructural point of view, the iliac and

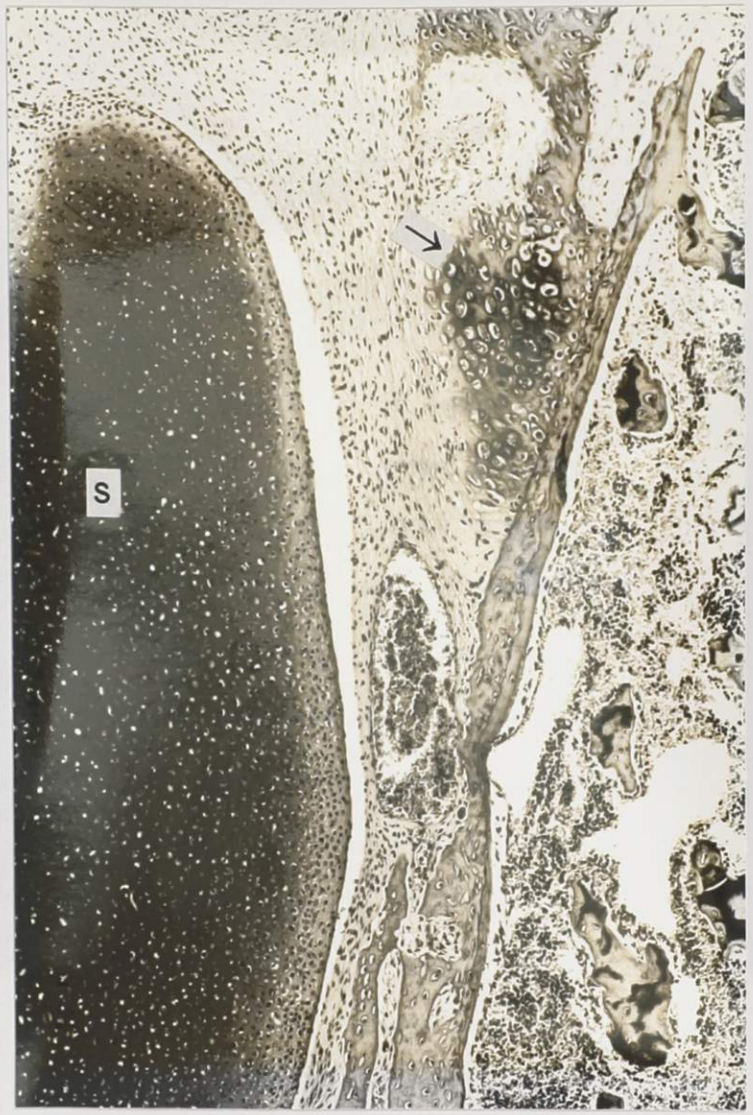

Figure 4.8a This 18 WG male specimen shows a well-developed joint space with the sacral cartilage (s) staining deeply metachromatic because of its high proteoglycan content. The iliac surface is composed primarily of undifferentiated cells with a small pocket of developing chondrocytes surrounded by a metachromatic-staining matrix (arrow). S-O, X 35

Figure 4.8b A high-power view shows the developing iliac chondrocytes in detail. The matrix surrounding these cells, and all of the sacral cartilage matrix, stains positively for proteoglycans. The large iliac chondrocytes appear to develop in columns. The overlying mesenchyme is composed of spindle cells in a loose connective tissue matrix. S-O, X 220

Figure 4.9 This is a more cranial section of the 16 WG female specimen shown in figure 4.7. Note that the joint space is better defined (arrowheads), indicating that the process of cavitation is further developed in more cranial regions. S-O, X 88

Figure 4.10 This 19.5 WG male specimen shows the process of cavitation (arrowheads) progressing in the caudal region of the sacroiliac joint. Note that there is no evidence of chondrocyte formation on the iliac (i) side of the joint in this plane of section. S-O, X 35

Figure 4.11 This 17 WG male specimen shows the beginning of joint cavitation. Minute spaces appear in the joint interzone (arrowheads). These spaces coalesce to form the joint cavity. At most levels, there are no chondrocytes on the iliac side at the time of cavitation. Instead, there are undifferentiated mesenchymal cells (m). S-O, X 88

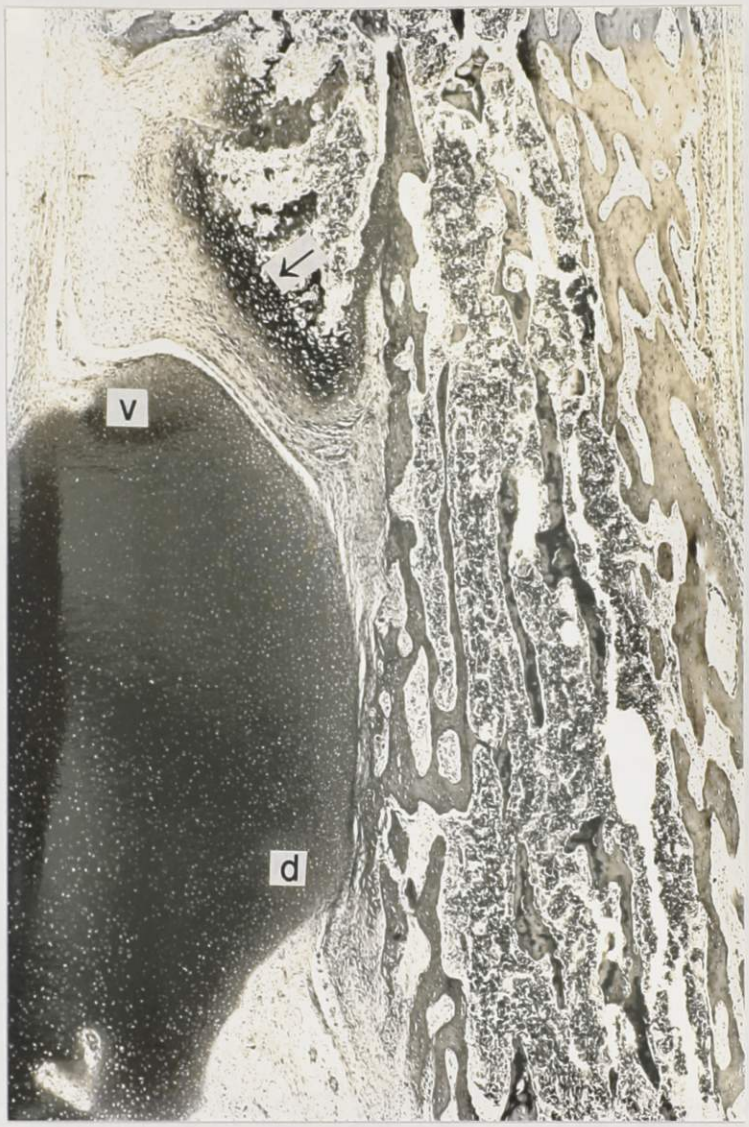

Figure 4.12a An 18 WG male specimen shows cavitation of the sacroiliac joint spreading from the ventral (v) to the dorsal (d) region. An area of chondrogenesis can be seen on the iliac side of the joint in the ventral region (arrow). It is characterized by large developing chondrocytes forming columns and staining positive for proteoglycans in the surrounding matrix. There are several fibrous septa across the caudal part of the joint. S-O, X 35

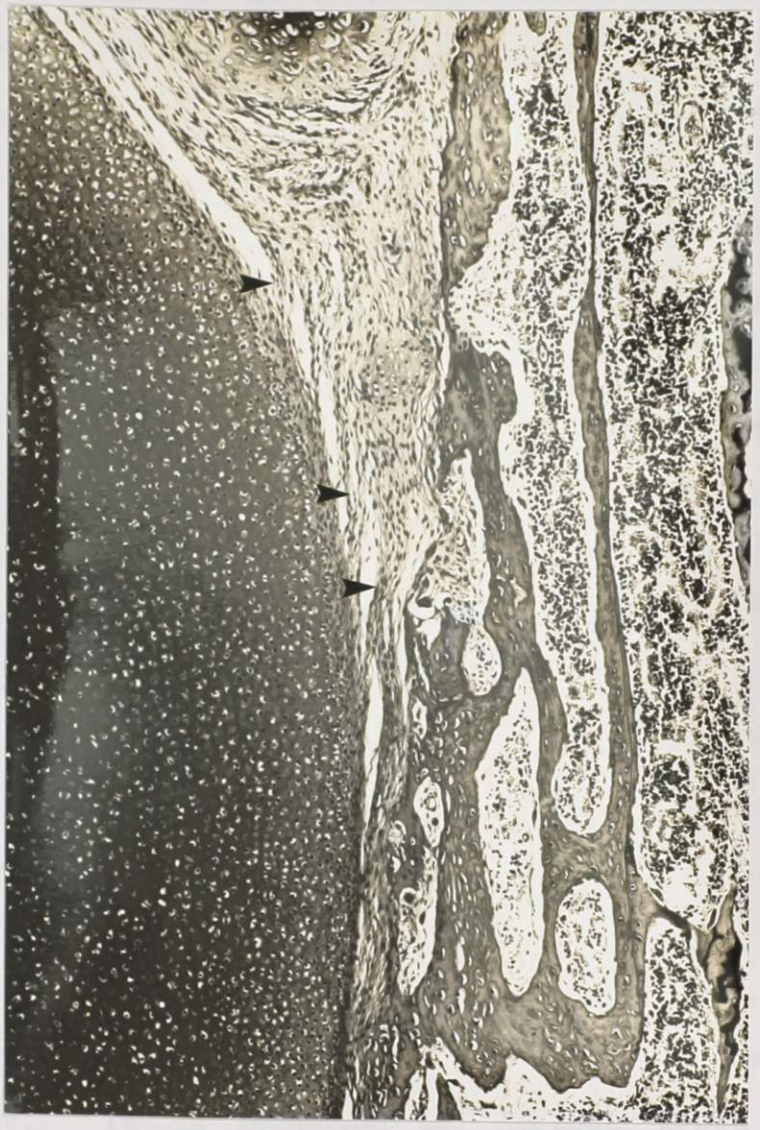

Figure 4.12b A high-power view of the dorsal region of the joint shows the intra-articular fibrous septa (arrowheads) bridging the joint space. They are composed of strands of mesenchyme from the iliac side of the joint that remain attached to the sacral cartilage surface. S-O, X 88

sacral joint surfaces appear quite different. The sacral side has the normal appearance of fetal hyaline articular cartilage. At the surface, the zone I chondrocytes have oval or elongated nuclei that are tangential to the surface. (Figure 4.13a) These cells are embedded in a thin, but prominent layer of collagen fibrils that run parallel to the joint surface. Just below this, the chondrocytes have oval to round nuclei and are evenly spaced within a hyaline matrix of proteoglycan particles (30 to 70nm in diameter) with associated filaments (about 5nm thick) and a moderate number of randomly-oriented collagen fibrils (ranging from 30 to 80nm). (Figure 4.13b) These young chondrocytes do not exhibit a well-defined territorial matrix. Since the sacral ala is entirely cartilaginous, there is no osteochondral junction, or zone III or IV morphology, typical of adult articular cartilage. Therefore, the entire sacral cartilage has the same appearance, except for the zone I surface region.

On the other hand, the iliac side appears quite different. It is composed of various types of cells, embedded in a loose connective tissue matrix filled with abundant collagen fibrils organized into fibres. Most of the cells are fibroblastic in nature. They exhibit a spindle form with elongated nuclei. At the surface of the joint, there is a zone I region with prominent collagen fibrils running parallel to the joint surface. (Figure 4.14a) The

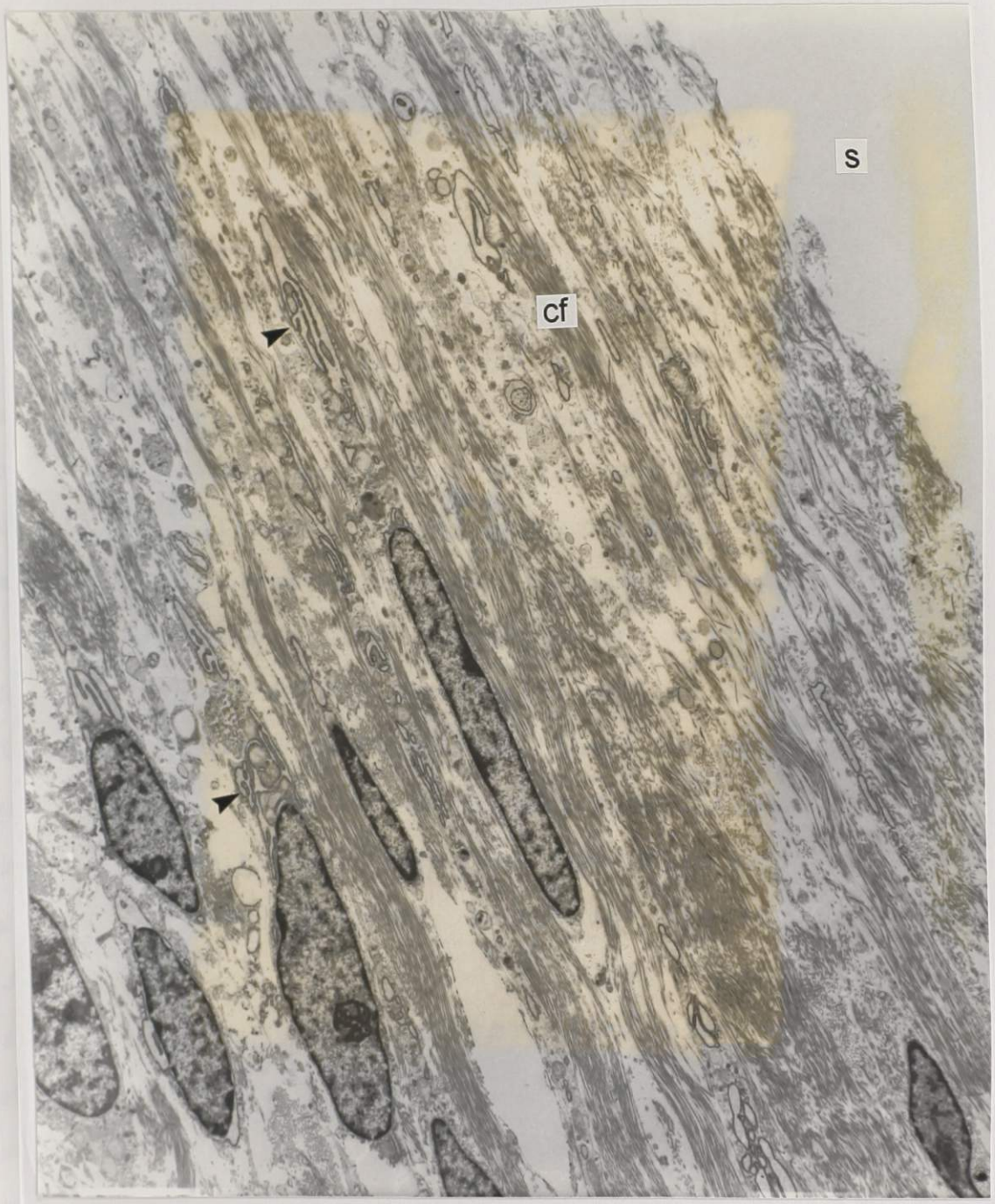

Figure 4.13a Ultrastructural details of the sacral surface of a 13 WG male specimen. Immediately below the joint surface (s) parallel collagen fibrils (cf) are prominent. The nuclei of the chondrocytes in this region are elongated and tangential to the surface. These cells contain sparse cytoplasm with some dilated rough endoplasmic reticulum (arrowheads) and occasional mitochondria. X 3,800

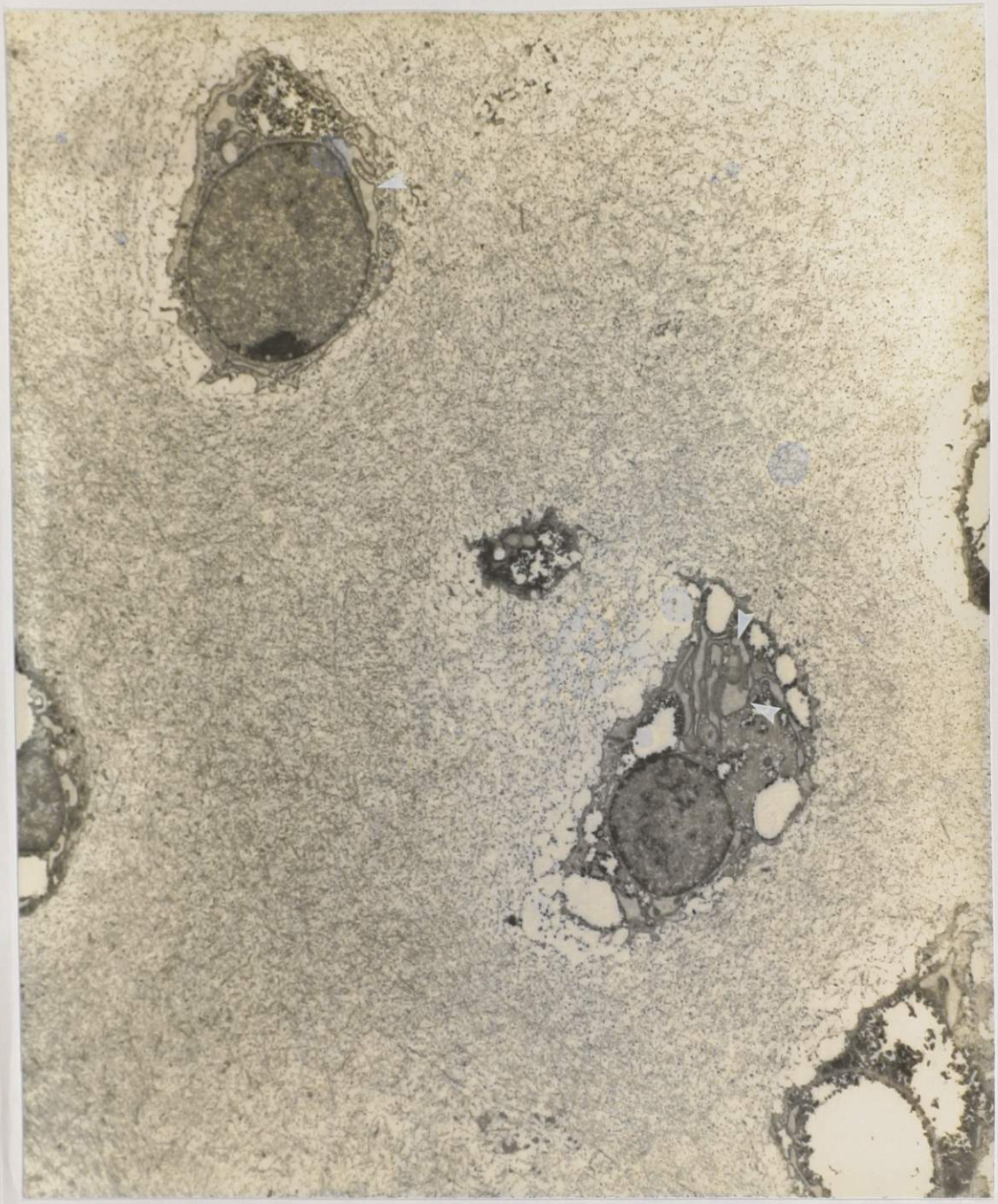

Figure 4.13b Just below the joint surface the chondrocyte nuclei are more round and the cell processes are small and short. The cisternae of the rough endoplasmic reticulum of the cells are dilated (arrowheads), which is a common and early autolytic change. The matrix is composed of electron-dense proteoglycan particles with associated filaments and randomly-oriented collagen fibrils. X 3,800

Figure 4.14a The joint surface region of this 13 WG male iliac specimen contains cells with elongated nuclei and long cell processes. There are focal accumulations of collagen fibrils (cf) forming fibres that are oriented parallel to the joint surface. X 7,600

cells in this region have elongated nuclei and long cell processes with scarce cytoplasm. Just below this region, there is a mixture of connective tissue cells, including endothelium forming capillaries, fibroblasts or mesenchymal cells, and cells with more rounded nuclei that resemble chondroblasts. (Figure 4.14b) These latter cells are an intermediate form, between fibroblasts and mature chondrocytes. The matrix at this level is composed of loosely packed collagen fibres. In some regions, there are more fully developed chondrocytes that are surrounded by a typical cartilage matrix. (Figure 4.15a) At the osteochondral junction, osteoblasts can be seen adjacent to areas of mineralization in the ilium. (Figure 4.15b)

As the two joint surfaces separate and become distinct entities, the zone I region on the sacral side decreases in thickness, and the matrix on the iliac side becomes more collagenous. (Figure 4.16) Pockets of chondroblasts occur on the iliac side of the joint, and short columns of chondrocytes can be seen at the osteochondral border. (Figure 4.17) Collagen fibres run between the columns of iliac chondrocytes and insert directly into the underlying bone. (Figure 4.18) Closer to the joint surface, there are randomly-oriented spindle cells embedded in a collagenous matrix. (Figure 4.19a) On the sacral side, the matrix is filled with proteoglycan aggregates in a meshwork of intermediate filaments and collagen fibrils. (Figure 4.19b)

Figure 4.14b An area of loose connective tissue is visible just below the surface region shown in figure 4.14a. A capillary lumen (cl) is surrounded by endothelial cells (e). Undifferentiated fibroblastic or mesenchymal cells have long cytoplasmic processes with an abundance of rough endoplasmic reticulum (arrows) and mitochondria (arrowheads). There are cells with more rounded nuclei and shorter cell processes that are chondroblasts (cb). X 4,750

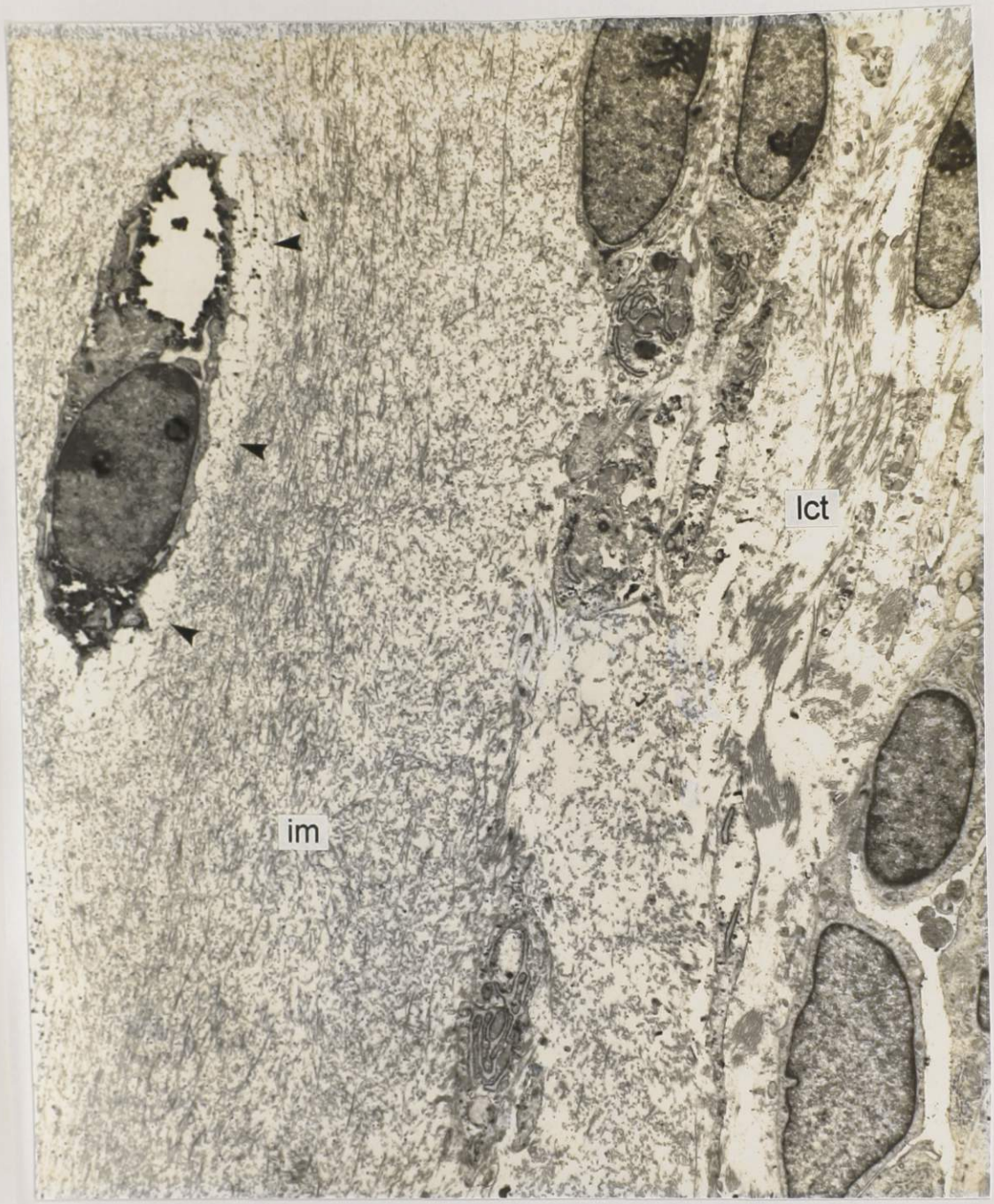

Figure 4.15a The region just below that seen in figure 4.14b contains a chondrocyte surrounded by a territorial matrix (arrowheads) that lies in a general matrix or interterritorial matrix (im) composed of proteoglycan particles and randomly-oriented filaments and collagen fibrils. A loose connective tissue (lct) area can be seen just adjacent to this region. It contains some spindle cells and an abundance of collagen fibrils. X 4,750

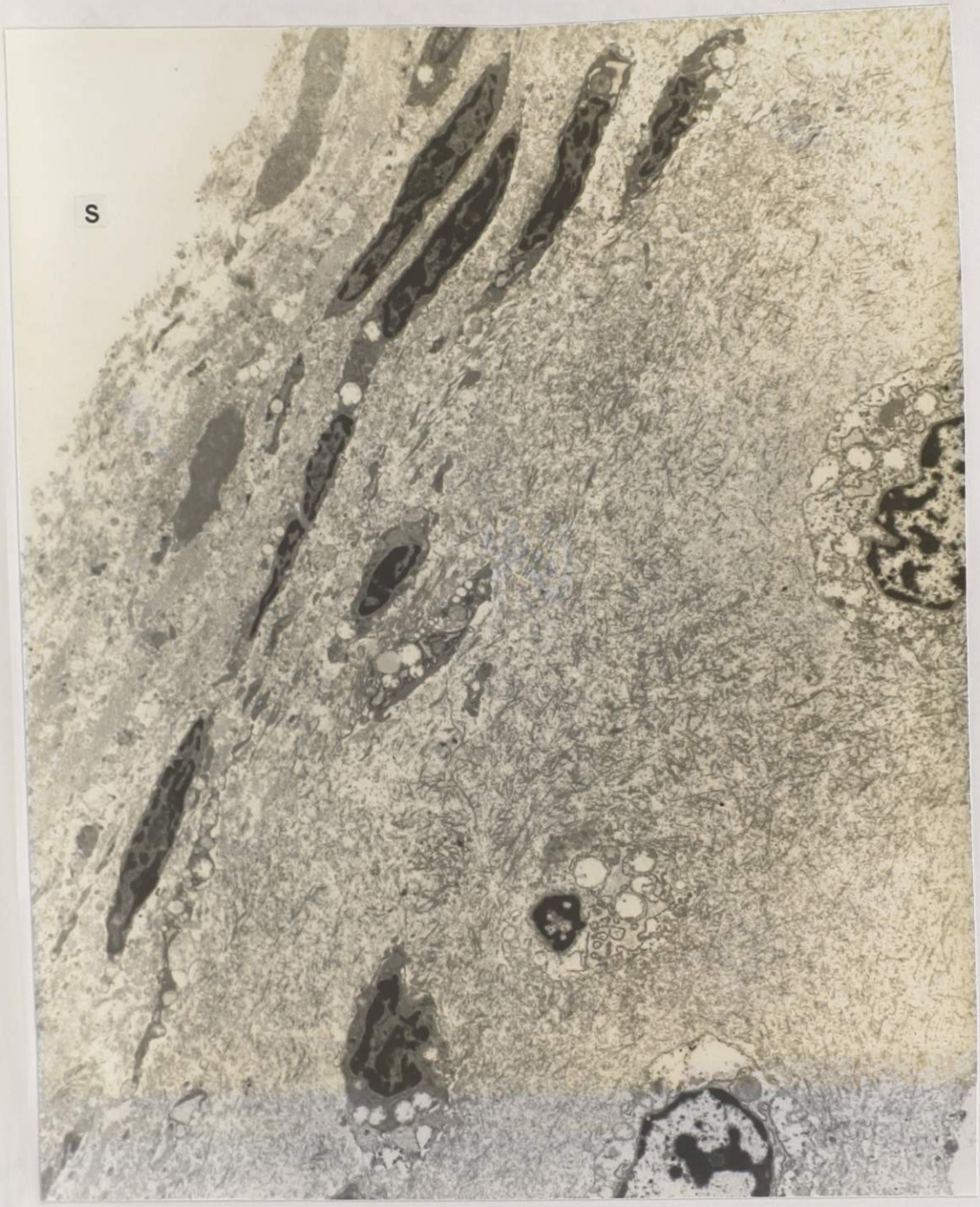

Figure 4.16a The zone I region of the sacral surface (s) of this 19 WG male specimen is composed of a thin layer of elongated chondrocytes. Immediately below this region, the cells are more round and contain more cytoplasm. X 3,800

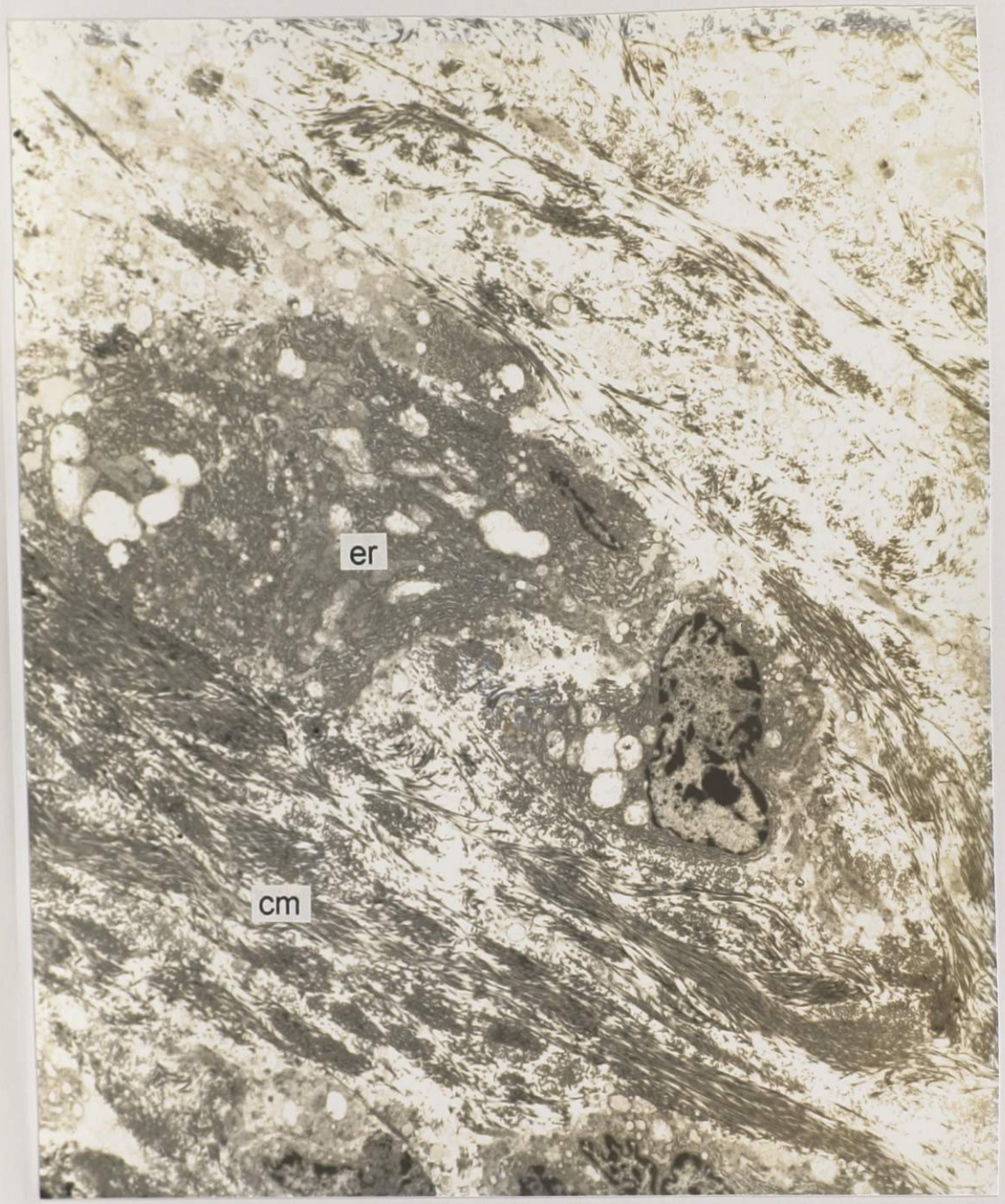

Figure 4.16b The iliac cartilage is characterized by a collagenous matrix (cm). Some of the cells appear metabolically active, with an increased amount of rough endoplasmic reticulum (er). These cells produce the collagen matrix and may eventually differentiate into chondrocytes. X 3,800

Figure 4.17 A pocket of chondrocyte development (c) can be seen on the iliac side of the sacroiliac joint in this 24 WG male specimen. In addition, there are short columns of chondrocytes, three to four cells high, at the osteochondral border (arrows). Undifferentiated mesenchyme (m) predominates on the iliac side of the joint. Cavitation is not yet complete in this caudal region of the joint (arrowheads). S-O, X 88

Figure 4.18a Columns of cells separated by bundles of collagen fibrils (cf) are visible in this area of the iliac osteochondral border in this 24 WG male specimen. These cells are intermediate between chondrocytes and fibroblasts. X 4,750

Figure 4.18b Collections of collagen fibrils pass between the iliac chondrocytes and insert directly into the underlying calcified tissue (arrow). X 11,970

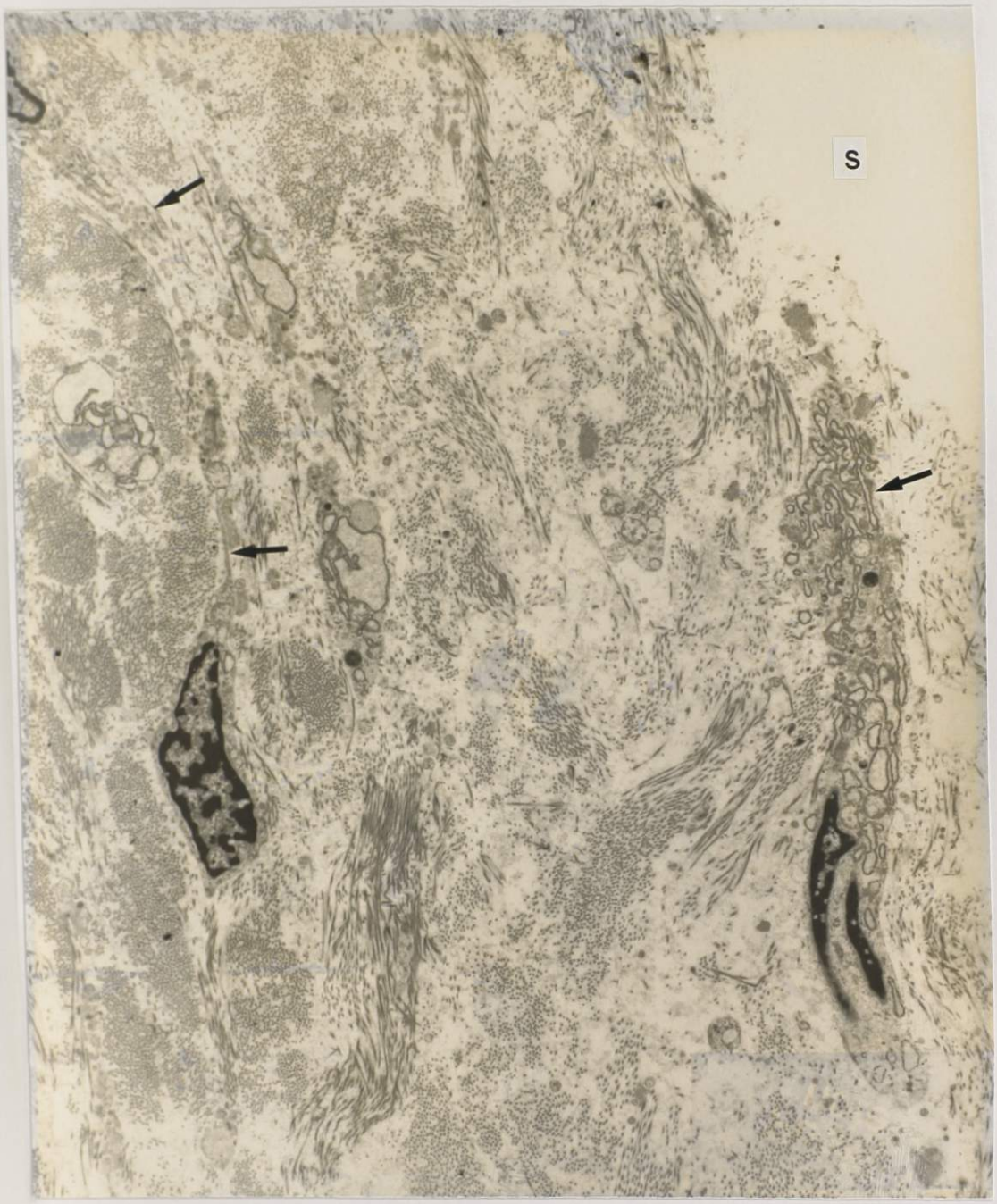

Figure 4.19a The iliac surface (s) of the same specimen seen in figures 4.17 and 4.18 shows an abundance of randomly-oriented collagen fibres with no visible filaments or proteoglycan particles. The cells have long cytoplasmic processes and resemble fibroblasts (arrows). X 4,750

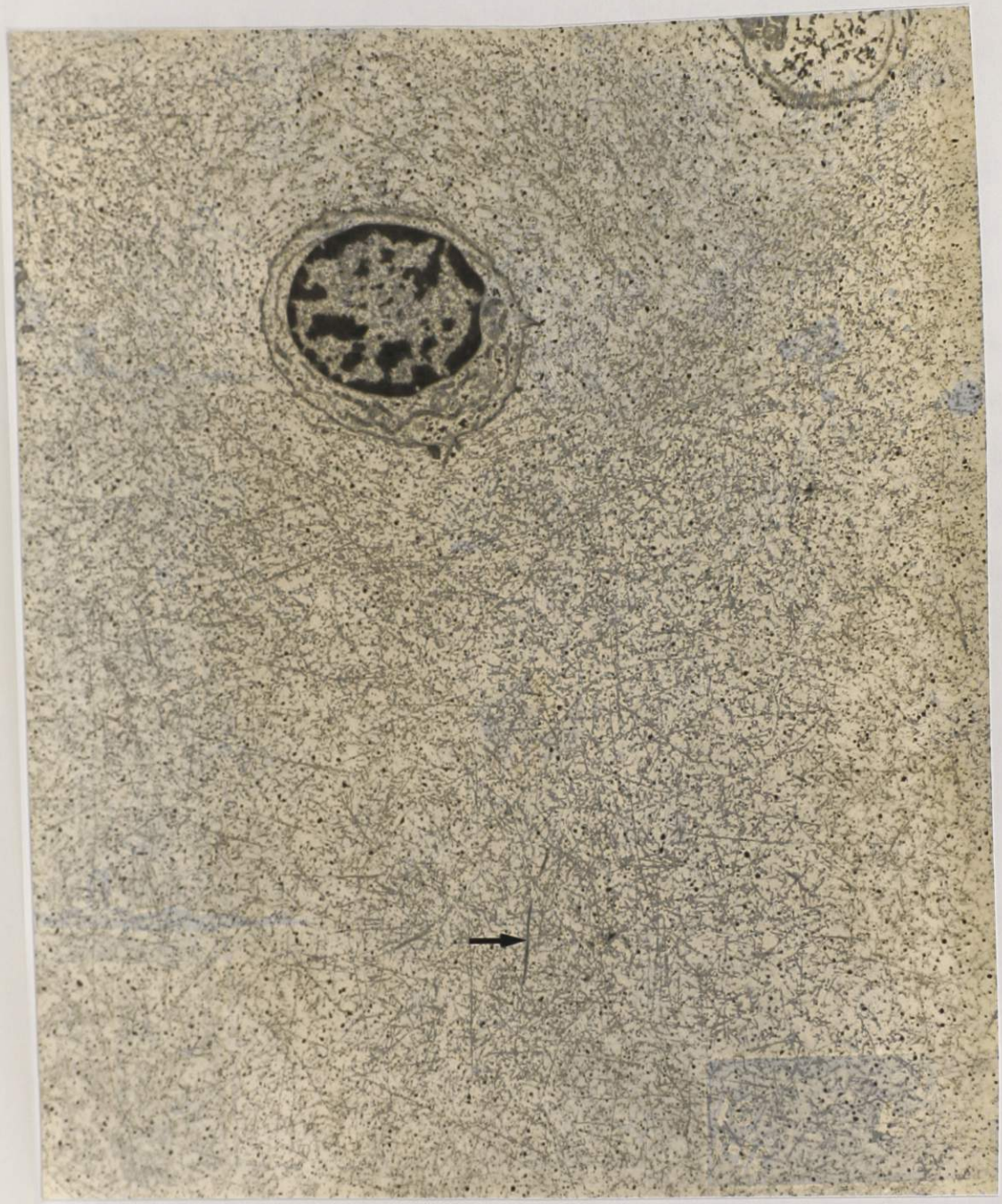

Figure 4.19b The matrix of the sacral cartilage is characterized by proteoglycan particles in a meshwork of intermediate filaments and collagen fibrils (arrow). The chondrocytes are round with short cell processes and lack a territorial matrix. X 4,750

Although the iliac side of the joint develops in an unusual manner, the sacral side is not without its own peculiarity. An intercellular or interlacunar network develops in the sacral cartilage matrix during the second trimester. (Figure 4.20) It stains more intensely metachromatic than the surrounding matrix. The network concentration seems to gradually increase with the distance from the articular surface, and the elements appear to extend from the individual chondrocytes as branching bundles of varying thickness. Their orientation changes from perpendicular to parallel to the joint surface with increasing depth from the surface. They are not always visible in paraffin sections, but are clearly visible in one-micron sections stained with toluidine blue. The network is also present in the iliac cartilage anlage, but not in the iliac joint fibrocartilage. (Figure 4.21)

The intercellular network appears to be an extension of the thin territorial matrix of the associated chondrocytes. (Figure 4.22) It has the ultrastructural appearance of a meshwork of densely-staining strands that contain filaments and granular material arranged in a loosely woven texture. (Figure 4.23) The individual elements vary in thickness and appear to branch, although branching might be a sectioning artifact. In many cases, several strands can be seen connecting two chondrocytes. This network can persist into childhood, but is never present on the iliac side of the

Figure 4.20 This one micron section through the sacral surface of a 13 WG male specimen shows the thin zone I region (arrow) and the typical appearance of the remainder of the sacral cartilage anlage. The nuclei of the cells in zone I are elongated and tangential to the joint surface. Below this region, the chondrocyte nuclei are oval to round, and the cells are distributed evenly within an abundant hyaline matrix. Some cells are paired and are seen lying in lacunae or clear spaces. An intercellular network of matrix streaks (arrowheads) can be seen connecting some of the chondrocytes. T-B, X 220

Figure 4.21a A prominent intercellular network is present in the iliac cartilage anlage of this 13 WG male specimen. This section was taken ventral to the sacroiliac joint interzone. Γ-B, X 88

'igure 4.21b A high-power view of the specimen shows the ıetwork in greater detail. It appears to be more prominent .n the centre of the anlage, and each part of the network ıppears to be made of a several strands. T-B, X 220

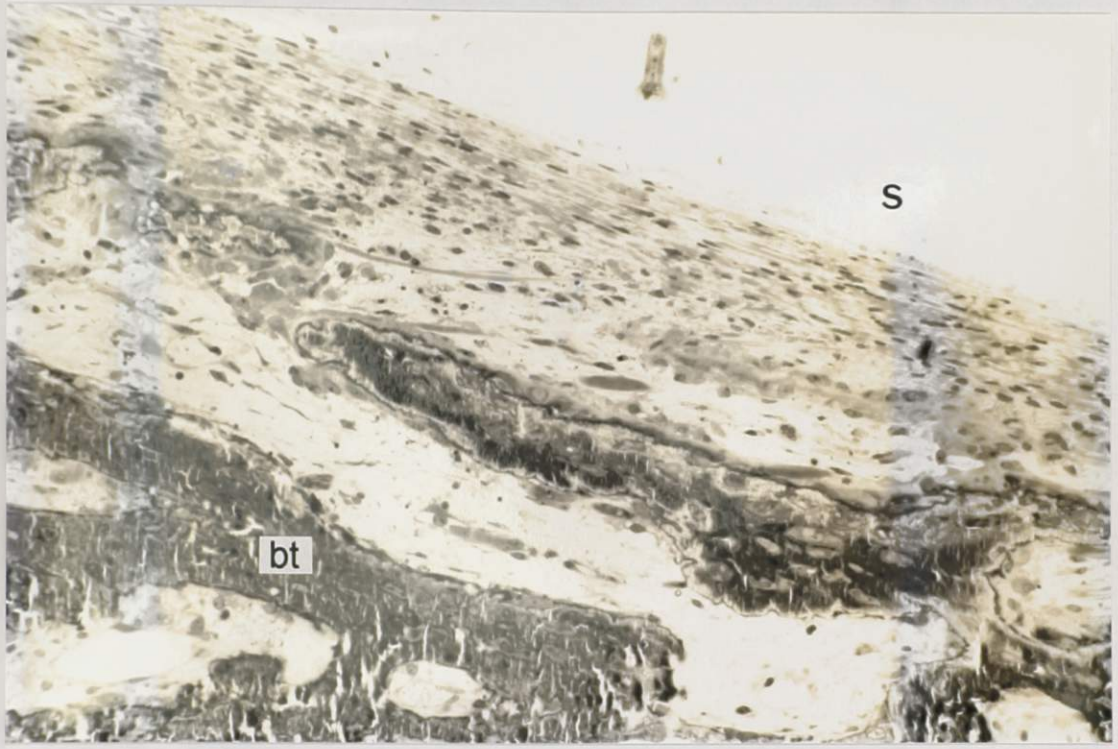

Figure 4.21c This one micron section through the iliac surface of the joint shows no evidence of an interlacunar network. Cells with elongated nuclei are clearly visible in this section. Collagen fibres can be seen running parallel to the joint surface (s) in the upper half of the joint. The cells below this region appear more pleomorphic. Bone trabeculae (bt) are visible just below the surface of the joint. T-B, X 220

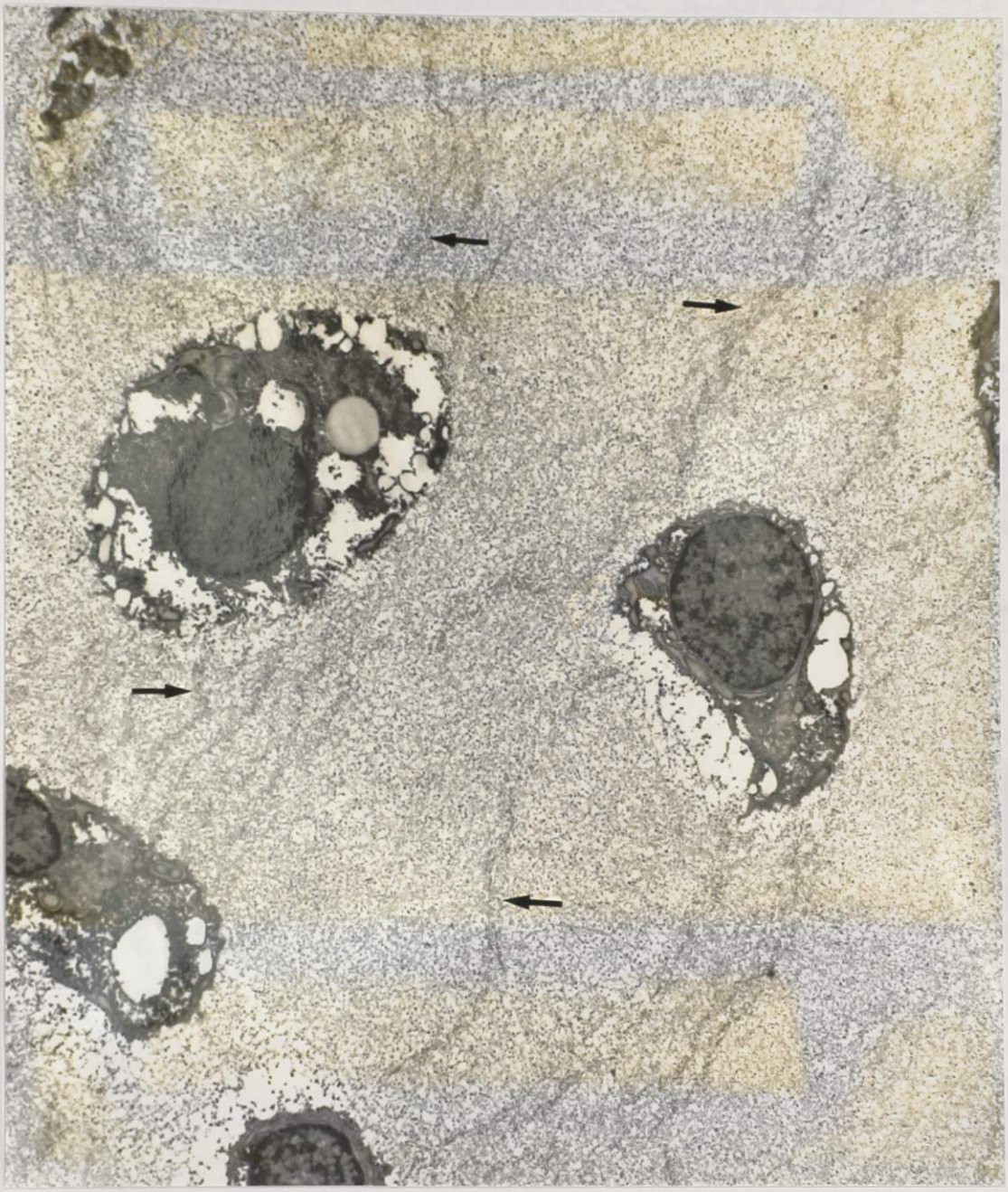

Figure 4.22 Several strands (arrows) of the intercellular network of the sacral cartilage of this 13 WG male specimen can be seen connecting each chondrocyte. The strands seem to take their origin from the thin territorial matrix surrounding the chondrocytes. X 3,800

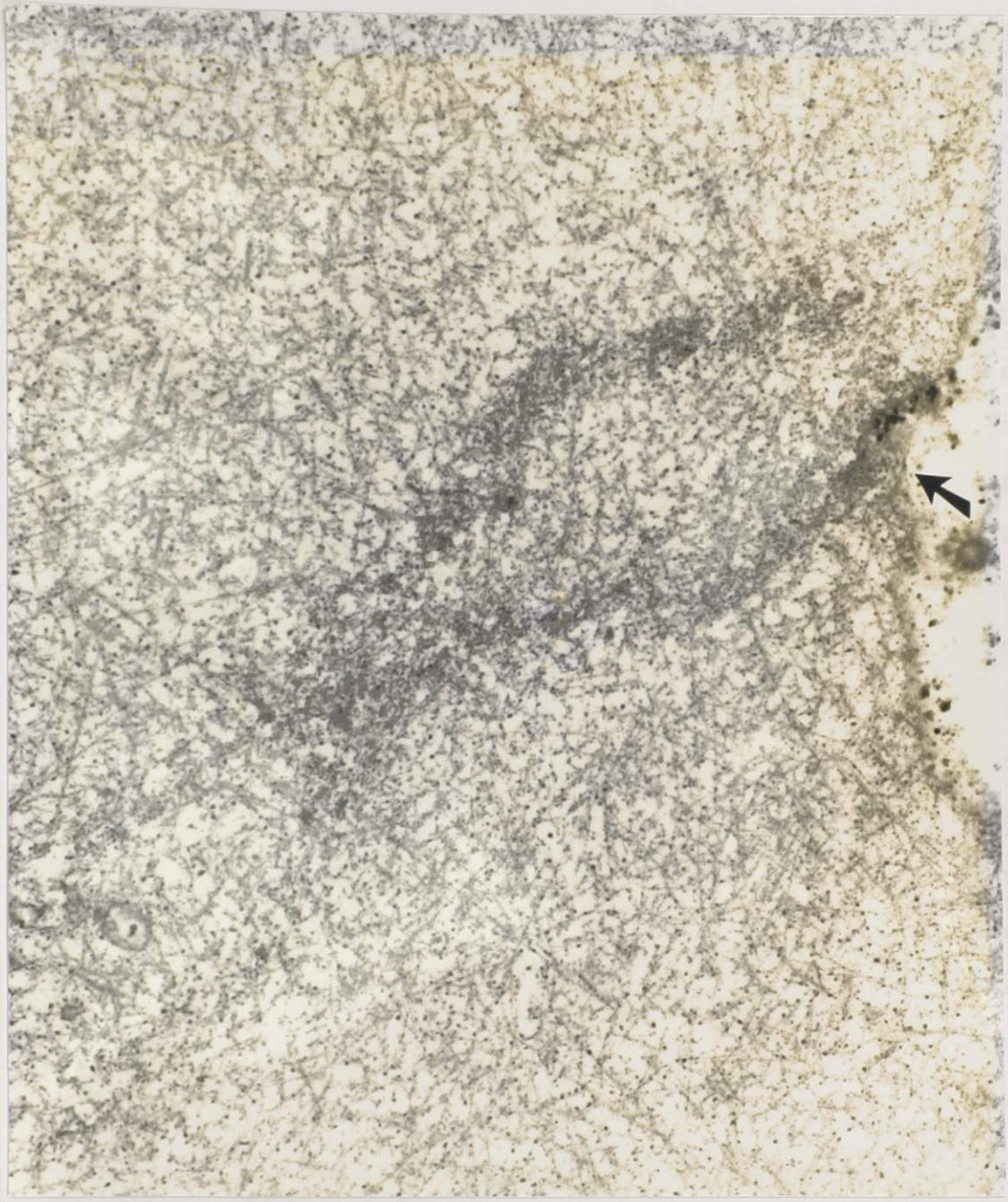

Figure 4.23 A high-power view of two strands from the intercellular network of the sacral cartilage of a 19 WG male specimen shows some of the ultrastructural details. The densely-staining strand appears to contain fibrillar and granular elements arranged in a loosely-woven texture. It appears to originate from the territorial matrix of the associated chondrocyte (arrow). X 15,200

joint. It can also be observed in the hyaline cartilage anlage of the vertebral body, adjacent to the fetal intervertebral disc, but is absent from the fibrocartilage of the adjacent annulus fibrosis. (Figure 4.24)

Scanning electron microscopy highlights the difference between the sacral and iliac sides. Generally, the sacral side appears smoother than the iliac side. (Figure 4.25) The iliac side is covered with fibrous strands, which represent the intra-articular fibrous septa that develop during cavitation. (Figure 4.26) The sacral side is characterized by numerous pits that represent surface chondrocytes that have shrunk during processing. (Figure 4.27) This is explained by the more cellular nature of the sacral cartilage, and the more hyaline nature of its matrix. On the other hand, the iliac surface appears less cellular and more fibrous. (Figure 4.28) This is in keeping with the abundance of collagen and the lack of proteoglycans in the matrix on the iliac side. In some cases, the sacral pits appear more like holes. (Figure 4.29) Perhaps some of the surface cells are removed during processing, leaving empty lacunae. In all cases, the iliac side has a very fibrous appearance with fewer cells. (Figure 4.30)

4.1.3 Third Trimester

During the third trimester, the sacroiliac joint matures, especially on the iliac side. (Figure 4.31) The

Figure 4.24a An intercellular network is present in the cartilage anlage of the L5 vertebral body of this 13 WG male specimen. It appears as a meshwork of electron-dense strands between chondrocytes (arrows). X 3,800

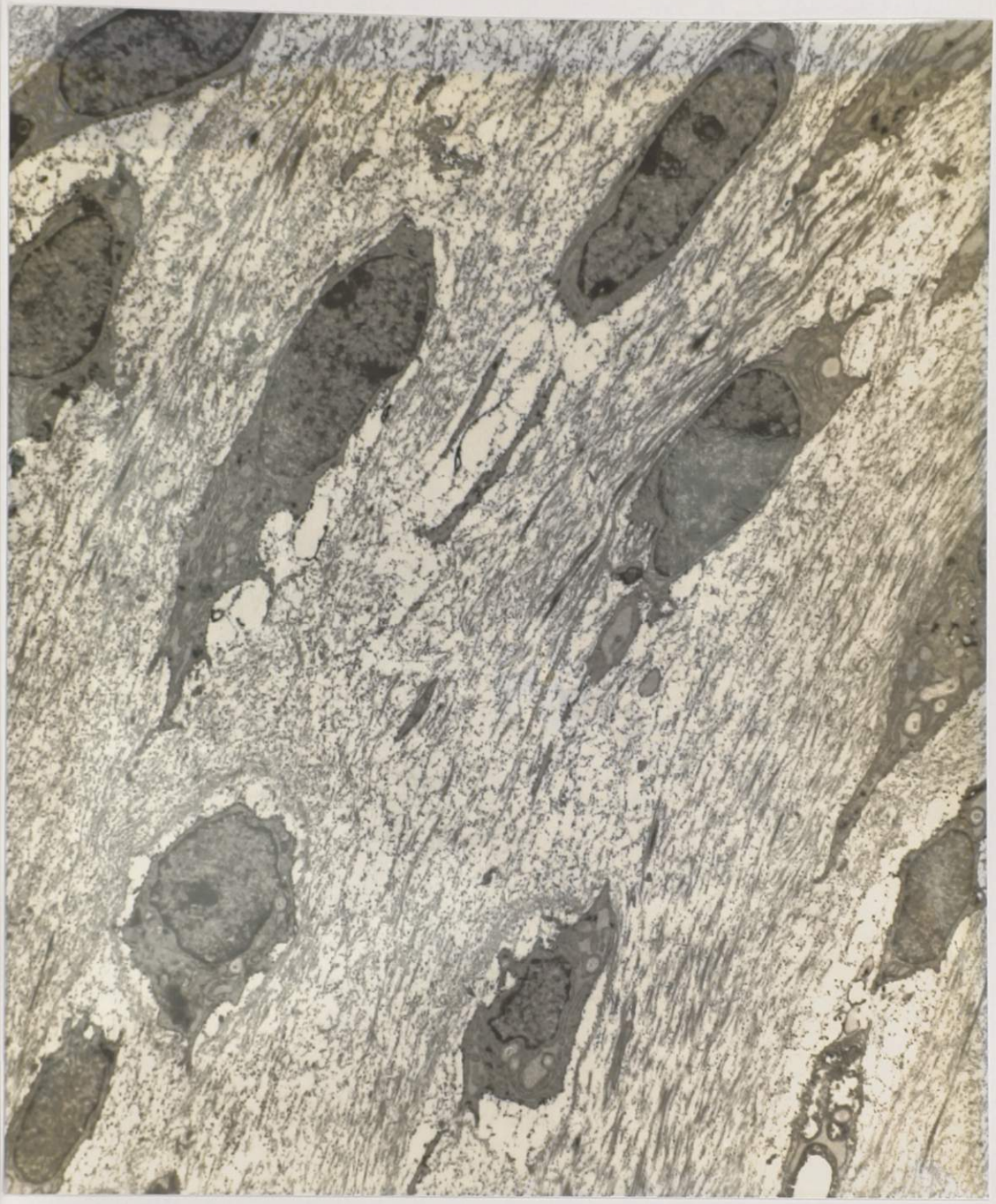

Figure 4.24b The annulus fibrosis of the L5 disc is composed of fibrocartilage, similar to the iliac cartilage. It contains elongated chondrocytes in a matrix dominated by collagen fibrils arranged in a parallel orientation to the cells. There is no evidence of an intercellular network. X 3,800

Figure 4.25a A low-power SEM of this 20 WG female sacral specimen shows a relatively smooth surface. At one end of the joint, there is a defect where several strips of cartilage were removed for transmission electron microscopy (arrows). At the other end of the joint there are some flakes of debris (arrowheads). X 70

Figure 4.25b A low-power SEM of the iliac surface shows numerous strands of broken intra-articular fibrous septa (arrows). X 70

Figure 4.26 A LM of the specimen seen in figure 4.25 explains why the iliac surface is covered by fibrous strands. The strands are broken intra-articular fibrous septa that form from the iliac surface during cavitation (arrowheads). Several vascular channels are visible in the sacral cartilage anlage (arrows). S-O, X 88

Figure 4.27a The sacral surface of this 18 WG male specimen shows depressions or pits (arrows) that represent underlying shrunken chondrocytes. The surface is not smooth, but wrinkled (arrowheads). Wrinkling is a drying artifact that develops during processing. X 696

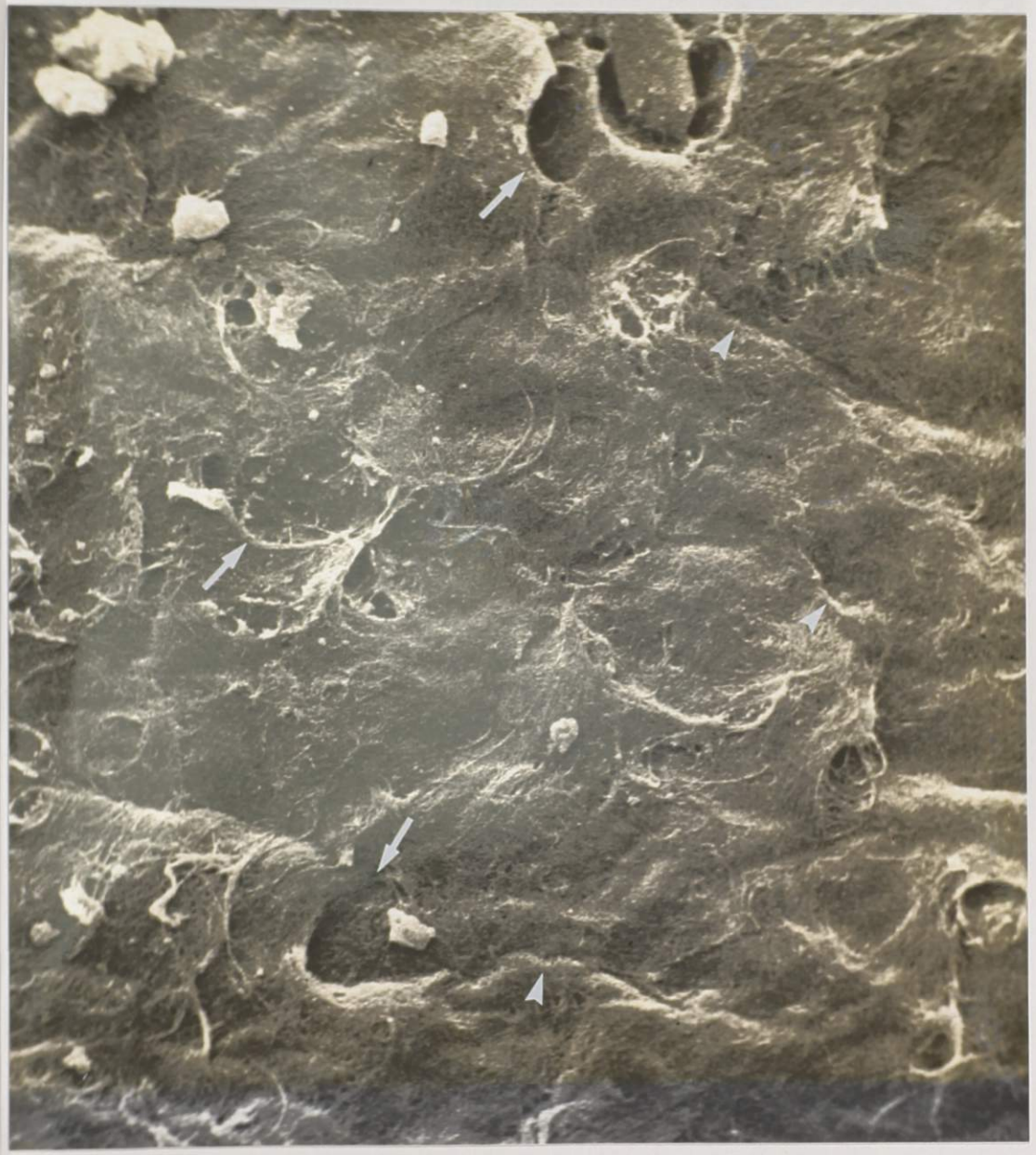

Figure 4.27b A high-power view shows the pits (arrows) and wrinkles (arrowheads) in detail. X 3,480

Figure 4.28a The iliac surface of the specimen in figure 4.25 is less cellular. Only one pit is visible, and it is elongated, like a spindle cell (arrow). Wrinkling (arrowheads) of the surface is present, and some debris remains on the surface, despite careful washing with saline. X 667

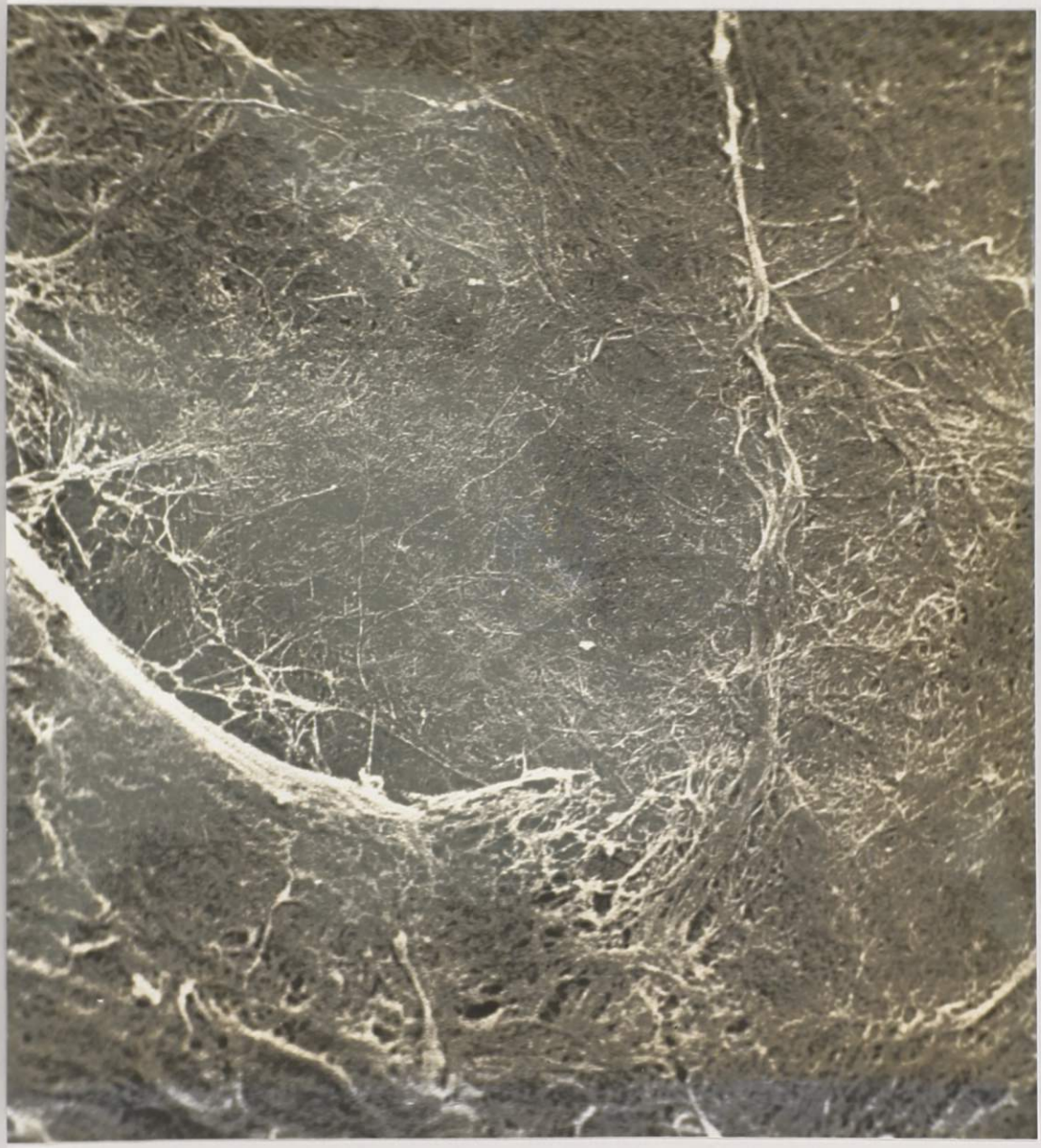

Figure 4.28b A high-power view shows the fibrous nature of the iliac surface. X 3,262

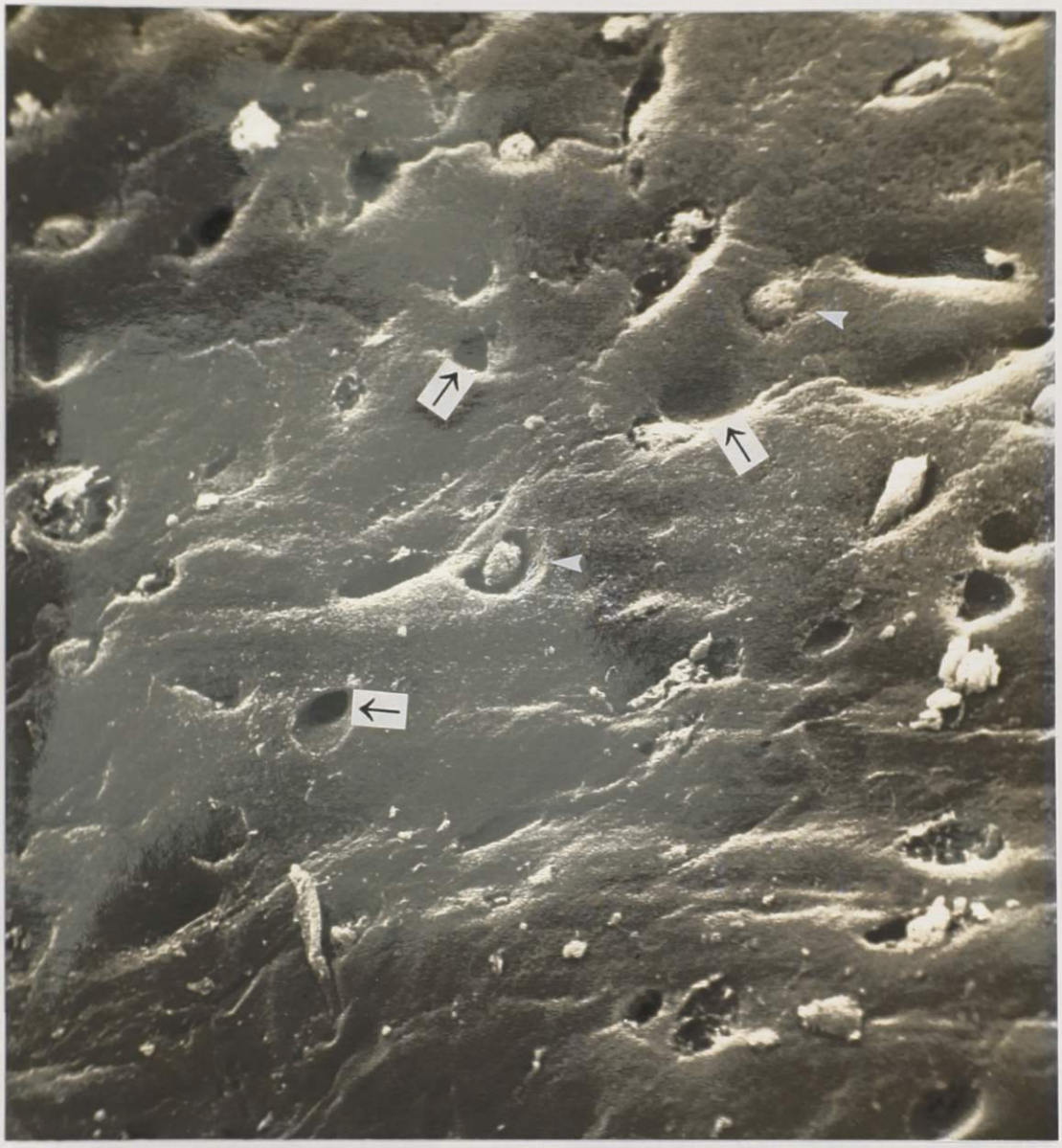

Figure 4.29a The sacral surface of this 19 WG male specimen SEM shows numerous pits (arrows). These represent surface chondrocytes that have collapsed. In some cases, the pits contain cells (arrowheads). X 1,566

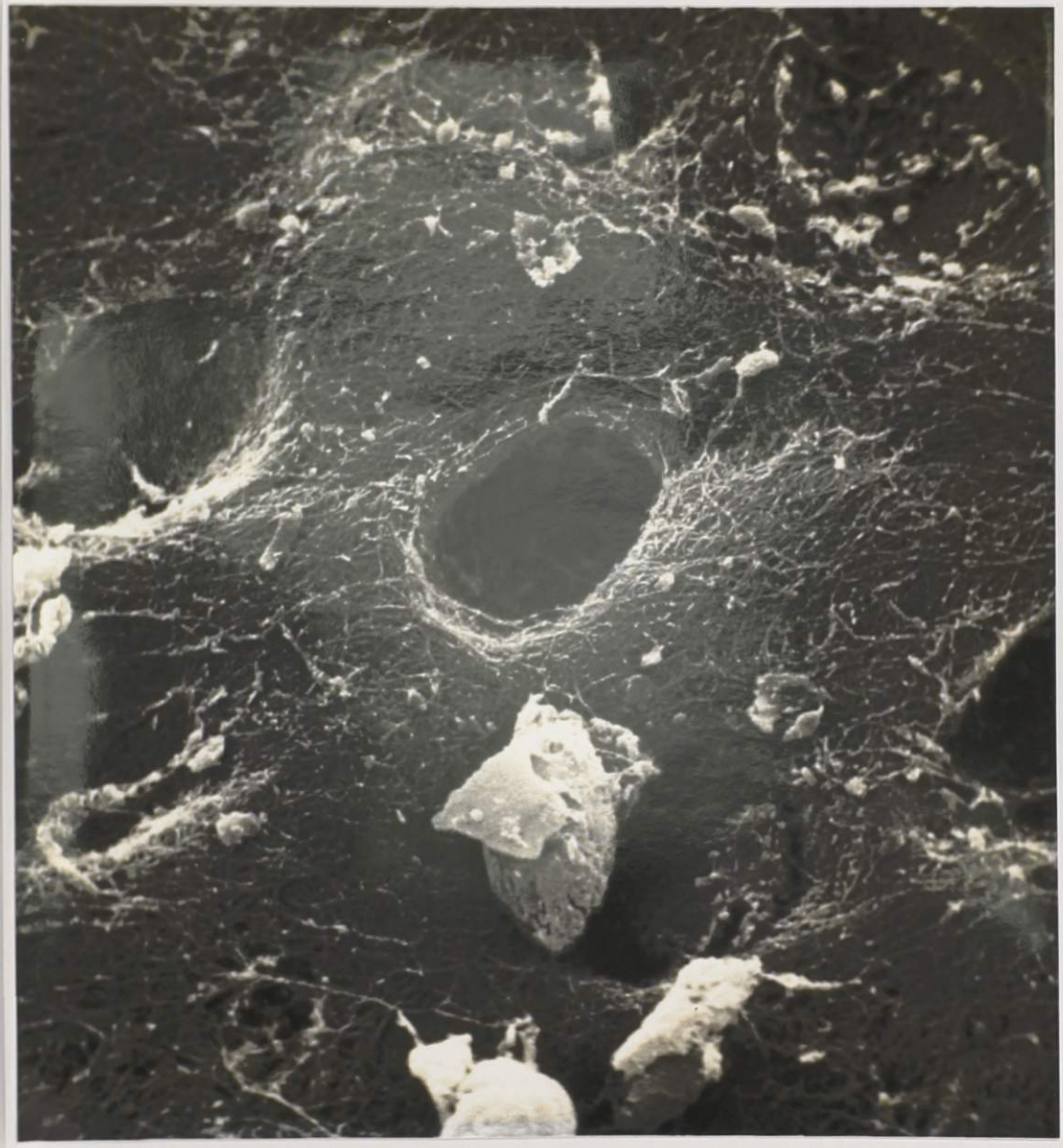

Figure 4.29b A high-power view of the above specimen shows that some of the pits appear very deep. At this power, the fine fibrillar zone I surface matrix is visible. X 6,090

Figure 4.30a The iliac surface of the 19 WG male specimen in figure 4.27 appears like a tangled web of fibres. Several cells are visible on the surface, including a fibroblastic cell with a long cell process (small arrow) and a larger elongated cell (large arrow). X 1,711

Figure 4.30b A high-power view shows cells (arrows) embedded in the fibrous matrix of the iliac surface. X 6,960

Figure 4.31a This low-power view of a 28 WG male specimen shows the continuation of chondrogenesis (arrowheads) on the iliac side. S-O, X 35

Figure 4.31b A higher-power view shows a band of developing chondrocytes adjacent to the ilium (il). These cells form columns that are surrounded by a metachromatic matrix. Most of the iliac side is composed of undifferentiated mesenchyme (m) that overlies the chondrocytes. S-0, X 88

.ntercellular network persists on the sacral side, and can ıave a variable presence, depending on the area of section. (Figure 4.32) Sacral chondrocytes are more commonly seen in ›airs with a more prominent territorial matrix. (Figure 4.33) Their cytoplasm contains more lipid and glycogen.

A variety of cells can be seen in the developing iliac cartilage, depending on the level of section. (Figure 4.34) At the surface, there are elongated cells, similar to zone I chondrocytes, embedded in a collagenous matrix. (Figure 4.35) Below the surface, there is a mixture of chondrocytes, chondroblasts and spindle cells. (Figure 4.36) Generally, the iliac matrix continues to be dominated by collagen and most of the cells do not have a territorial matrix. However, near the osteochondral border, the cells appear more like chondrocytes and do have a territorial matrix. (Figure 4.37) These cells also appear in pairs and contain more lipid and glycogen than the undifferentiated cells near the joint surface. In addition, some of the chondrocytes contain intracytoplasmic filaments. (Figure 4.38) These are most likely vimentin filaments, which are sometimes seen in zone III chondrocytes of normal articular cartilage (Ghadially, 1983). Since there are some small blood vessels present on the iliac side, the occasional macrophage and mast cell are present. (Figure 4.39)

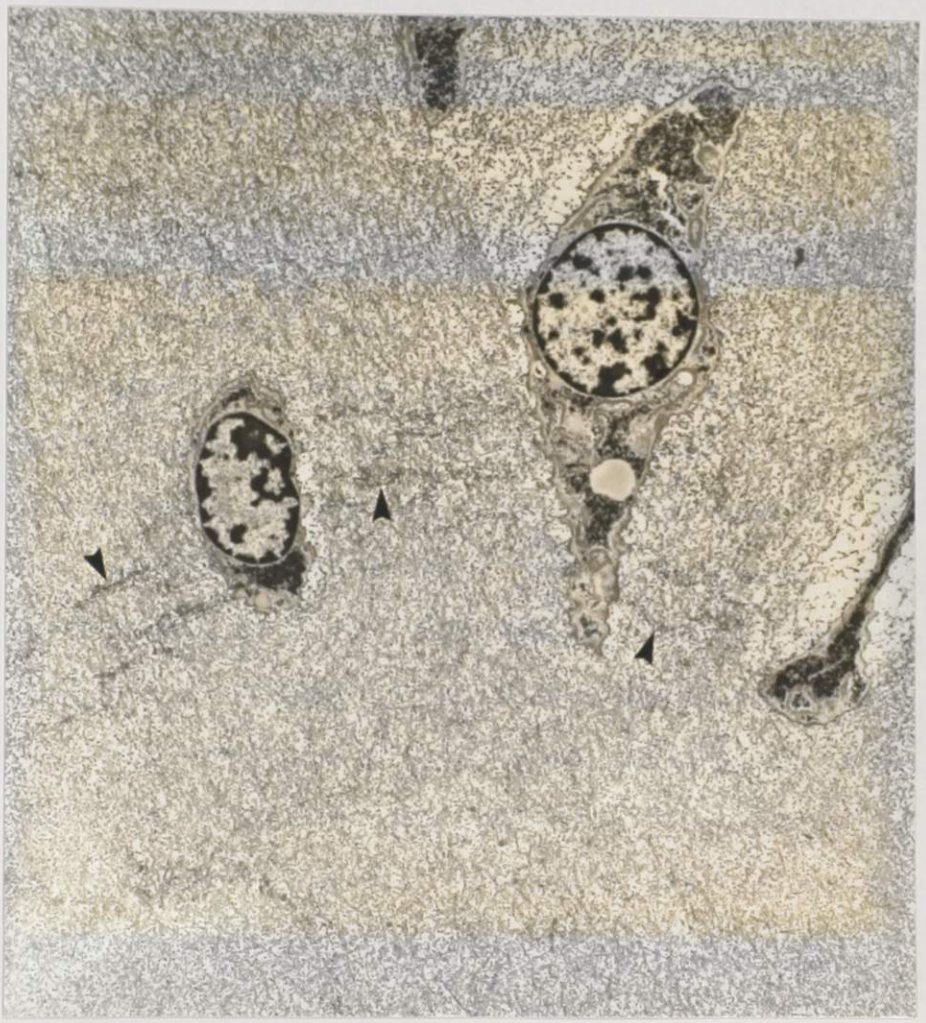

Figure 4.32 The intercellular network is less prominent in the sacral cartilage of this 28 WG male specimen. Several strands (arrowheads) are present connecting two sacral chondrocytes. The network can have a variable presence, depending on the area of section. X 4,600

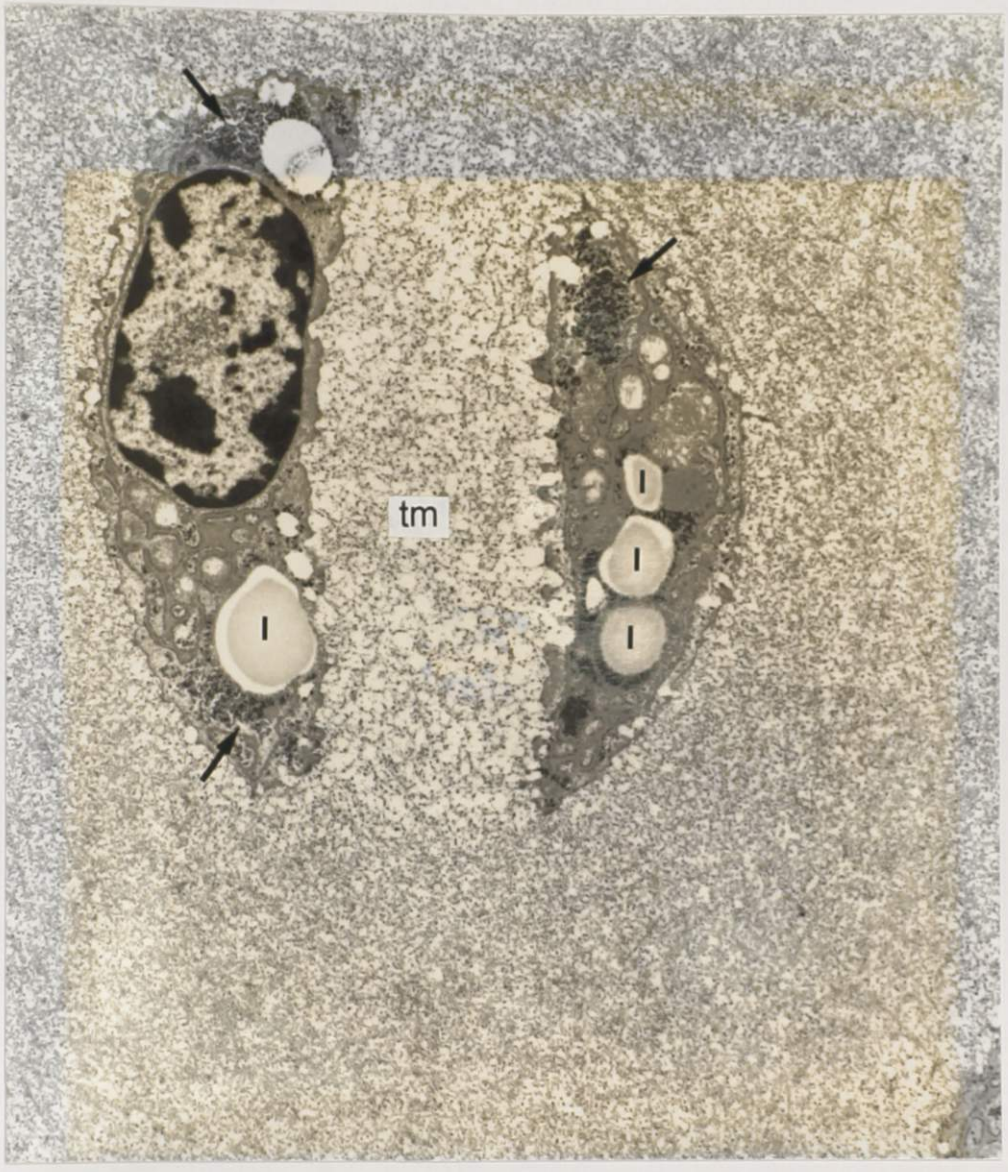

Figure 4.33 During the third trimester, the sacral chondrocytes mature. The cells contain more glycogen (arrows) and lipid droplets (l), which are often closely associated. The two chondrocytes in this 32 WG female specimen share a common territorial matrix (tm). X 5,985

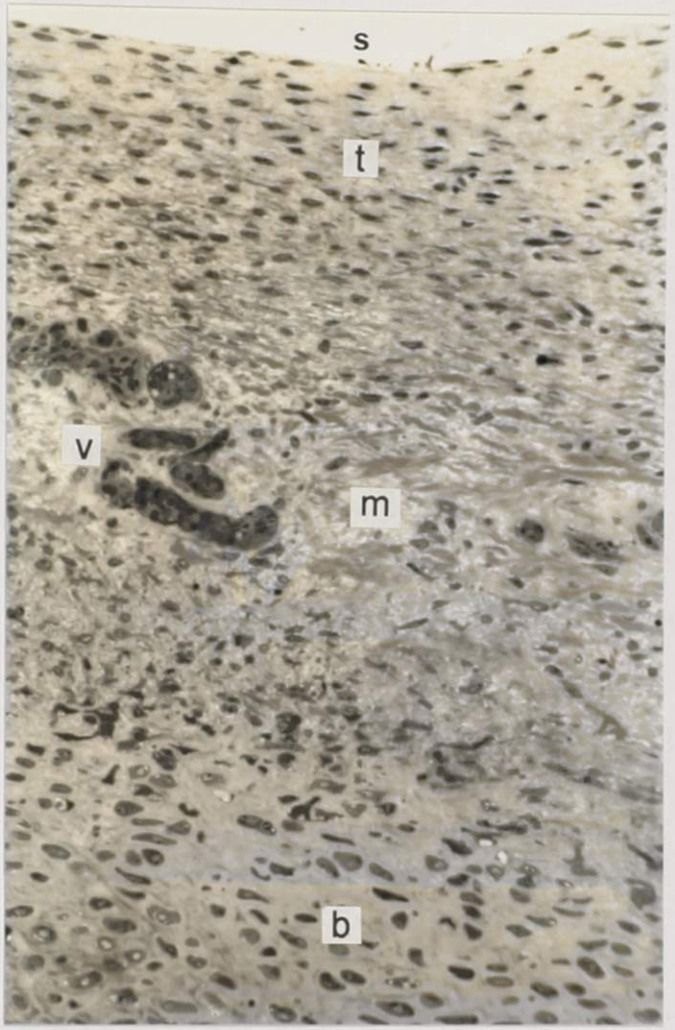

Figure 4.34 The iliac side of the sacroiliac joint in this 37 WG male specimen is composed of a variety of tissues and cells. Near the surface (s), the top third (t) is composed of spindle cells embedded in a collagenous matrix. The middle third (m) contains small blood vessels (v) and a variety of cells in a more loose connective tissue matrix. The bottom third (b) is composed of developing chondrocytes, adjacent to the ilium. T-B, X 220

igure 4.35 The iliac joint surface (s) of this 34 WG male pecimen is composed of parallel collagen fibrils and longated fibroblastic cells. X 4,750

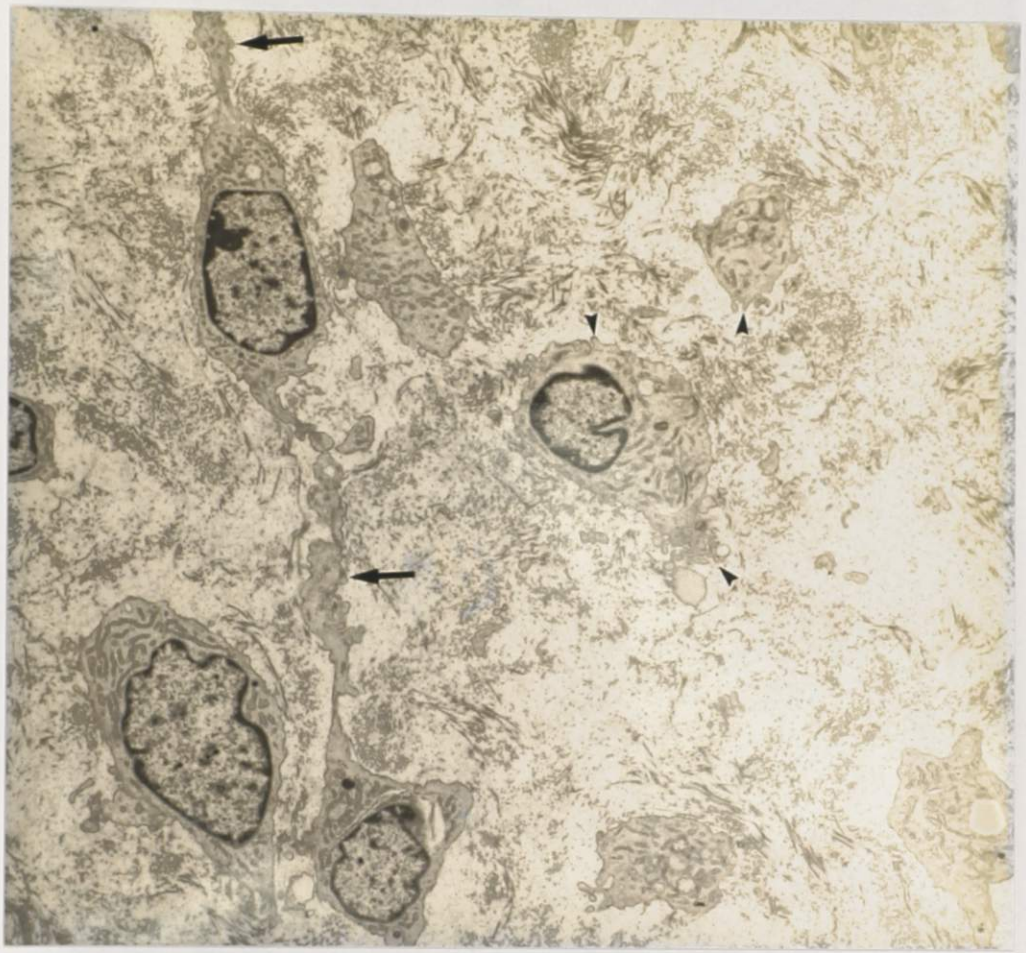

Figure 4.36 A variety of undifferentiated cells are present in this TEM of the iliac cartilage of a 28 WG male. Some cells have elongated cell processes (arrows), similar to fibroblasts. Others are round with short processes (arrowheads), similar to chondrocytes. The matrix contains an abundance of collagen fibrils. None of the cells have a territorial matrix. X 11,500

Figure 4.37 Two paired chondrocytes, surrounded by a well-developed territorial matrix (tm), are visible in this 32 WG female specimen. These cells have the typical features of chondrocytes, including short cell processes, glycogen particles (arrows), a lipid droplet (l), and rough endoplasmic reticulum (arrowheads). X 4,750

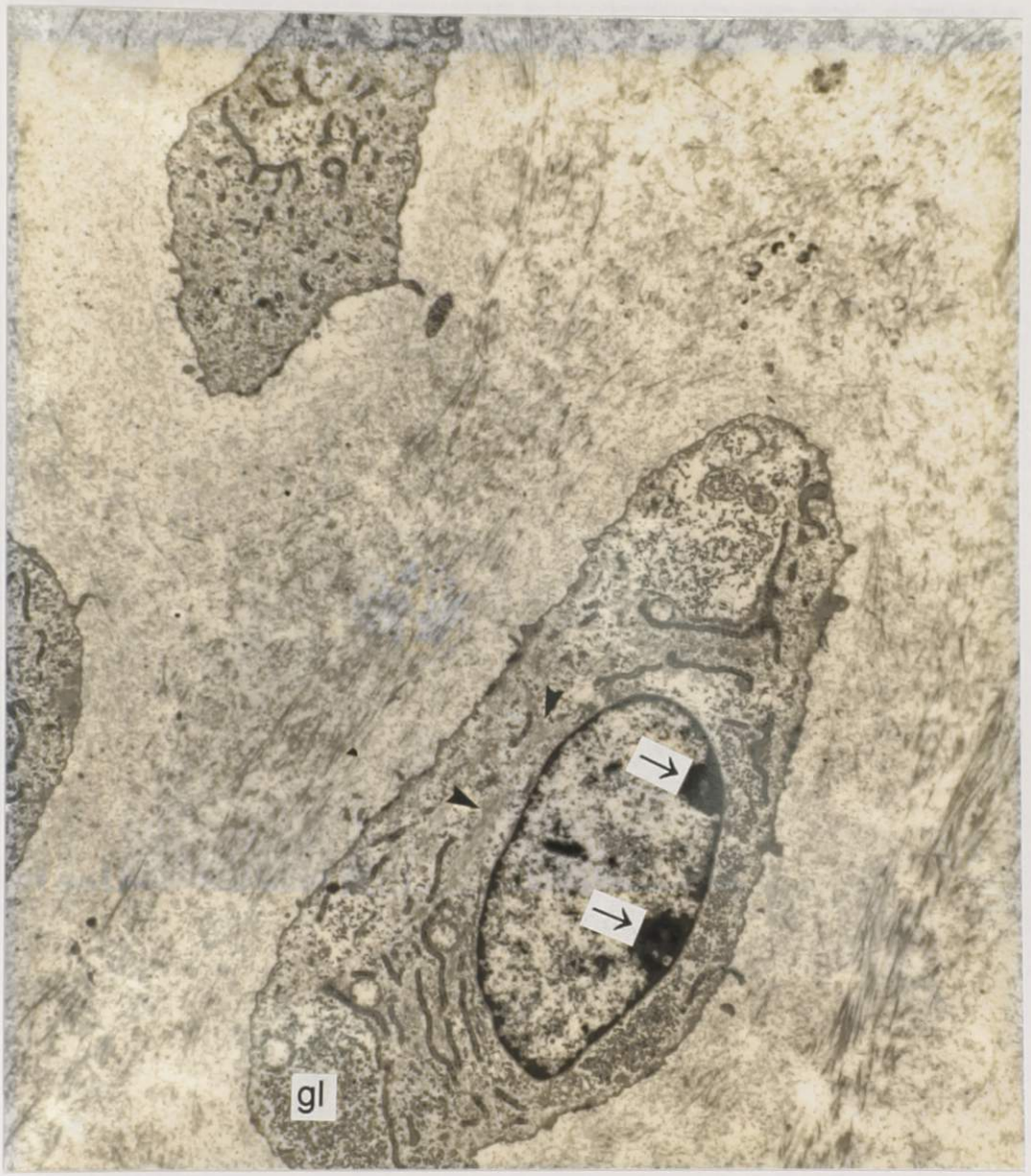

Figure 4.38 An iliac chondrocyte, located adjacent to the osteochondral border in a 34 WG male specimen, contains intracytoplasmic filaments (arrowheads). This plane of section shows two nucleoli (arrows). In addition, the cell contains an abundance of glycogen (gl). X 4,750

Figure 4.39 A mast cell is present in this section from a 34 WG male iliac specimen. It contains electron-dense secretory granules (arrows) that contain heparin and histamine. The cell has well-developed cell processes. X 5,985

Figure 4.40 A photograph of the gross appearance of a newborn male sacroiliac joint. The sacral surface (s) has a well-defined, creamy-white appearance, and an auricular shape. In contrast, the iliac surface (i) is difficult to distinguish from the surrounding bone. X 6

Figure 4.41a This low-power view of a two-month old female sacroiliac joint shows the staining characteristics of the two distinct areas of the iliac cartilage. At the iliac osteochondral border and throughout the sacral side, the cartilage stains deeply metachromatic (arrows). In these regions, chondrocytes are producing proteoglycans that are responsible for this reaction. There is no evidence of metachromasia in the other areas of the iliac cartilage. This indicates a lack of proteoglycan-producing chondrocytes. In addition, there is a large intra-articular fibrous septum running between the two joint surfaces (arrowhead). S-O, X 22

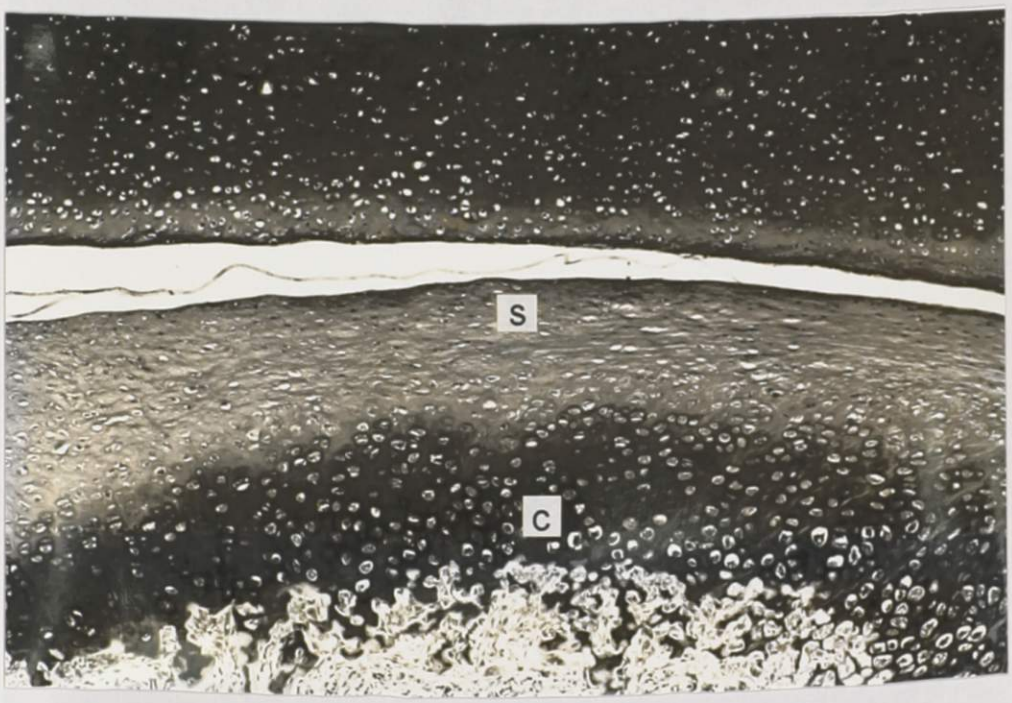

Figure 4.41b The high-power view shows columns of round chondrocytes (c) in the metachromatic region of the iliac cartilage. Above this area, there are spindle-cells (s), embedded in a collagenous matrix. S-O, X 35

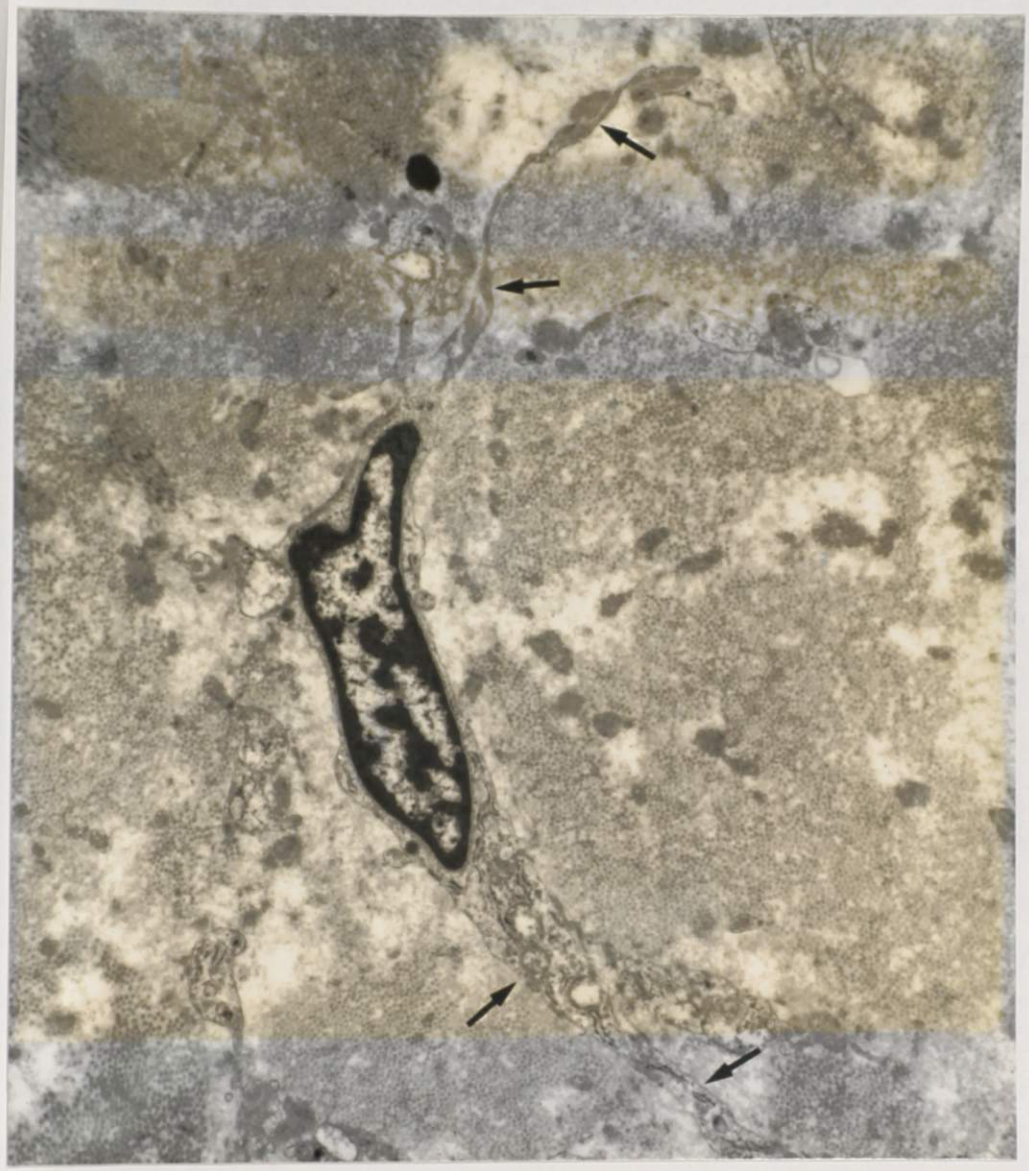

Figure 4.42 A TEM of a cell from the upper region of the iliac surface of a two-month-old male has several long cell processes (arrows). Its scant cytoplasm contains a few profiles of rough endoplasmic reticulum and a Golgi complex. X 7,600

Figure 4.43 A TEM of the iliac fibrocartilage region of a one-month-old male specimen shows cells that appear more like chondrocytes than fibroblasts. They have rounder nuclei, shorter cell processes, and more organelles, such as mitochondria and rough endoplasmic reticulum. One of the cells contains some intracytoplasmic filaments in the perinuclear region (arrowheads). The surrounding matrix is dominated by collagen fibrils (cf), and the cells do not have a surrounding territorial matrix. X 4,750

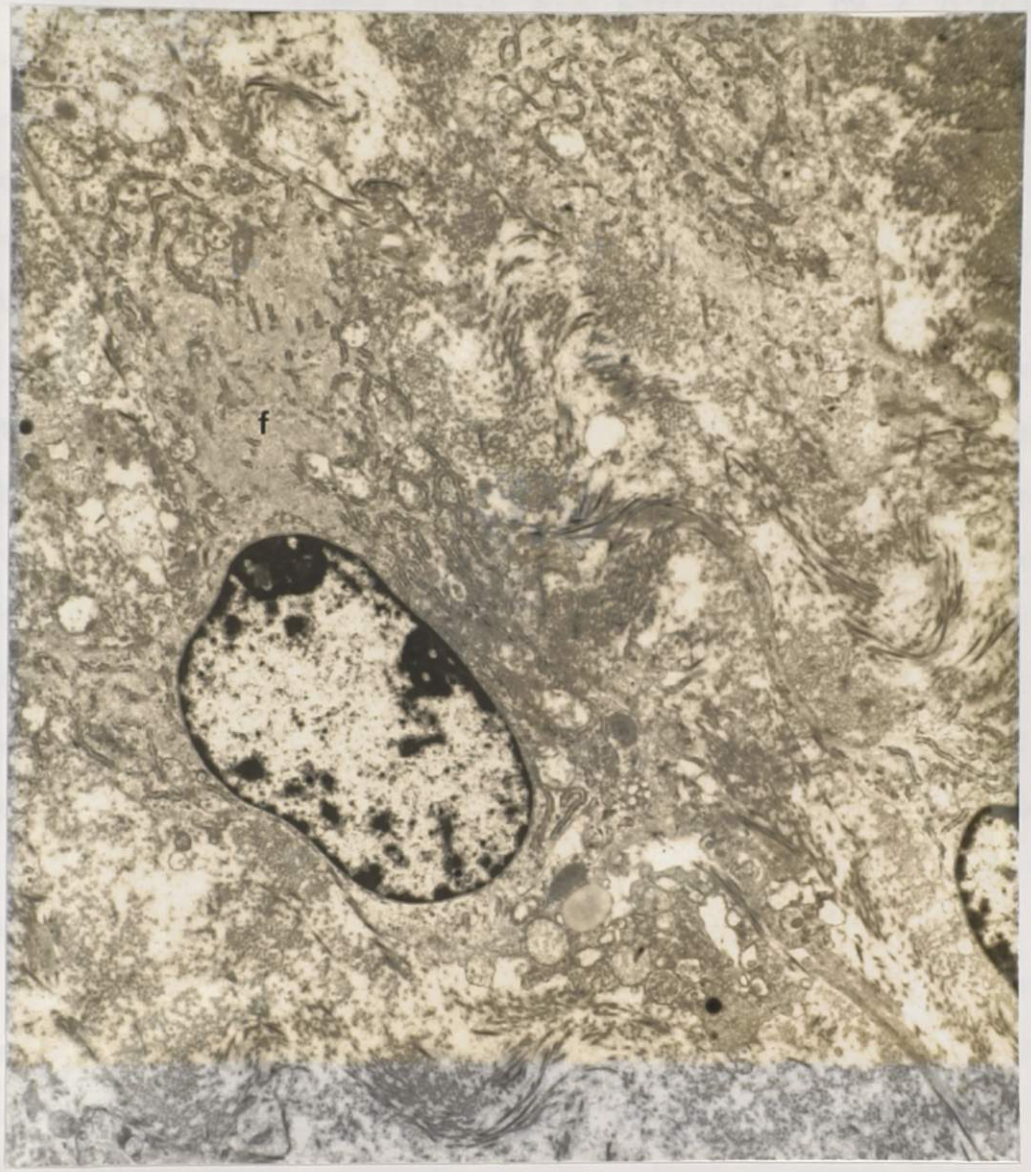

Figure 4.44 An iliac chondroblast in this two-month-old male specimen contains a considerable amount of intracytoplasmic filaments (f). The surrounding matrix is full of collagen. X 5,985

of the iliac cartilage contains columns of large chondrocytes, separated by bundles of collagen fibrils. (Figure 4.45) These cells are surrounded by a distinct territorial matrix, rich in proteoglycans. At the osteochondral border, there are necrotic chondrocytes, adjacent to new bone formation. (Figure 4.46) These cells eventually disappear as they are incorporated into the ilium during periosteal apposition.

At birth, the sacral cartilage appears much the same as it does during the embryonic period. There are areas where the interlacunar network is prominent, and other areas where it is absent. (Figure 4.47) The ultrastructural appearance of the network can vary from the usual single, densely-staining strand, to a group of closely-related strands connecting chondrocytes. (Figures 4.48 and 4.49) In some cases, the network appears thicker and more globular. (Figure 4.50) It is also present in the articular cartilage of the newborn's femoral head. (Figure 4.51)

During early childhood, the primary ossification centre in the ala of the sacrum expands by endochondral ossification, until it approaches the surface of the sacroiliac joint. (Figure 4.52) This process leaves an articular cartilage cap on the sacral side of the joint. On the iliac side, there remains a thin layer of fibrocartilage, and throughout childhood the two joint surfaces appear quite distinct. (Figure 4.53) Their gross appearance reflects this

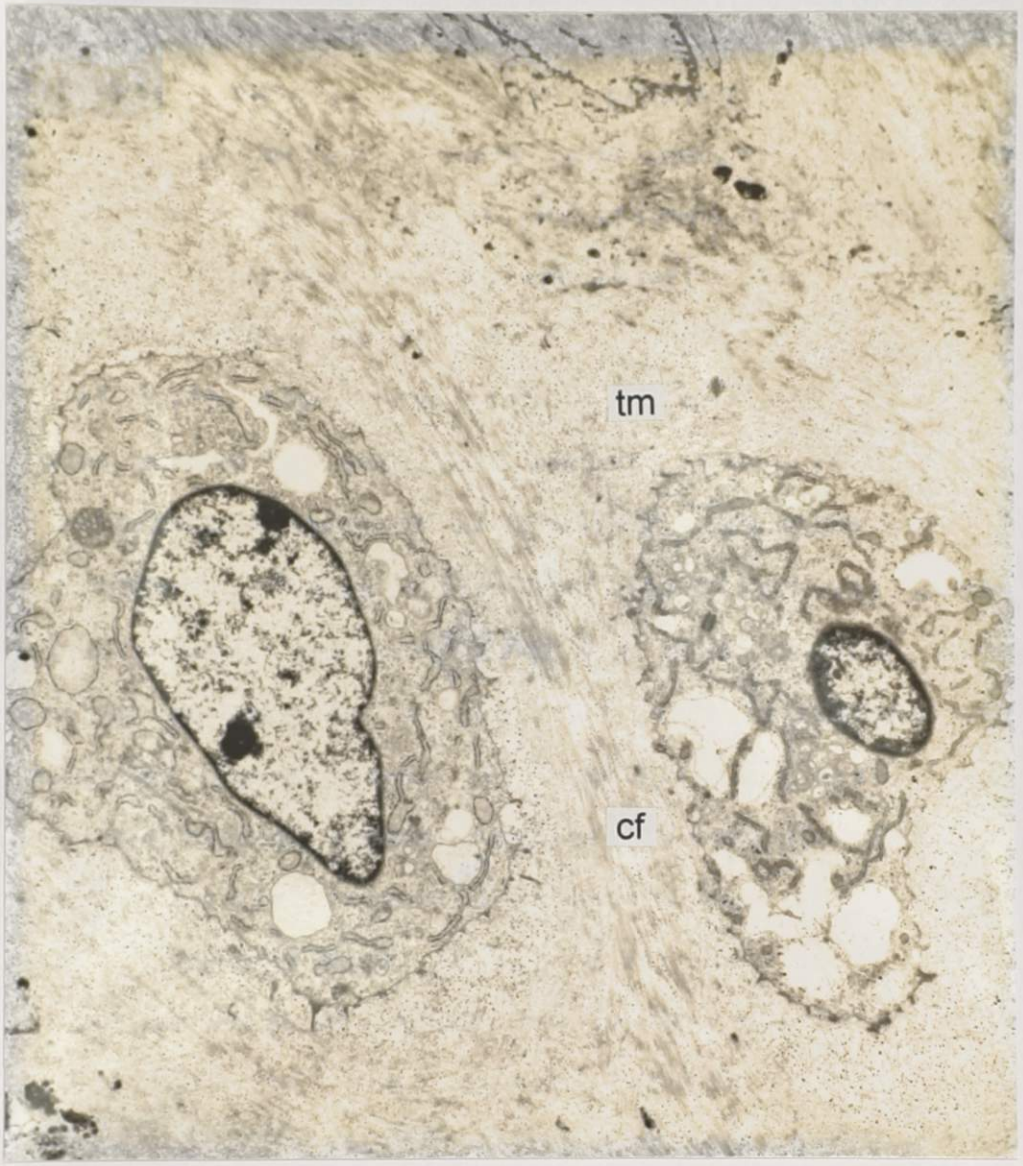

Figure 4.45 The deepest portion of the iliac cartilage of this one-month-old male specimen contains columns of large chondrocytes, separated by bundles of collagen fibrils (cf). These cells are surrounded by a distinct territorial matrix (tm) that is rich in proteoglycans. X 4,750

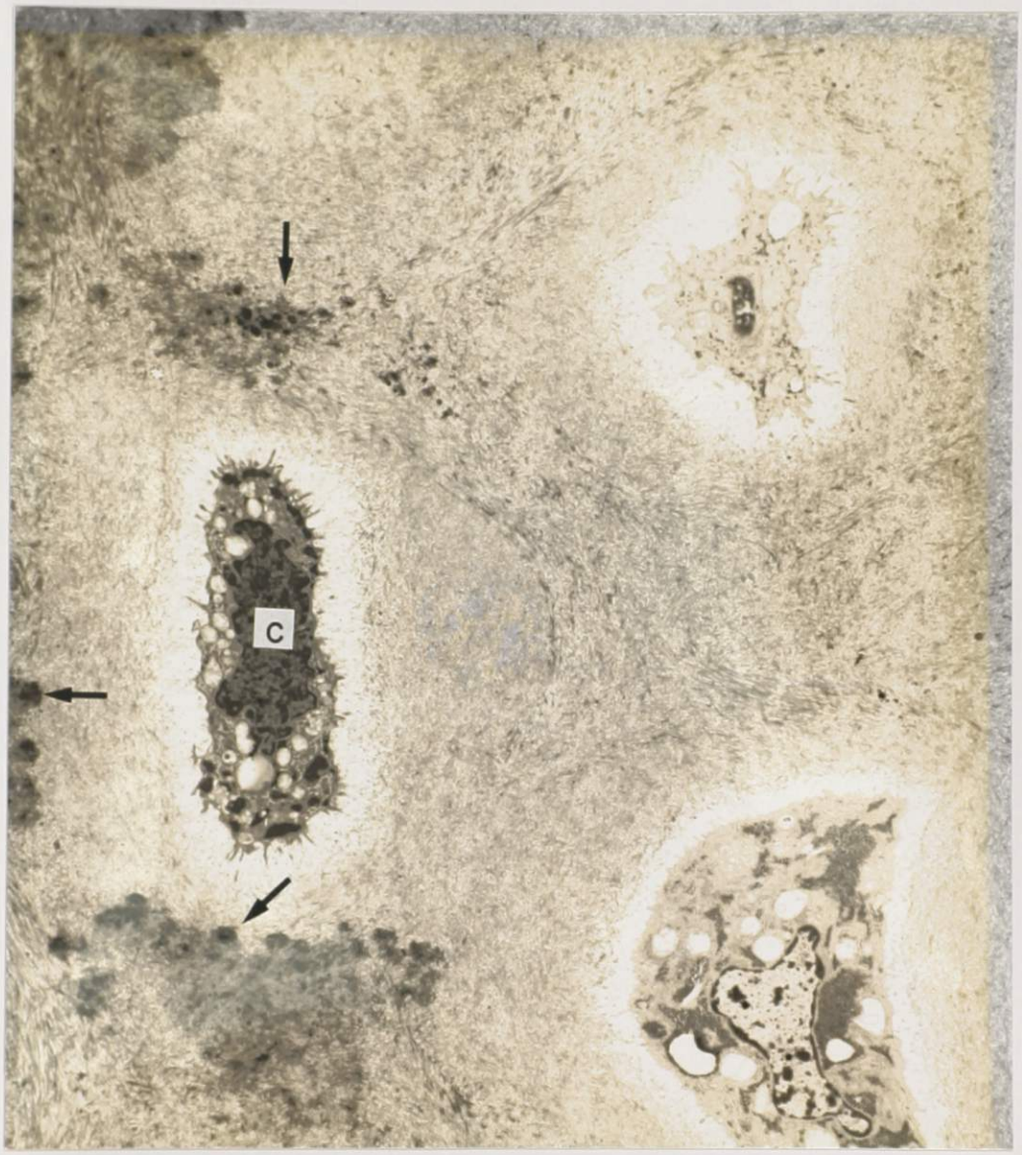

Figure 4.46 At the iliac osteochondral border of this five-month-old male specimen numerous electron-dense foci of mineralization can be seen in the collagen-rich matrix (arrows). A shrunken, dense chondrocyte (c) is visible near the osteochondral border. X 3,800

Figure 4.47 The interlacunar network is present in varying degrees in this one-micron section of a two-month-old sacral specimen. T-B, X 220

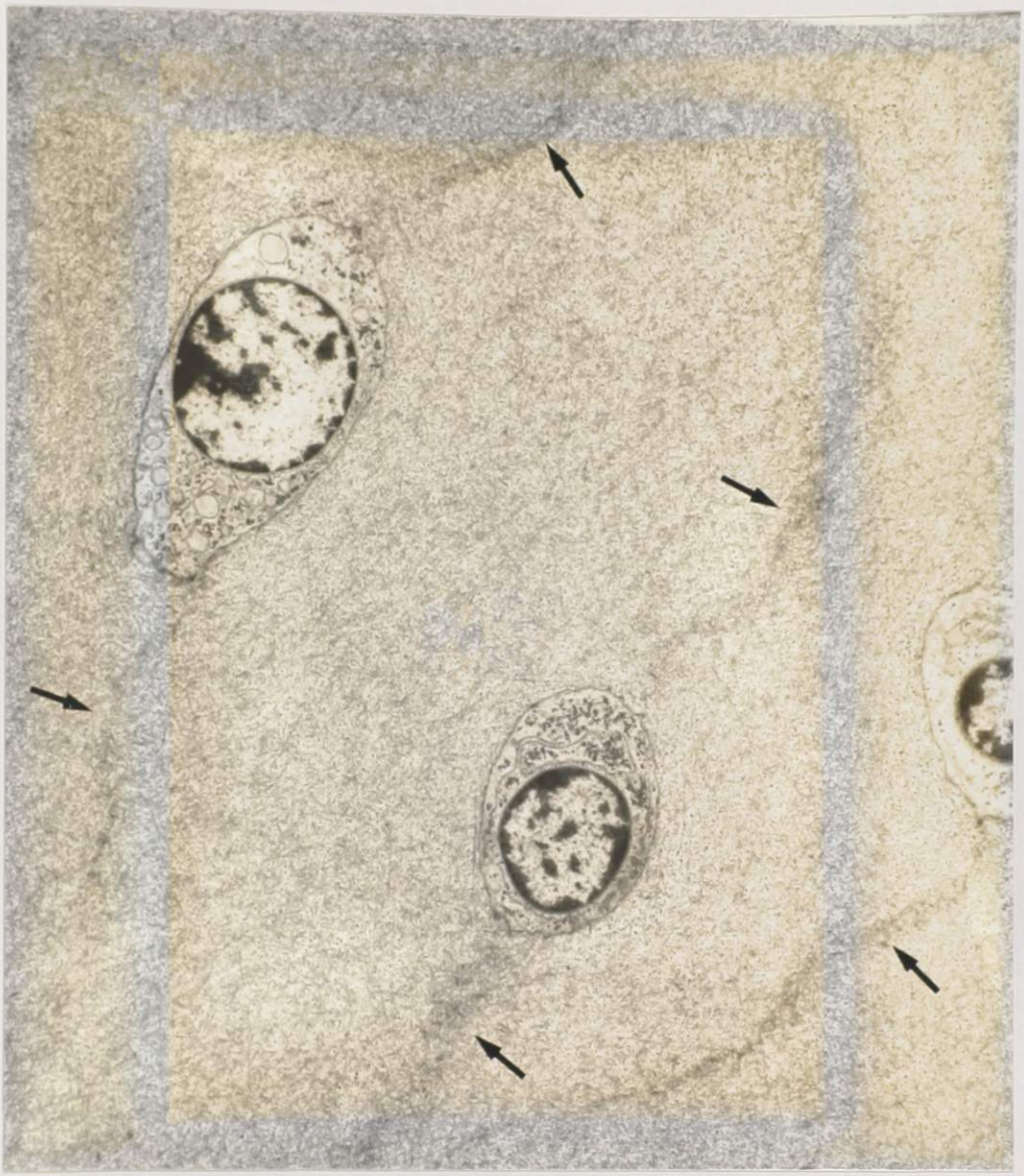

Figure 4.48 The interlacunar network usually appears as a single, electron-dense strand of material connecting two chondrocytes. In this two-month-old male sacral specimen, each chondrocyte has a single strand (arrows) originating from each pole of the cell. X 3,800

Figure 4.49 In some cases, the interlacunar network appears as a group of closely-related strands connecting chondrocytes. In this five-month-old male sacral specimen, there are branching groups of strands between the chondrocytes. X 3,800

Figure 4.50 The interlacunar network in this two-month-old male sacral specimen has a thick and globular appearance (arrows). X 3,800

Figure 4.51 An interlacunar network is present in the femoral head cartilage of this one-month-old male specimen. T-B, X 220

Figure 4.52 This low-power micrograph of a two-month-old female sacral specimen shows the advancing border of the sacral epiphyseal plate (arrows). During childhood, the plate advances towards the joint surface, leaving a hyaline cartilage cap, which forms the articular surface of the sacrum. S-O, X 22

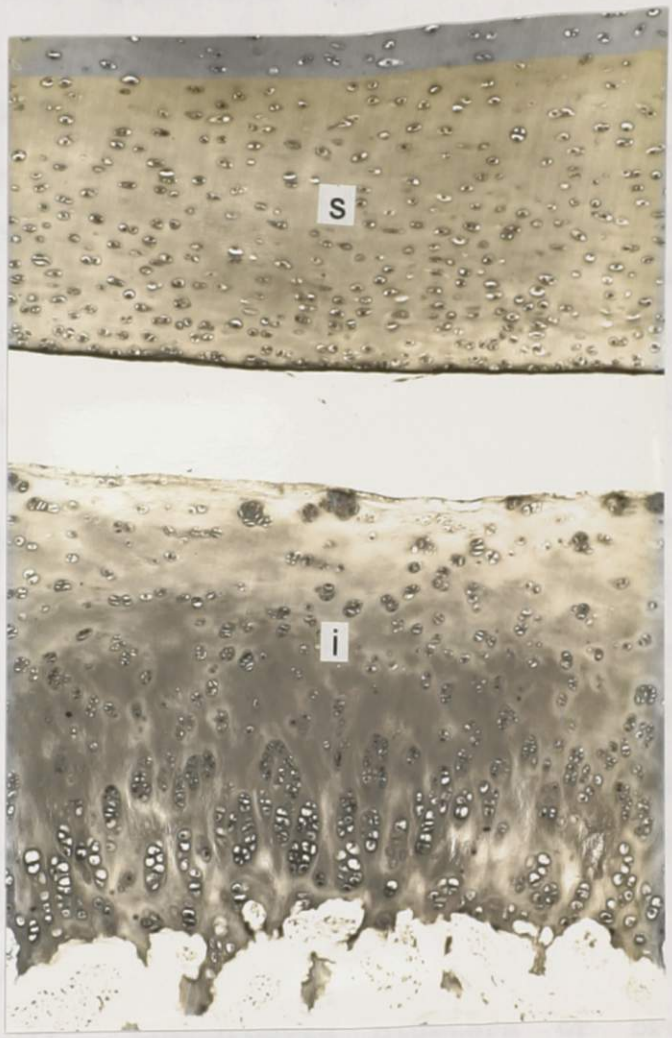

Figure 4.53 This micrograph of a two-year-old male sacroiliac joint shows the distinct morphology of the two articular surfaces. The sacral side (s) has the appearance of normal articular cartilage. Chondrocytes are evenly dispersed throughout the hyaline matrix. On the iliac side (i), the chondrocytes are grouped together into columns and small clusters known as brood capsules. The matrix does not have an even hyaline appearance. S-O, X 88

difference. (Figure 4.54) The sacral side has a smooth, creamy white appearance that is typical of articular cartilage. The iliac side has a more roughened appearance. It has a blueish tinge because the underlying blood and bone are visible through the thin transparent fibrocartilage. In addition, there is a well-developed anterior joint capsule, but there is no visible posterior joint capsule. (Figure 4.55) The posterior border of the sacral and iliac cartilage blends into the interosseous ligament, which must be considered an intra-articular ligament.

By the latter part of childhood, there is visible evidence of degenerative changes on the iliac side of the sacroiliac joint. The iliac surface appears rough and uneven, in contrast to the smooth sacral surface. (Figure 4.56) In places, the iliac fibrocartilage appears normal, but in other areas, the surface is frayed and split (fibrillation) and chondrocyte hyperplasia (clusters of cells) is present in the upper half of the joint cartilage. (Figure 4.57) Chondrocyte clusters or brood capsules represent cell proliferation in an attempt to repair the damage to the cartilage. The cells in the clusters are endowed with glycogen particles and prominent lipid droplets. In addition, the territorial matrix is thickened and intramatrical lipidic debris is present. (Figure 4.58) In some cells, the rough endoplasmic reticulum is dilated and the nucleus appears shrunken. (Figure 4.59) All of these

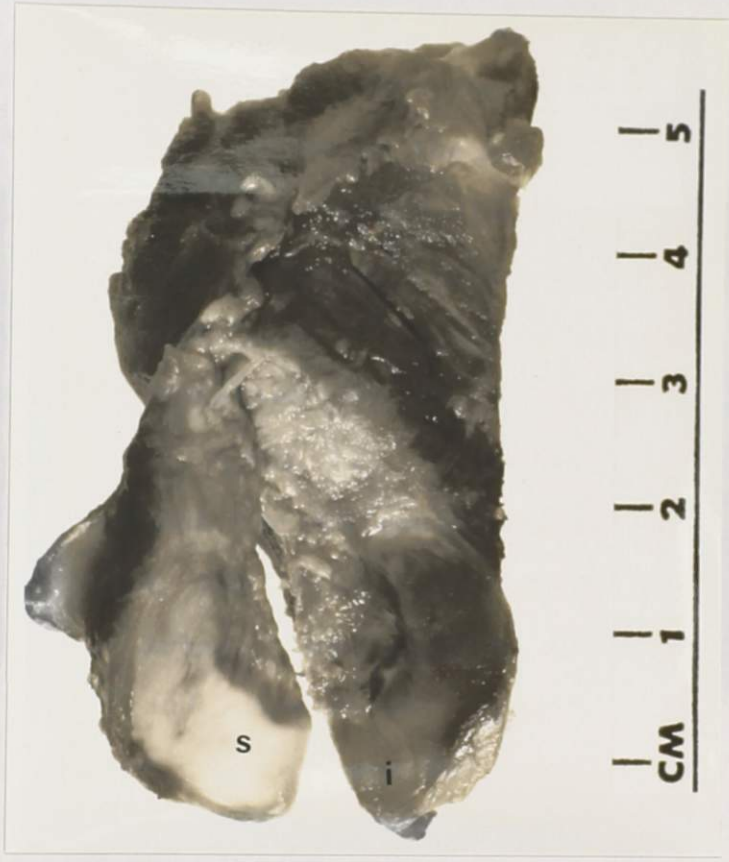

Figure 4.54 A photograph of a two-year-old male specimen reflects the different morphology of the articular surfaces. The sacral side (s) has a smooth, creamy-white appearance. The iliac side (i) has a more rough and dark appearance. X 1.7

Figure 4.55 A photograph of a six-year-old female specimen shows the distinct morphology of the two joint surfaces. The iliac surface (i) appears dark because the thin fibrocartilage is transparent. The joint capsule is prominent anteriorly (arrows), but absent posteriorly. The interosseous ligament (l) can be seen to insert directly (arrowheads) into the cartilage surface (s) of the sacrum. Since a joint capsule is not present posteriorly, the interosseous ligament should be considered an intra-articular ligament. X 2.8

Figure 4.56 The iliac surface (i) of this of this nine-year-old male specimen appears very rough and uneven. The insertion of the interosseous ligament (l) into the articular surface of the sacrum can be seen (arrowheads). X 1.2

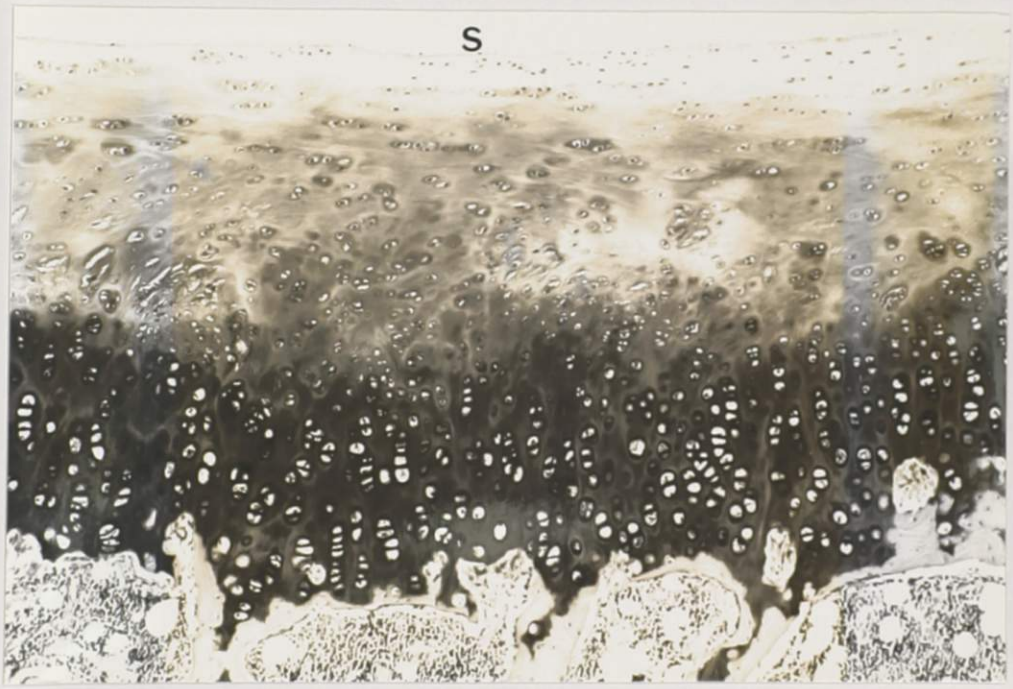

Figure 4.57a In places, the iliac surface (s) of the nine-year-old boy in figure 4.56 appears smooth and intact. S-O, X 88

Figure 4.57b In some other places, the iliac surface (s) appears roughened and fibrillated. There is an increased number of chondrocyte clusters (arrows). This proliferation of cells is an attempt to repair the surface damage. S-O, X 88

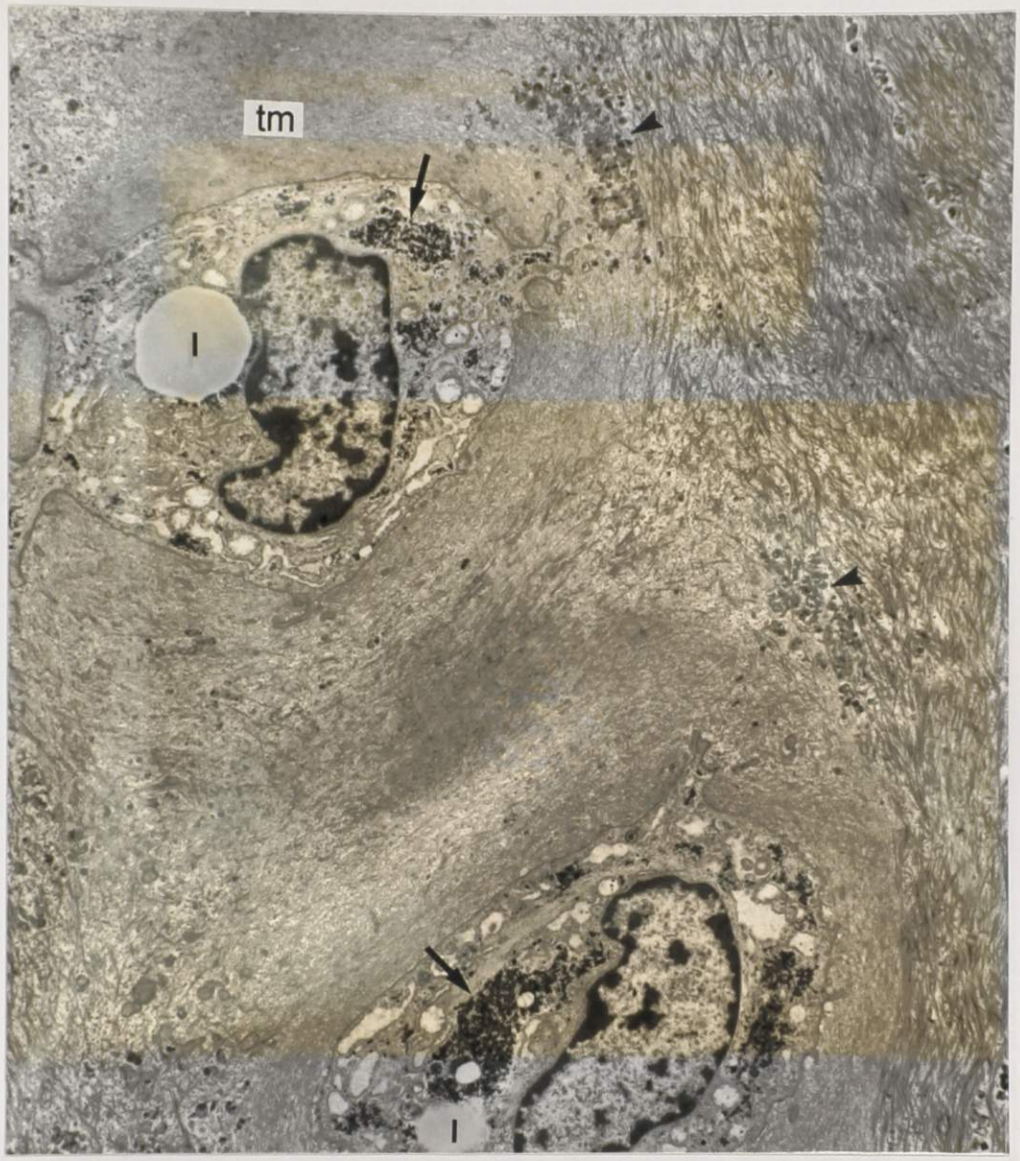

Figure 4.58 Chondrocytes from a cell cluster taken from the iliac cartilage of the nine-year-old boy in figure 4.56 have a thickened territorial matrix (tm) and contain glycogen particles (arrows) and lipid droplets (l). Intramatrical lipidic debris (arrowheads) is present and is generally regarded as a sign of chondrocyte degeneration (Ghadially, 1983). X 4,750

Figure 4.59 The cells in this cluster, from the same specimen as figure 4.56, have a dilated rough endoplasmic reticulum (arrows). In one of the cells, the nucleus (n) appears shrunken. X 5,985

findings have been associated with osteoarthrosis and ageing, but are an unusual finding in such young specimens.

The above changes are even more prominent in teenage specimens. The iliac surface is marred by surface erosions and flaking, while the sacral surface has the normal smooth appearance of articular cartilage. (Figure 4.60) With increasing age, the joint surfaces change from flat to irregular. (Figure 4.61) The sacral side develops a central depression or groove, into which an iliac ridge articulates. The sacral cartilage is thinner at the bottom of the groove and appears less smooth and more worn than the surrounding areas. This interdigitation of ridge and groove is similar to a tram rail, and is more conspicuous in male specimens.

Chondrocyte clusters are pronounced throughout the upper portion of the iliac cartilage. In some cases, their cell processes are irregular and folded. (Figure 4.62) The territorial matrix is thick and intramatrical lipidic debris is present. In other areas, there are cells associated with a predominately collagenous matrix. (Figure 4.63) Even on the sacral side, there are noticeable accumulations of intramatrical lipidic debris. It appears as electron-dense granular material. (Figure 4.64) These osmiophilic lipidic accumulations result from shedding of cell processes and in situ necrosis of chondrocytes. In most teenage cases, the sacral side has the histological appearance of normal articular cartilage. (Figure 4.65)

Figure 4.60 A photograph of a 17-year-old male specimen shows obvious roughening and surface irregularities on the iliac (i) side of the joint. On the other side, the sacral surface (s) appears smooth. X 0.84

Figure 4.61 This photograph of a 19-year-old male specimen shows an iliac ridge (i) that fits into a corresponding sacral depression (s). This type of surface irregularity is common, particularly in male specimens. X 0.83

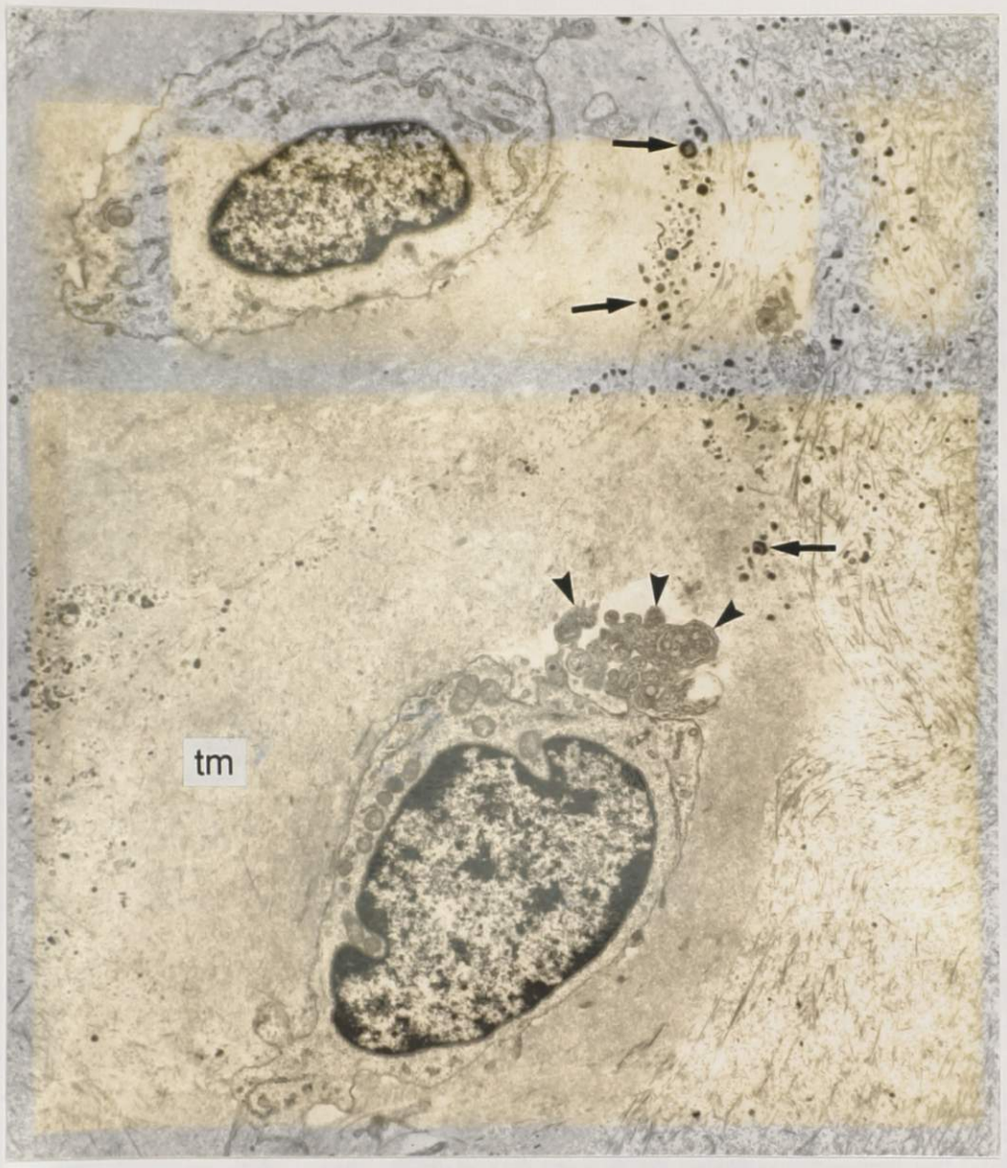

Figure 4.62 An iliac chondrocyte within a cluster in a 16-year-old male specimen has irregular and folded cell processes (arrowheads). The surrounding territorial matrix (tm) is thickened and contains some intramatrical lipidic debris (arrows). X 5,985

Figure 4.63 This atypical chondrocyte from a 16-year-old iliac specimen contains some intracytoplasmic filaments (arrowheads). It is located in a collagenous matrix and does not have an associated territorial matrix. X 4,750

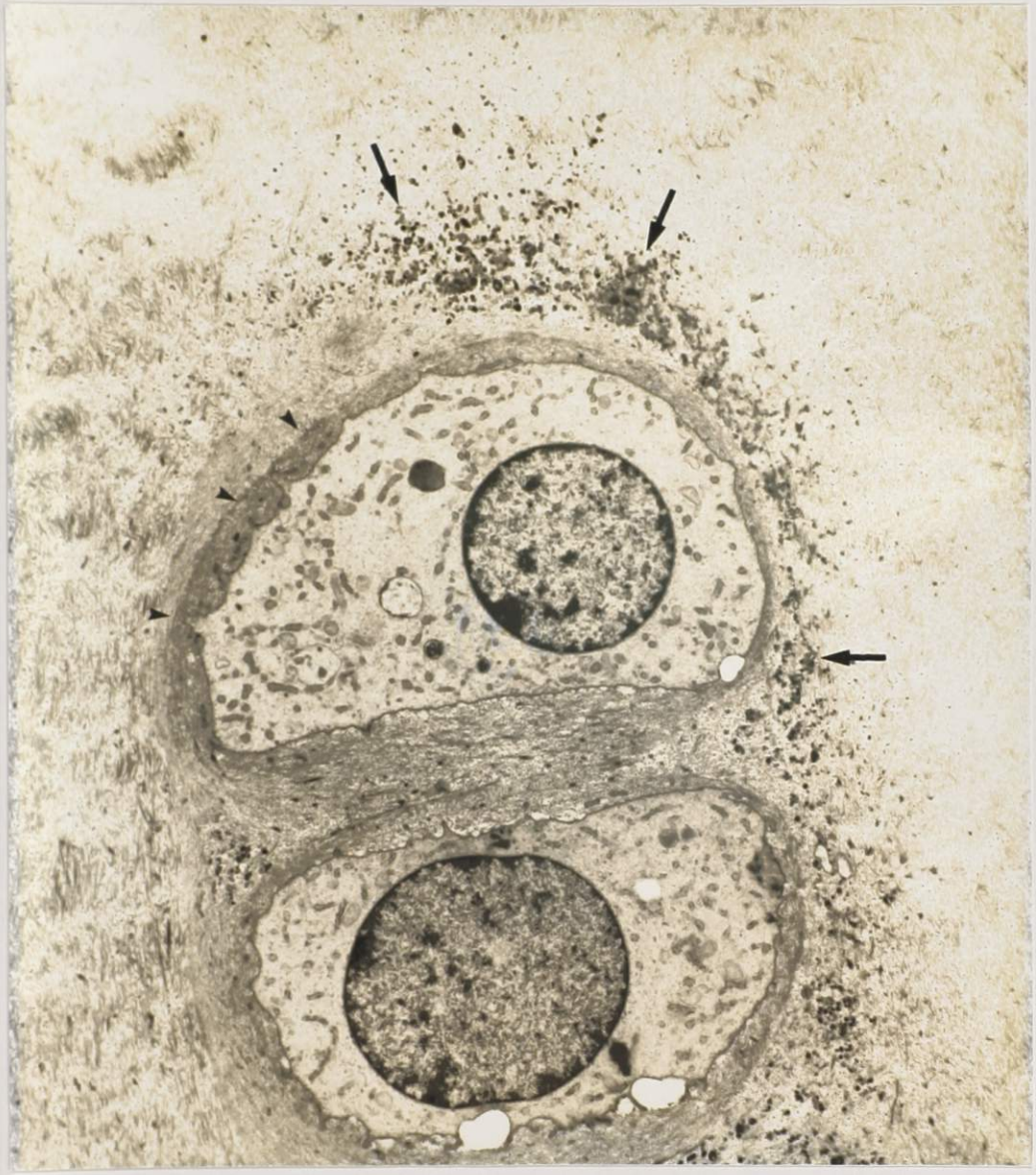

Figure 4.64 Two paired sacral chondrocytes from a 16-year-old sacral specimen are surrounded by a thin territorial matrix (arrowheads). There is a noticeable accumulation of intramatrical lipidic debris (arrows). X 4,750

Figure 4.65 The sacral cartilage of a 16-year-old male specimen appears like normal articular cartilage. There are no surface (s) irregularities or evidence of chondrocyte clustering. S-O, X 35

The gross appearance of all of the joints was graded according to the degree of degenerative change visible. With the exception of one specimen, all the joints were graded as smooth, or devoid of degenerative change. (Appendix A) One 19-year-old male specimen was graded as showing signs of moderate degeneration. (Figure 4.61)

4.2.2 Young Adults

The most prominent finding in young adult specimens is the gross, microscopic, and ultrastructural evidence of premature osteoarthrosis. The evidence is most marked on the iliac side of the joint, but the sacral side is affected too. In all the specimens, the iliac cartilage appears very rough with deep crevices and loose flakes of surface material. (Figure 4.66) In the older specimens, the surface can be so rough that it is difficult to identify the posterior border of the joint. (Figure 4.67) The absence of a posterior joint capsule contributes to this difficulty. Although the sacral side is similarly affected, there are some areas of smooth articular cartilage visible in the younger specimens. However, by the fourth decade of life, the sacral side also appears very rough. On gross inspection of all the specimens, five were rated as smooth, eight as showing moderate degeneration, and two appeared to be severely degenerated. (Appendix A)

Histological examination confirms the gross

Figure 4.66 The iliac cartilage (i) of this 23-year-old male specimen is roughened by deep crevices and loose flakes of surface material. On the sacral side (s) the cartilage surface is much smoother, but there are also some roughened areas.

Figure 4.67 By the fourth decade, the joint surfaces of the sacroiliac joint are extremely rough. In this 36-year-old male, it is difficult to differentiate the sacral from the iliac surface. On both sides, there is marked surface erosion and deep crevice formation. In addition, there is a prominent iliac ridge (i) that articulates into a deep sacral depression (s). This interdigitation of surface topography is a fairly constant feature in adult joints.

observations. By the third decade of life, the iliac surface of the sacroiliac joint has undergone obvious degenerative change. (Figure 4.68) There is marked surface erosion, fibrillation, and deep crevice formation that extends down to the underlying bone. The chondrocytes form large clusters, in an attempt at proliferative repair. Although it is possible to find areas of the iliac surface that are intact, chondrocyte clustering is always present. (Figure 4.69) On the other side, most of the sacral surface appears to be normal in younger specimens. However, at the base of the sacral surface depression, degenerative changes are often present. (Figure 4.70)

By the fourth decade, metachromatic staining of the sacroiliac joint shows marked depletion of proteoglycan content in both the sacral and iliac cartilages. (Figure 4.71) In addition, there are cellular signs of degenerative change at the surface of the sacral cartilage. These include surface fibrillation, erosion, and chondrocyte clusters. By the end of the fourth decade, the surface topography of the joint is quite irregular. (Figure 4.72)

Ultrastructural examination of young adult specimens confirms the presence of osteoarthrosis. In the sacral cartilage, the matrix contains more collagen, a paucity of proteoglycan particles, and an increase in intramatrical lipidic debris. This debris is the result of extruded chondrocyte cell processes and in situ necrosis of

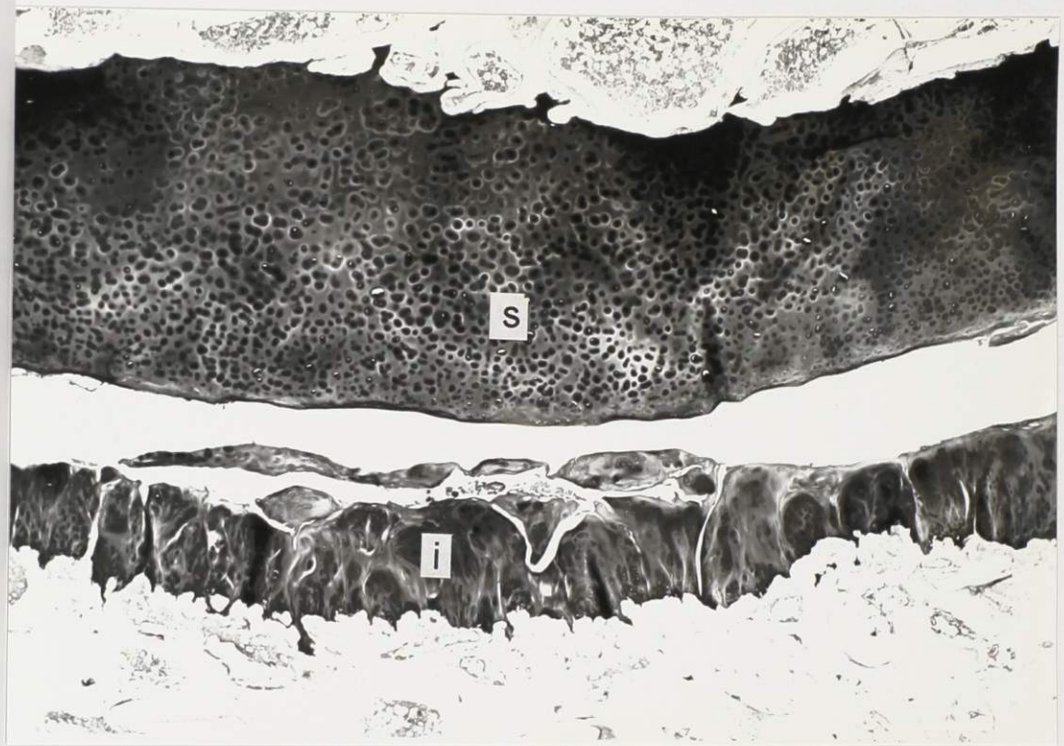

gure 4.68a This cross section of a 20-year-old male ecimen contrasts the sacral (s) and iliac (i) surfaces. e sacral surface is about three times as thick as the iliac rface and appears as relatively smooth articular cartilage. wever, the iliac side has undergone marked degenerative ange, with surface erosion and crevice formation. S-O, 22.

Figure 4.68b A high-power view of the iliac cartilage shows proliferative clustering of chondrocytes (arrows), secondary to the degenerative changes. There are deep crevices and erosion of the superficial layer of the joint surface. S-O, X 88

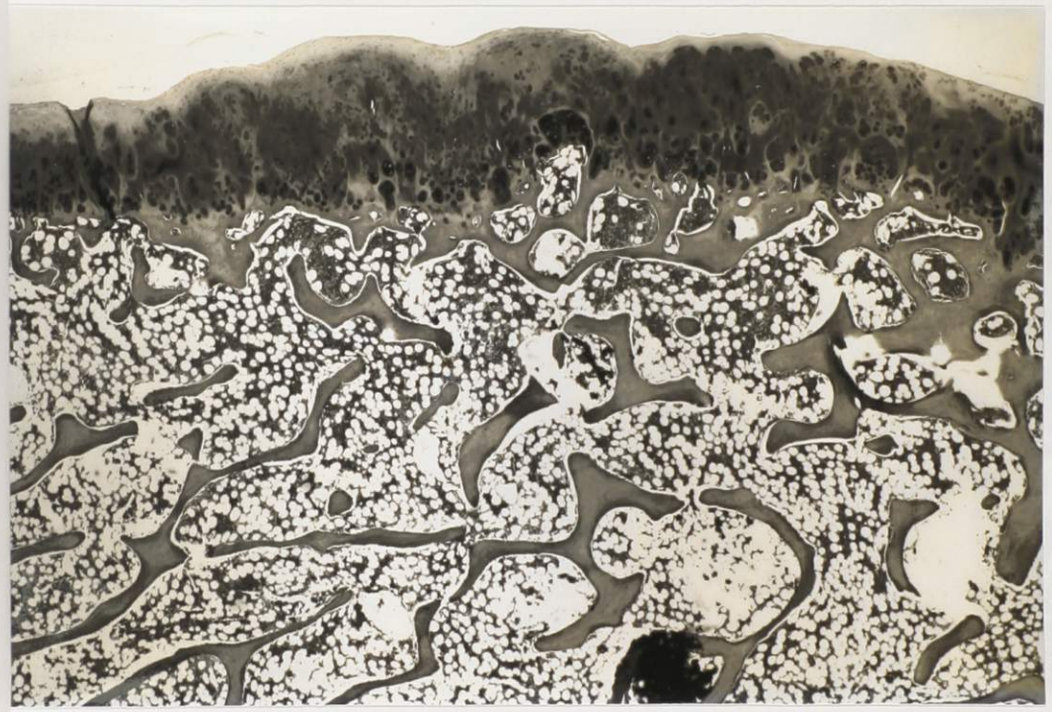

gure 4.69a The iliac surface of this 23-year-old male ecimen is intact, but there is marked chondrocyte ustering. S-O, X 22

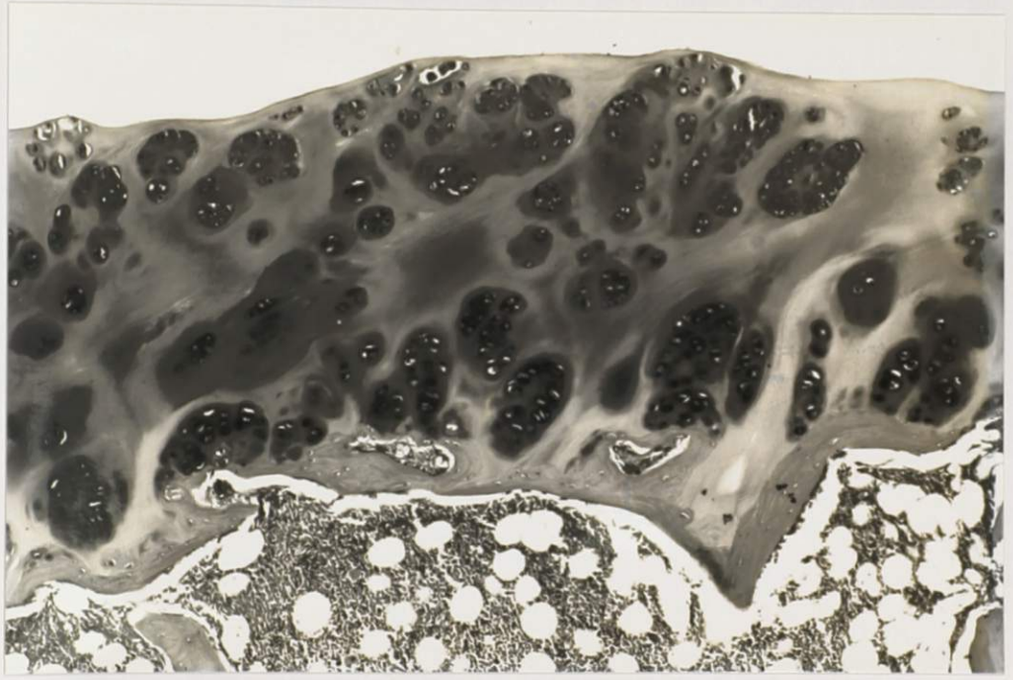

Figure 4.69b A high-power view shows the extent of the chondrocyte clusters. These clusters are an attempt at repair of the damaged articular cartilage. The matrix immediately surrounding the clusters stains metachromatically for the presence of proteoglycans. S-O, X 88

Figure 4.70a The sacral surface of this 23-year-old male appears relatively normal. Columns of chondrocytes have secreted enough proteoglycans to give the matrix a deep stain. Although the surface appears smooth, there is some decrease in proteoglycan production (arrowheads). These changes are suggestive of early osteoarthrosis. S-O, X 22

Figure 4.70b A section through the sacral depression reveals obvious degenerative changes. There is fibrillation and erosion of the surface (s), an absence of proteoglycan content, and clustering of chondrocytes. This depression fits into a prominent ridge on the iliac surface. S-O, X 22

Figure 4.71a The sacral cartilage of this 36-year-old male specimen shows very little metachromasia, indicating a depletion of the proteoglycan content in the matrix. There is some surface fibrillation (arrowheads) and chondrocyte clustering. S-O, X 22

Figure 4.71b The iliac cartilage also shows marked depletion of proteoglycans. In addition, there is chondrocyte clustering and joint surface fibrillation (arrowheads). The cell density is decreased in the surface region. S-O, X 22

Figure 4.72 A low-power view of the sacral surface (s) of a 38-year-old specimen shows the irregular topography of a fourth decade sacroiliac joint. S-O, X 22

chondrocytes. (Figure 4.73) The interterritorial matrix is depleted of proteoglycan particles, and there is an increase in collagen content. Giant collagen fibres are present and form microscars at sites of chondrocyte necrosis. (Figure 4.74) This is often referred to as amianthoid (asbestoid) degeneration. In other areas, matrix streaks are present, similar to the fetal interlacunar network. (Figure 4.75) In some cases, the territorial matrix is thick and contains more collagen than usual. (Figure 4.76)

Sacral chondrocyte morphology is also suggestive of degenerative changes. The cells contain more lysosomes, lipid droplets and intracytoplasmic filaments. (Figures 4.73a and 4.77) Some dense, shrunken, necrotic chondrocytes are also encountered. (Figures 4.73b and 4.78) Whorls of intracytoplasmic filaments are common. (Figure 4.77 and 4.79) These intermediate filaments are presumably vimentin, and are thought to be a regressive or degenerative change. Often they are closely associated to a lipid droplet or, they are present in the perinuclear region. The joint surface is often composed of amorphous material, collagen fibrils and chondrocyte clusters. (Figure 4.80)

Most of the ultrastructural changes seen on the sacral side of the joint are present on the iliac side, but they are more advanced. All of the chondrocytes are grouped into clusters. (Figure 4.81) These occur as a result of an attempt at proliferative repair of the degenerating

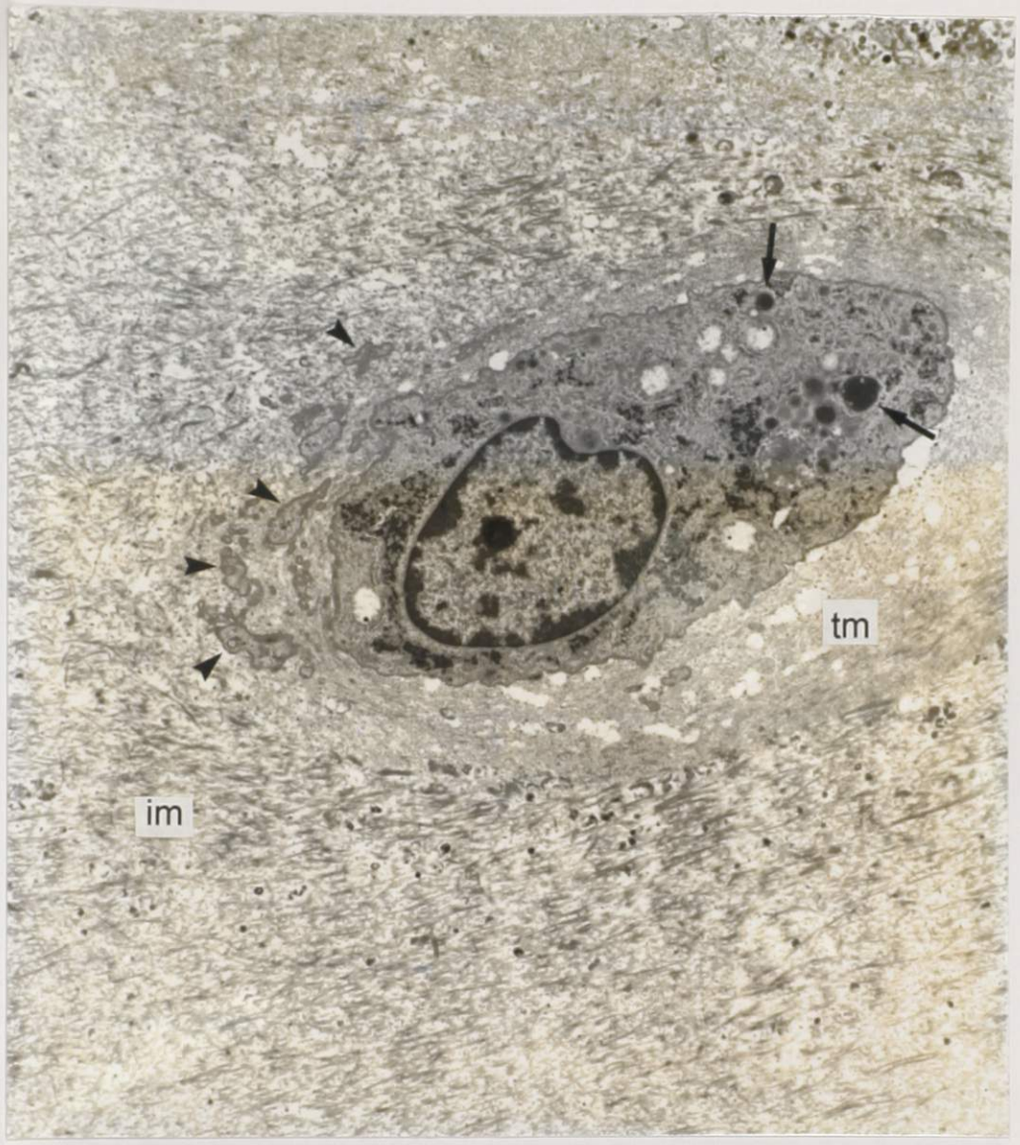

Figure 4.73a A sacral chondrocyte from a 23-year-old male specimen contains dense bodies or lysosomes (arrows). Convoluted cell processes (arrowheads) are present. These may separate from the cell and contribute to the presence of matrical lipidic debris (Ghadially, 1983). The territorial matrix (tm) contains an ample amount of proteoglycans, but in the interterritorial matrix (im), there is more collagen and lipidic debris and fewer electron-dense proteoglycan aggregates. X 5,985

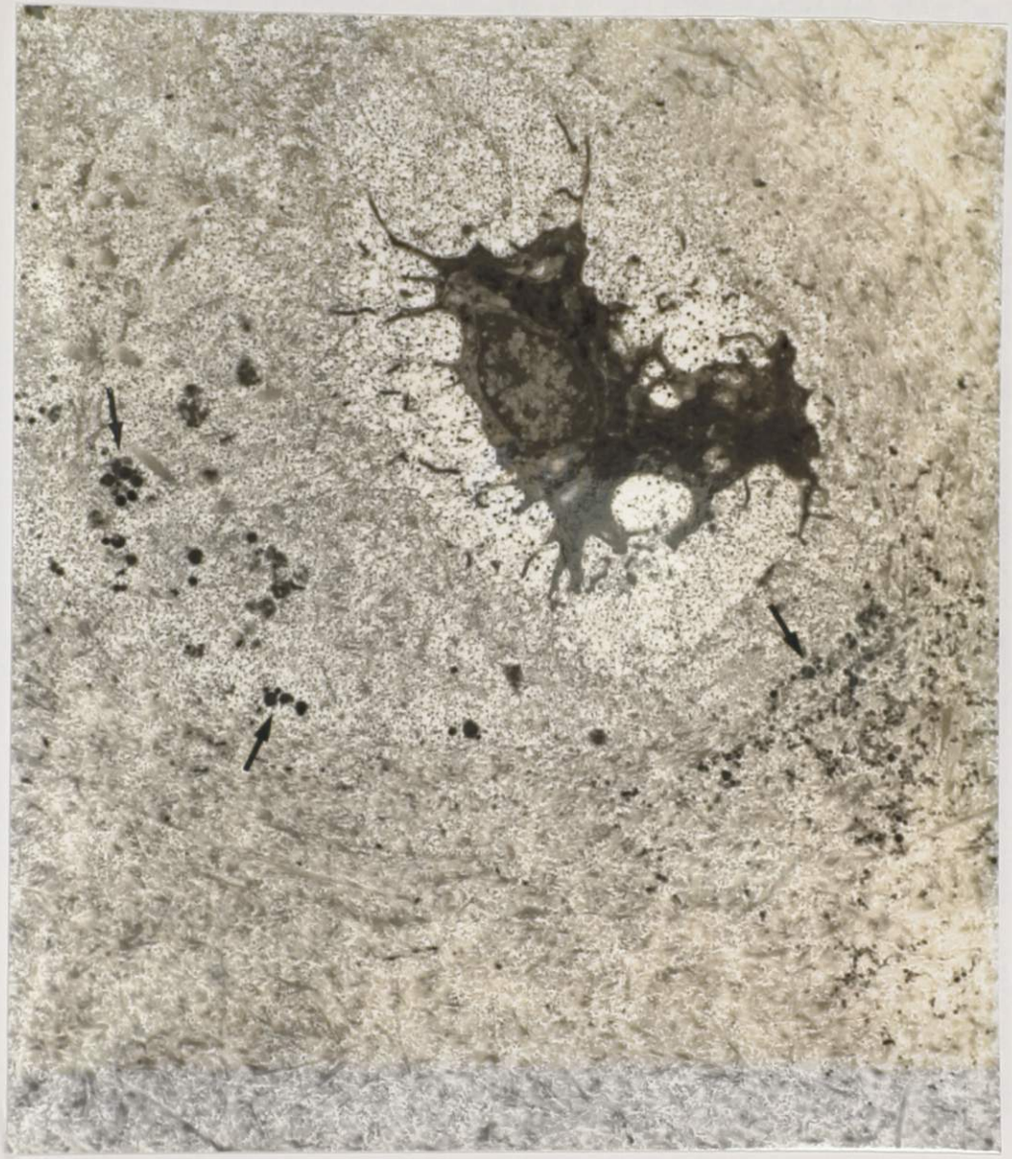

Figure 4.73b In situ necrosis of a chondrocyte contributes to the matrical debris found in this 23-year-old specimen. The cell is dense, dark and shrunken. The surrounding matrix is full of lipidic debris (arrows). X 5,985

Figure 4.74 A microscar of giant collagen fibres (arrows) is present in the territorial matrix of a 23-year-old sacral specimen. This condition is often referred to as amianthoid degeneration. It is most common at the site of chondrocyte necrosis. X 9,500

Figure 4.75a Matrix streaks (arrows), similar to the fetal interlacunar network, are present in this 22-year-old male sacral specimen. X 3,800

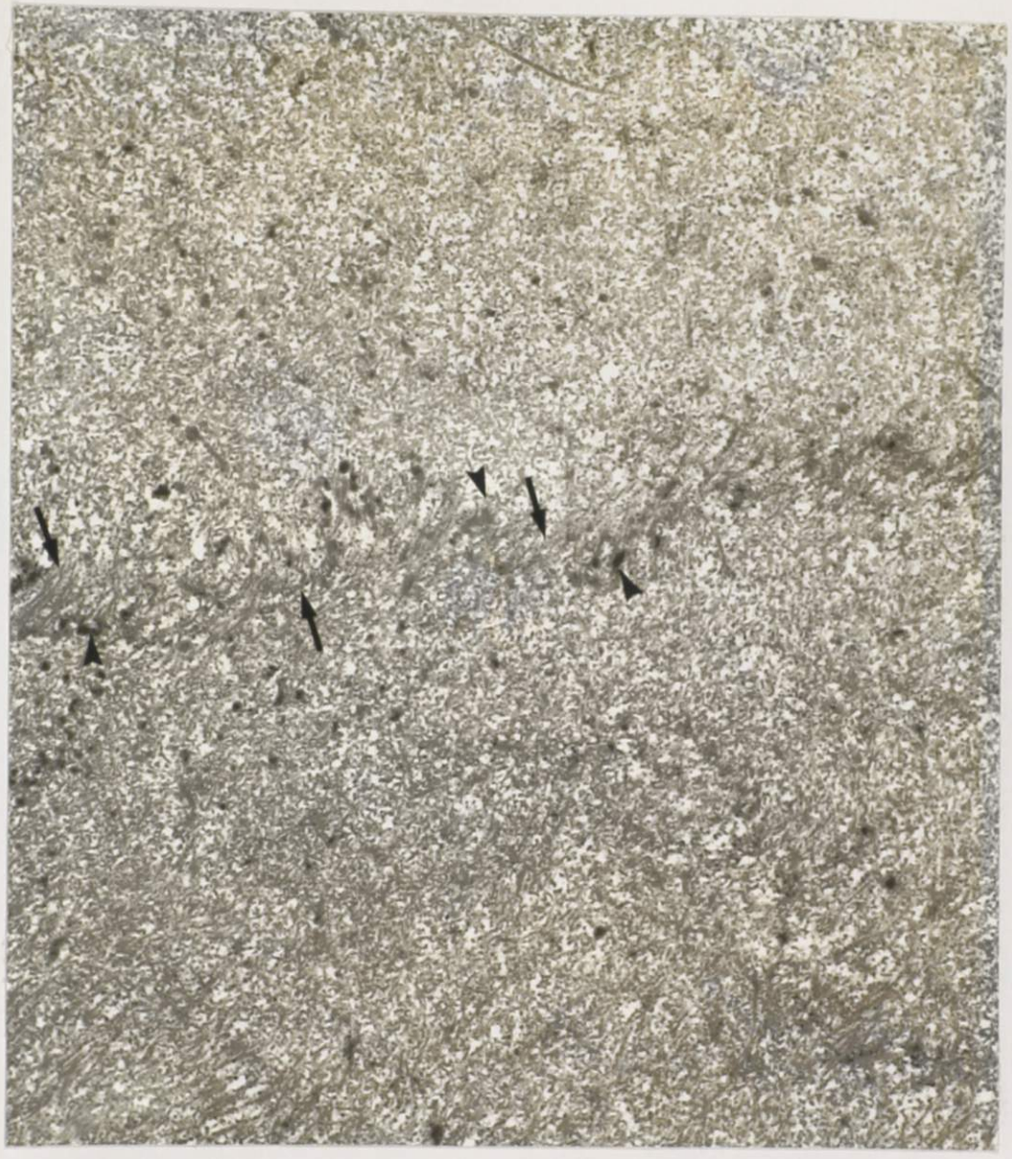

Figure 4.75b A high-power view shows that the streak is composed of both globular (arrowheads) and fibrillar (arrows) material. X 11,970

Figure 4.76 The territorial matrix (tm) surrounding this chondrocyte from a 23-year-old male specimen appears thick and contains a considerable amount of collagen fibrils. X 5,985

Figure 4.77 A sacral chondrocyte from a 23-year-old male specimen contains three lipid droplets (l). Two are surrounded by glycogen particles and the other is in the centre of a whorl (w) of intracytoplasmic filaments. A large tertiary lysosome (arrow) appears to be present. X 5,985

Figure 4.78 A dense and shrunken chondrocyte that is undergoing in situ necrosis is visible in this sacral specimen from a 33-year-old male. It is difficult to identify any of the cytoplasmic organelles, which appear to be fragmented. There is an increased amount of collagen and lipidic debris in the surrounding matrix. X 9,500

Figure 4.79a A whorl of intracytoplasmic filaments (w) is present in this chondrocyte from a 22-year-old male specimen. X 5,985

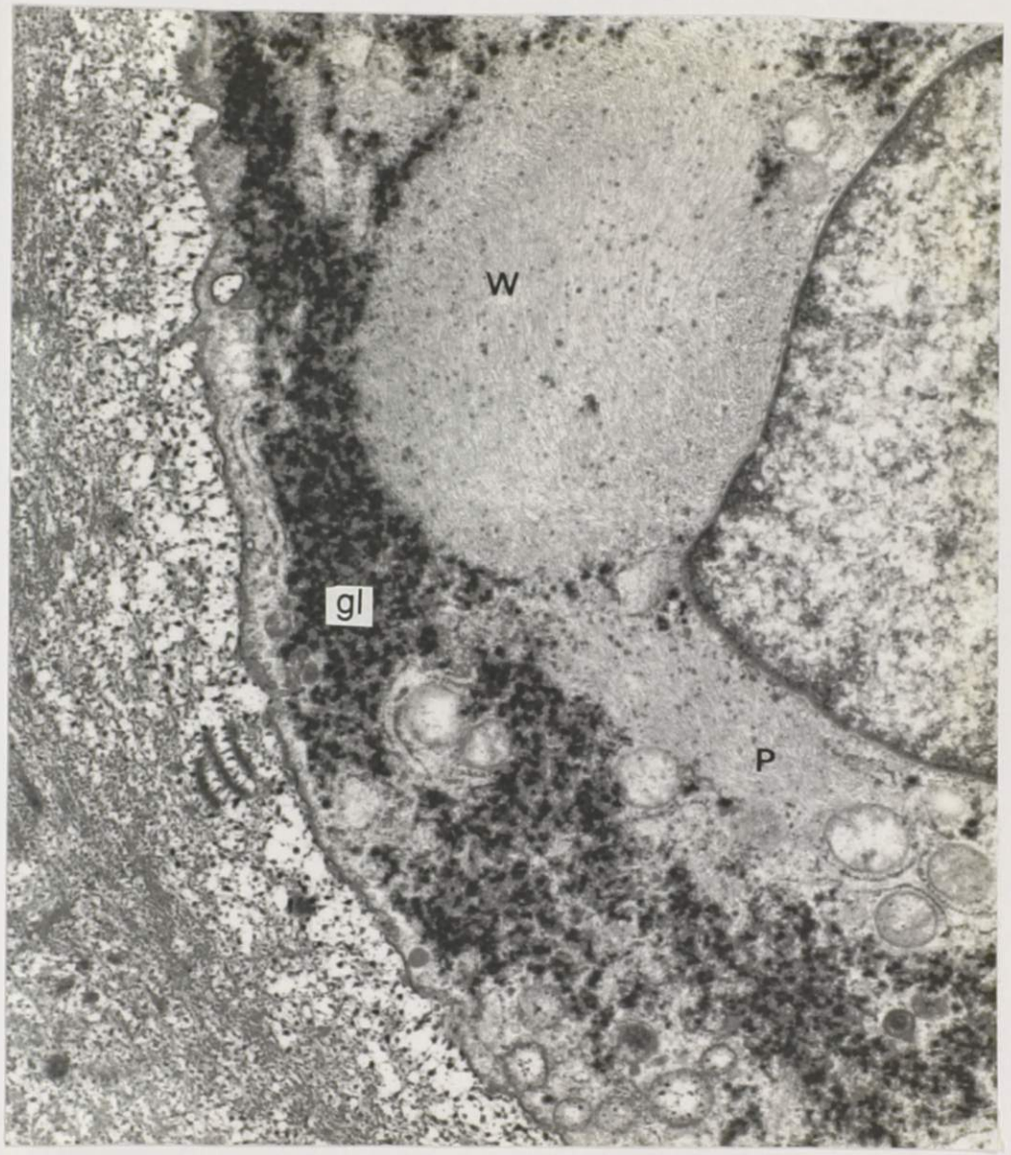

Figure 4.79b A high-power view of the above specimen confirms the presence of a whorl (w) of intermediate filaments in the cytoplasm that extend around the perinuclear region (p). The cell also contains a considerable amount of glycogen (gl). X 19,000

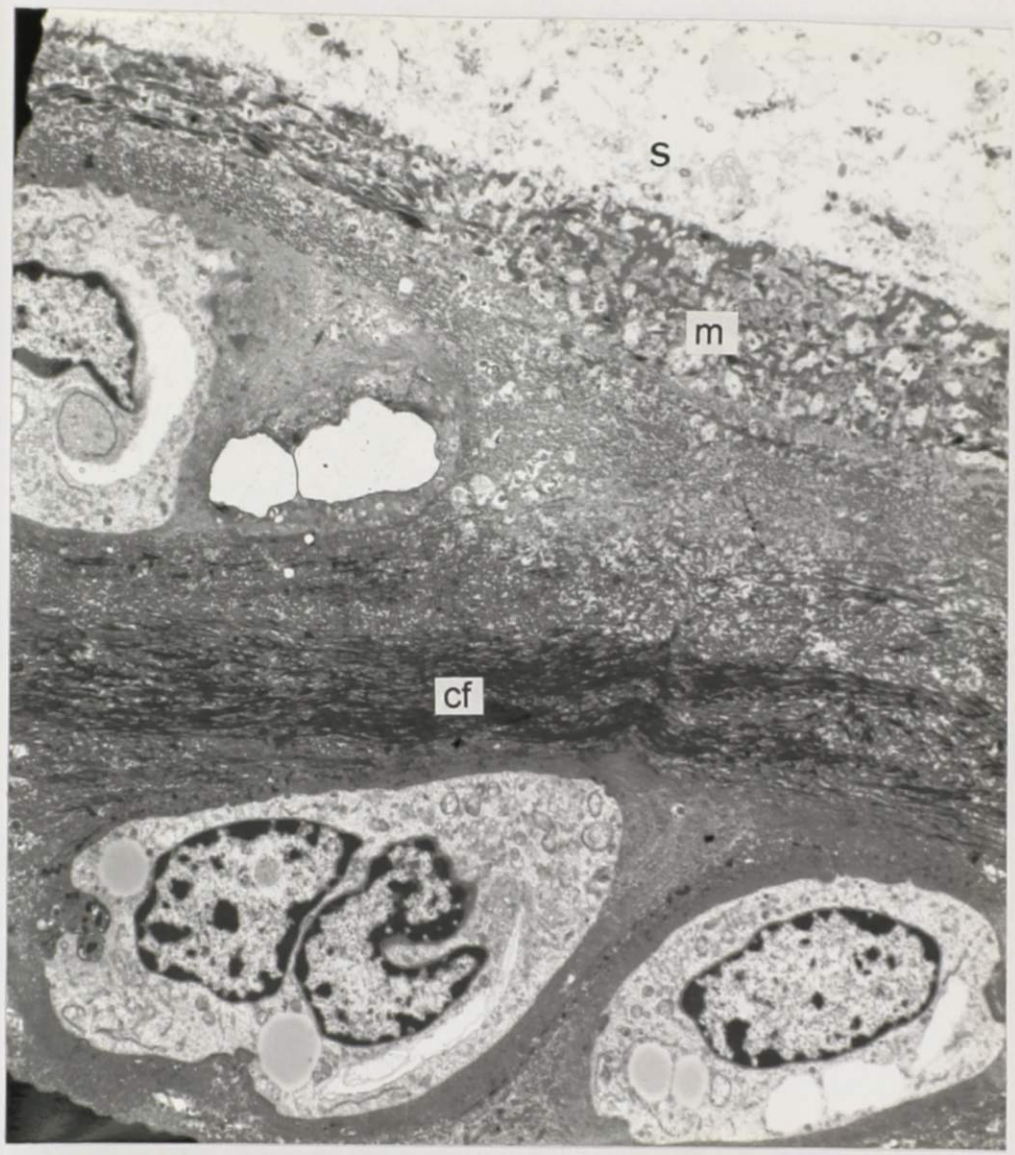

Figure 4.80 The joint surface (s) of this 33-year-old male specimen is covered by amorphous, degenerate material (m). Beneath this, there is a chondrocyte cluster and collagen fibres (cf) that run parallel to the joint surface. One of the chondrocytes appears to have two nuclei (n). However, this appearance is likely due to folding of a single nucleus. X 4,750

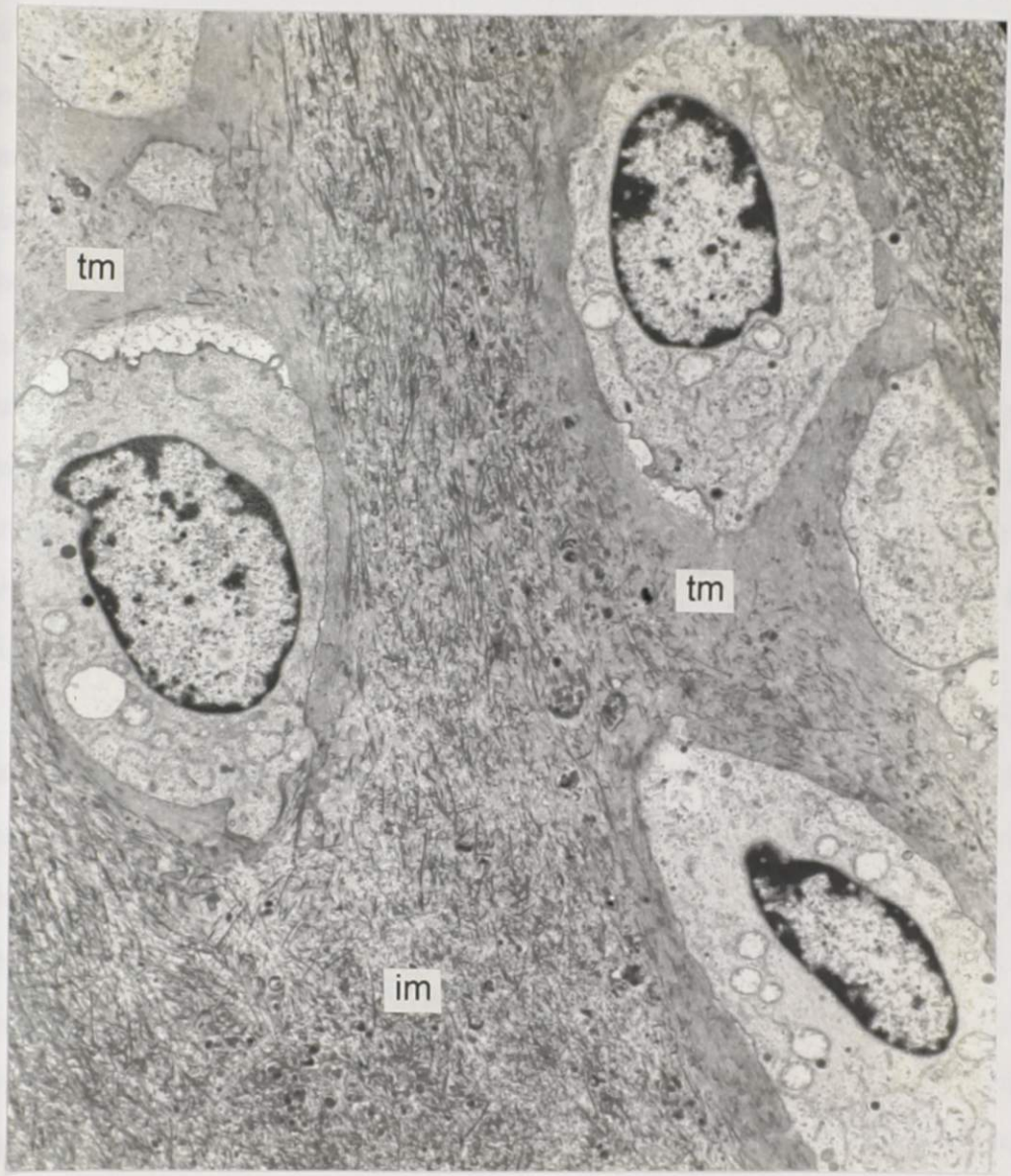

Figure 4.81 Two clusters of chondrocytes from a 23-year-old male iliac specimen are defined by their territorial matrix (tm) and separated by a collagenous interterritorial matrix (im). X 4,750

cartilage. As a result, dividing chondrocytes may be observed within a cluster. (Figure 4.82) Many of the cells within the clusters appear necrotic. (Figure 4.83) Some contain myelin figures that reflect the presence of lipidic residues that occur during cell death. Most of the clusters contain both viable and necrotic-looking cells. However, there are areas where all the cells within a cluster have died, leaving their remnants still surrounded by a territorial matrix. (Figure 4.84) In most cases, the territorial matrix is thick and contains filaments and proteoglycans. However, the remaining matrix is depleted of proteoglycans and is composed mostly of collagen fibrils and lipidic debris. (Figure 4.85)

Scanning electron micrographs of the sacroiliac joint surfaces in young adults shows a spectrum of changes. For the most part, the sacral surface is smooth and intact. There are characteristic surface humps and pits that are caused by chondrocytes just under the surface. (Figures 4.86 and 4.87) If the underlying chondrocyte shrinks during processing, a pit is produced. If it does not shrink, a hump is produced. In some cases, the sacral surface appears more roughened. Surface undulations (i.e. alternating ridges and furrows) and wrinkles (i.e. fine undulations) are common surface artifacts caused by curling and shrinkage of the specimen. (Figure 4.88) In some limited areas, there is surface fibrillation and even small crevice formation.

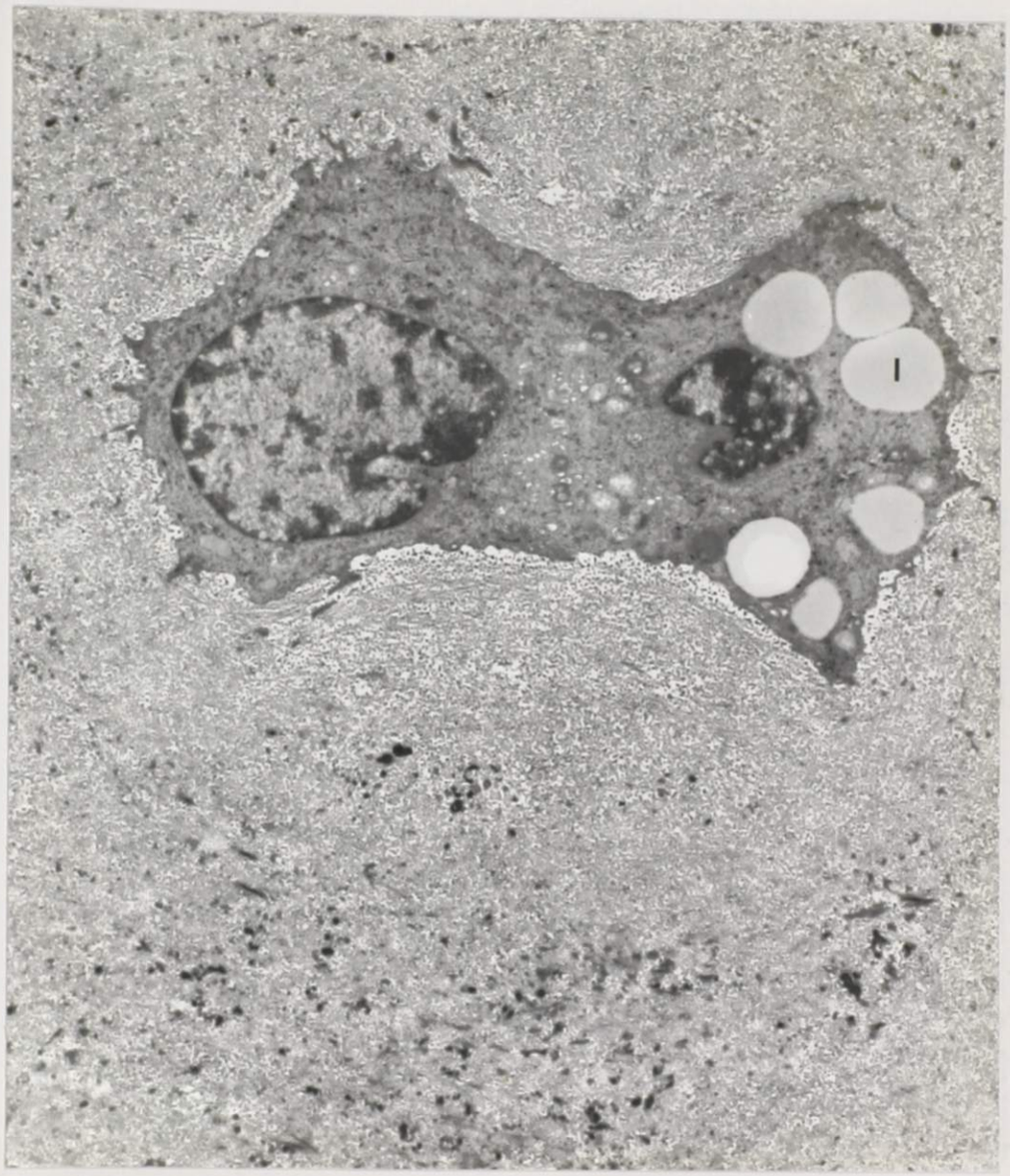

Figure 4.82 The appearance of this chondrocyte from a 22-year-old female iliac specimen is suggestive of cell division. There appears to be two nuclei, but it could be a single convoluted nucleus. In addition, the cells appears to be separating centrally. There are several lipid droplets (l) at one pole of the cell. X 5,985

Figure 4.83 The two chondrocytes in this 23-year-old male iliac specimen are undergoing in situ necrosis. They are dark and dense, with poorly-defined cytoplasmic organelles. Both cells contain numerous lipid droplets (l) and appear to be fragmenting. There is a considerable amount of lipidic debris in the surrounding matrix (curved arrows). X 5,985

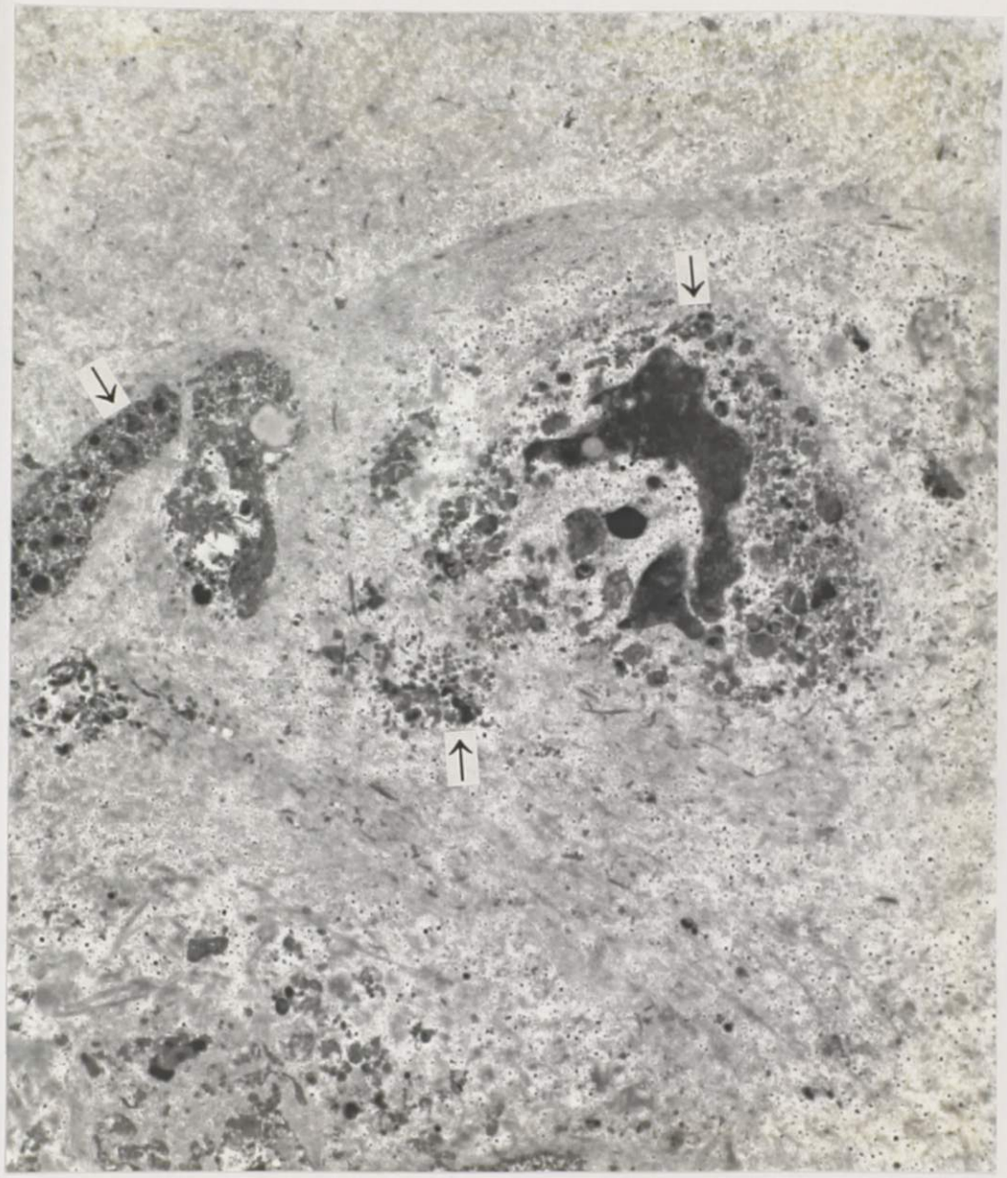

Figure 4.84 Fragmented pieces of cell remnants are present within an area of territorial matrix in this 23-year-old iliac specimen. The process of in situ necrosis of chondrocytes contributes to the lipidic debris (arrows) in the matrix. X 5,985

Figure 4.85 The two necrotic-looking chondrocytes in this 23-year-old male iliac specimen are surrounded by a territorial matrix (tm) that contains filaments and proteoglycan particles. However, the interterritorial matrix (im) is composed almost entirely of collagen fibrils and some lipidic debris (arrows). X 7,600

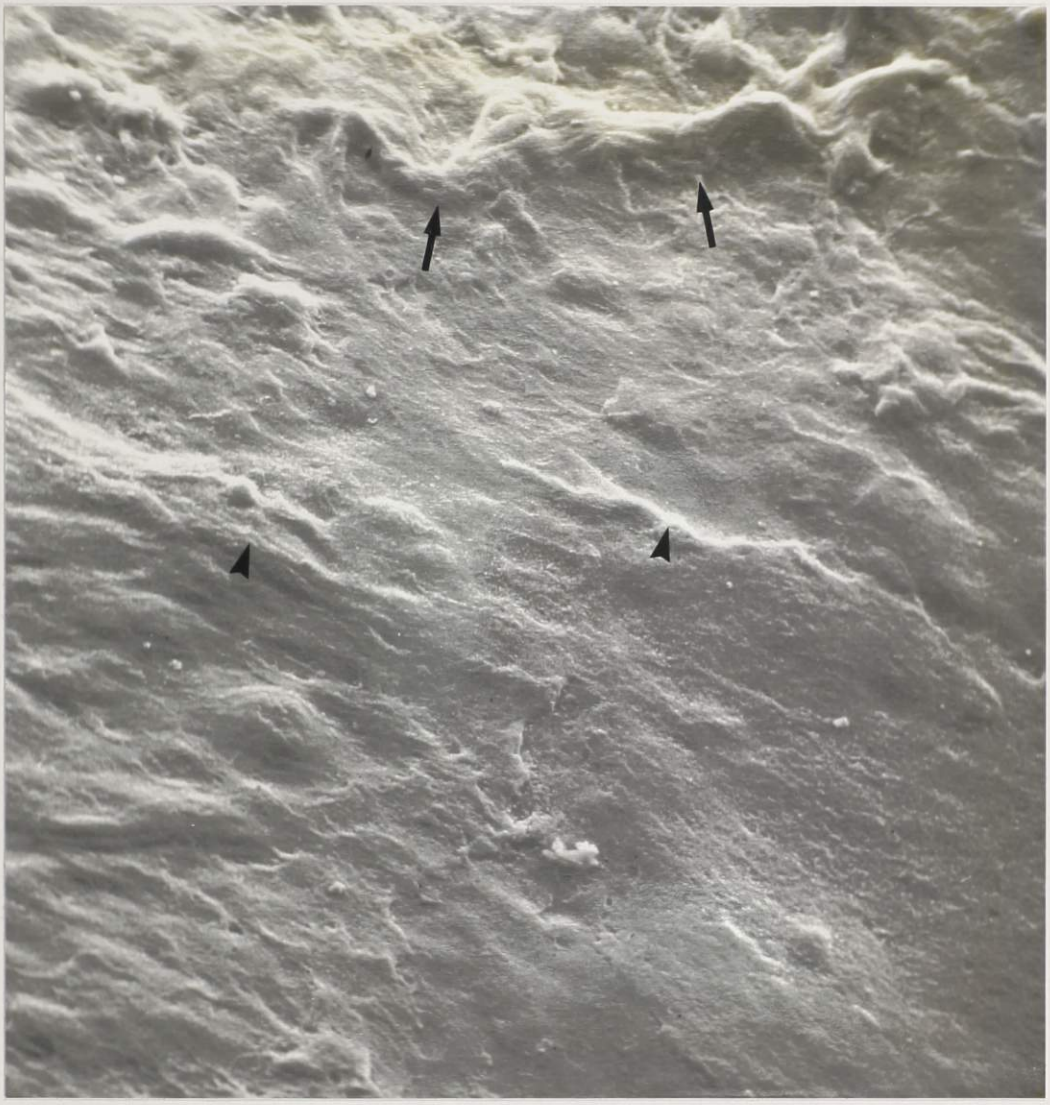

Figure 4.88 The sacral surface of this 22-year-old male specimen is roughened by both coarse (arrows) and fine (arrowheads) undulations. X 250

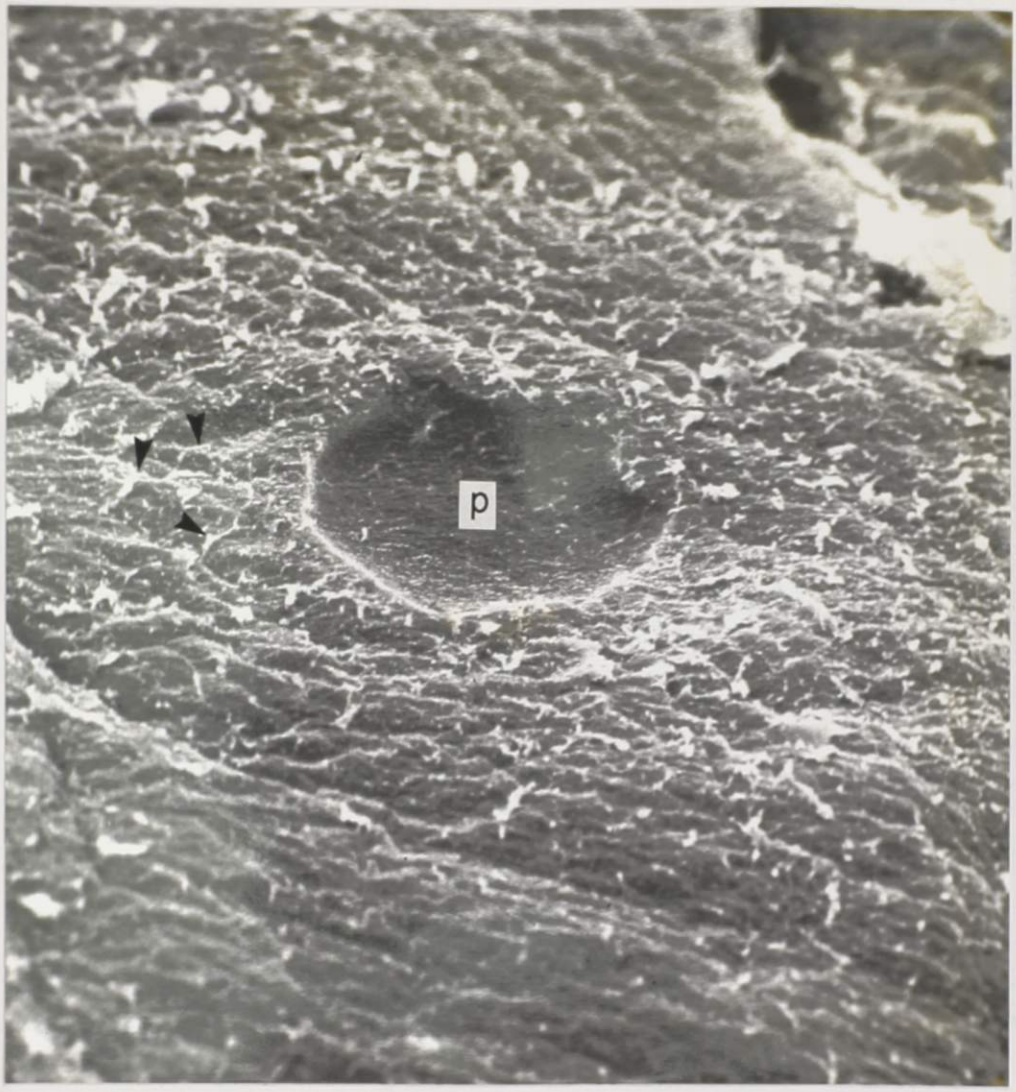

Figure 4.87 A high-power view of the sacral surface of a 23-year-old male specimen shows a pit (p). Like humps, pits are thought to result from underlying chondrocytes. Precipitated synovial fluid has formed a reticulum on the joint surface (arrowheads). X 1,562

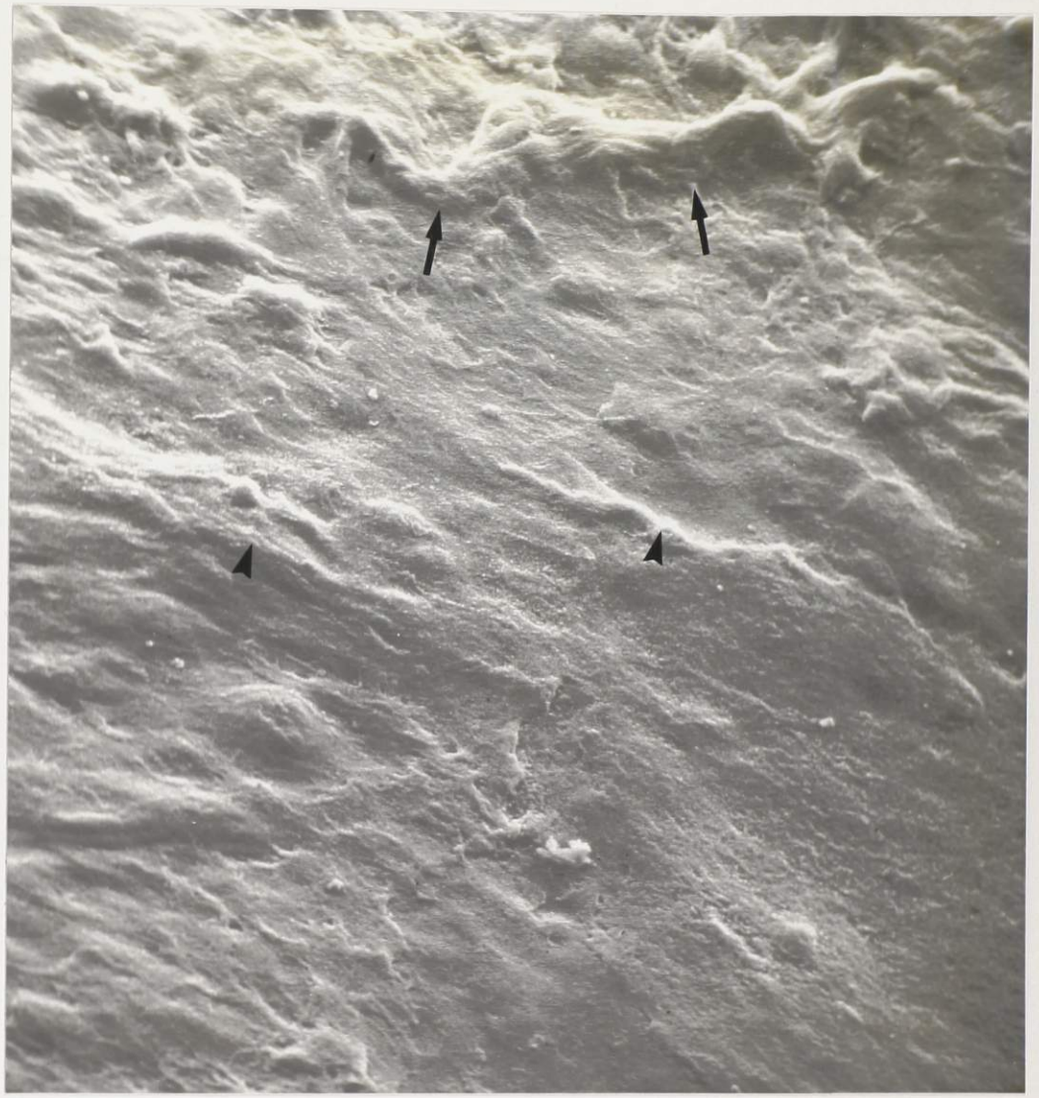

Figure 4.88 The sacral surface of this 22-year-old male specimen is roughened by both coarse (arrows) and fine (arrowheads) undulations. X 250